**University of Dundee**

**MASTER OF SCIENCE**

# Regulation of Phosphorylation of PPARγ by CDK5 in Obesity

Saul, Louise

*Award date:*
2014

# Regulation of Phosphorylation of PPARγ by Cdk5 in Obesity

By Louise Saul

A thesis submitted for the Degree of Master of Science University of Dundee

## Table of Contents 1-4

## Abbreviations

| | |
|---|---|
| ANOVA | Analysis of Variance |
| ATP | Adenosine Triphosphate |
| BES | N,N-bis(2-hydroxyethyl)-2-aminoethanesulfonic Acid |
| CDK | Cyclin-Dependent Kinase |
| CDK5 | Cyclin Dependent Kinase 5 |
| CDK7 | Cyclin Dependent Kinase 7 |
| CDK9 | Cyclin Dependent Kinase 9 |
| CDKL | CyclinDependent Kinase-Like |
| CLK2 | CDC2-Like Kinase |
| DNA | Deoxyribonucleic Acid |
| DMEM | Dulbecco's Modified Eagle Medium |
| DSTT | Division of Signal Transduction Therapy |
| DYRK1A | Dual Specificity Tyrosine Phosphorylation Regulated Kinase 1A |
| DYRK1B | Dual Specificity Tyrosine Phosphorylation Regulated Kinase 1B |
| DYRK2 | Dual Specificity Tyrosine Phosphorylation Regulated Kinase 2 |
| EDTA | Ethylene DiamineTetra Acetic Acid |
| EGTA | Ethylene Glycol Tetra Acetic Acid |
| ERK2 | Extracellular Regulated Kinase 2 |
| ERK8 | Extracellular Regulated Kinase 8 |
| FFA | Free Fatty Acids |
| GRB-2 | Growth Factor Receptor-Bound Protein 2 |
| GSK | Glycogen Synthase Kinase |
| GSK3-β | Glycogen Synthase Kinase 3 Beta |
| Hek-293 | Human Embryonic Kidney Cells-293 |
| HeLa cells | Henrietta Lacks Cells |
| HGP | Hepatic Glucose Production |
| HGU | Hepatic Glucose Utilization |
| HIPK1 | Homeodomain Interacting Protein Kinase 1 |
| IRS | Insulin Receptor Substrate |
| JNK1 | C-Jun N-terminal Kinase 1 |
| JNK3 | C-Jun N-terminal Kinase 3 |
| LDS | Lithium Dodecyl Sulfate |
| MAP kinase | Mitogen Activated Protein Kinase |

| | |
|---|---|
| MBP | Myelin Basic Protein |
| PAGE | Polyacrylamide Gel Electrophoresis |
| PBS | Phosphate Buffered Saline |
| PCR | Polymerase Chain Reaction |
| PI 3-kinase | Phosphatidylinositol 3-kinase |
| PPARα | Peroxisome Proliferator Activated ReceptorAlpha |
| PPARβ | Peroxisome Proliferator Activated ReceptorBeta |
| PPARγ | Peroxisome Proliferator Activated ReceptorGamma |
| PPRE | Peroxisome Proliferator Response Element |
| PTD | Phosphatidylinositol |
| PTPases | Protein Tyrosine Phosphatases |
| PTP1B | Protein-tyrosine Phosphatase 1B |
| PTEN | Phosphatase and Tensin Homolog Deleted On Chromosome-10 |
| RNA | Ribonucleic Acid |
| SAP | Shrimp Alkaline Phosphatase |
| SAPK2β | Stress-Activated Protein Kinase 2 Beta |
| SAPK4 | Stress-Activated Protein Kinase 4 |
| SDS | Sodium Dodecyl Sulfate |
| SHIP2 | SH2-containing Inositol Phosphatase-2 |
| SIRP | Signal Regulatory Protein |
| SRC2 | SrcHomology 2 |
| SRPK1 | Serine/Arginine-Rich Protein-Specific Kinase |
| T2DM | Type 2 diabetes Mellitus |
| TAE | Tris Acetate EDTA |
| TBST | Tris Buffered Saline Tween20 |
| TNF-α | Tumour Necrosis Factor Alpha |
| TZD | Thiazolidinediones |

## List of Figures

Figure 3.5: Immunoblot of GST-Flag-PPARγ1 and PPARγ2, following incubation with CDK5/p35, CDK5/p25 or ERK2 using antibodies as indicated (MW ~80KD). Control is PPARγ1 or PPARγ2 alone.

Figure 3.6: CMGC Kinase Screen with activity matched to myelin basic protein and incubated with PPARγ2 wild type and [Ser273Ala]PPARγ2(x, n=2)

Figure 3.7: Autoradiograph showing examples of the data used to generate Fig 3.6. Incubations were Mg[32P]ATP plus kinase alone (-) or kinase + PPARγ2 (+) as indicated.

Figure 3.8: CMGC kinases that phosphorylated PPARγ2 were incubated with non radioactive MgATP and GST-Flag-PPARγ2 followed by western blot with PPARγ, CDK substrate, p-Ser273and p-Ser112 antibodies as indicated (MW ~80KD). Control is PPARγ2 alone and band intensity is compared with control to see any increase in phosphorylation.

Figure 3.9: Coomassie stained SDS-PAGE gel of the GST-PPARγ2 mutants (upper gel), with lower gel showing areas quantified to generate the normalization ratios in Table 3.1.

Figure 3.10: (A) Graphical representation of mol/mol stoichiometry of PPARγ2 mutants byCDK5 and (B) a representative autoradiograph of phosphorylation, including control CDK5 alone lane (no PPARγ2 present)

Figure 3.11: Graph (A) representing mol/mol stoichiometry of the phosphorylation of PPARγ2 mutants byCDK9 and autorad (B) showing phosphorylationof PPARγ2 mutants, including control CDK9 alone lane (no PPARγ2 present)

Figure 3.12: Graph (A) representing mol/mol stoichiometry of the phosphorylation of PPARγ2 mutants byERK2 and autorad (B) showing phosphorylationof PPARγ2 mutants, including control ERK2 alone lane (no PPARγ2 present)

Figure 4.4: Analysis of PPARγ phosphorylation in FT-293LS1 cells treated with harmine and U0126, UI= un-induced,DMSO as a control(MW ~58KD)

Figure 4.5: Images of 3t3L1 fibroblasts at different stages of differentiation into adipocyte like cells stained with oil red O.

Figure 4.6: Images of 3t3L1 fibroblasts at different stages of induction to differentiate into adipocyte like cells under low and high light microscopy magnification

Figure 4.7 Expression of PPARγ, FABP, p35 and CDK5 during differentiation of 3T3-L1 cells (control = undifferentiated, Mid Diff =day 2, ibmx+insulin, diff= differentiated, +ve control is recombinant PPARγ2)

Figure 4.8: Analysis of PPARγ phosphorylation by immunoblotbefore and after differentiation of 3T3-L1 cells, with PPARγ p-Ser112, p-Ser273 and CDK-substrate antibodies (control = undifferentiated, Day 2=ibmx+insulin, Day4= insulin, Diff= differentiated)

Figure 4.9: PPARγ was immunoprecipitated from differentiated 3T3-L1 cells and analysed by immunoblot using a second PPARγ antibody and the anti-CDK substrate antibody (+ve control= recombinant PPARγ1).

Figure 4.10: Analysis of PPARγ phosphorylation by immunoblot, in differentiated 3T3 cells treated with 500nM palmitate, with PPARγ p-Ser112, p-Ser273 and CDK-substrate antibodies

Figure 4.11: Analysis of PPARγ phosphorylation by immunoblotin differentiated 3T3 cells treated with 50ng TNF-α or 167nm insulin for 1 hour,with PPARγ, p-Ser112, p-Ser273, CDK-substrate, IKB and p-ERK antibodies (MW PPARγ1 ~55 and PPARγ~58kd, control- vehicle treated)

Figure 4.12: Adipose tissue (from rats fed either standard chow or high fat diet as indicated) was homogenized in RIPA buffer (as described in Methods) and lysates probed by immunoblot by antibodies indicated

Figure 4.13: PPARγ was immunoprecipitated using anti-PPARγ (from Santa Cruz) from either (A) Hek-293 cells expressing WT PPARγ1 or Ser273A PPARγ1, or from adipose tissue (B), prior to immunoblot analysis with anti-PPARγ (generated by Prof. Colin Palmer, University of Dundee)

Figure 4.14: Adipose tissue from chow fed rats was either (A) homogenized in Hepes buffer or (B) solvent extracted as described in Methods section. Protein fractions were analysed by immunoblot using the antibodies indicated

## List of Tables

## Amino Acid Codes

Table 1.1 - Table showing the amino acids, their codes and possible codon combinations

| One Letter Code | Three Letter Code | Amino Acid | Possible Codons |
|---|---|---|---|
| A | Ala | Alanine | GCA,GCC,GCG,GCT |
| B | Asx | Asparagine/Aspartic Acid | AAC, AAT, GAC, GAT |
| C | Cys | Cysteine | TGC, TGT |
| D | Asp | Aspartic Acid | GAC, GAT |
| E | Glu | Glutamic Acid | GAA, GAG |
| F | Phe | Phenylalanine | TTC, TTT |
| G | Gly | Glycine | GGA, GGC, GGG, GGT |
| H | His | Histidine | CAC, CAT |
| I | Ile | Isoleucine | ATA, ATC, ATT |
| K | Lys | Lysine | AAA, AAG |
| L | Leu | Leucine | CTA, CTC, CTG, CTT, TTA, TTG |
| M | Met | Methionine | ATG |
| N | Asn | Asparagine | AAC, AAT |
| P | Pro | Proline | CCA, CCC, CCG, CCT |
| Q | Gln | Glutamine | CAA, CAG |
| R | Arg | Arginine | AGA, AGG, CGA, CGC, CGG, CGT |
| S | Ser | Serine | AGC, AGT, TCA, TCC, TCG, TCT |
| T | Thr | Theonine | ACA, ACC, ACG, ACT |
| V | Val | Valine | GTA, GTC, GTG, GTT |
| W | Trp | Tryptophan | TGG |
| Y | Tyr | Tyrosine | TAC, TAT |
| | | STOP CODON | TAA, TAG, TGA |

## Acknowledgements

I would like to thank my supervisor DrCalum Sutherland for giving me the opportunity to undertake this research project for my masters, and thank him for his advice and support throughout.

I would also like thank Diabetes UK for funding the project, and allowing the chance for this study to be carried out

A big thank-you and acknowledgement also to all members of the Sutherland and Ashford labs for their help and support throughout my masters degree. I would also like to thank other departments within the university, such as the DSTT and sequencing service, for the services they provide to enable better quality research to be done in a shorter time frame.

A final acknowledgment and thanks goes to my friends and family for their support throughout my degree.

## Declarations

I declare that the following thesis is based on the results of investigations conducted by myself, and that this thesis is of my own composition. Work that is not my own is clearly indicated in the text by references to the relevant publications. This thesis has not in part or in whole been previously submitted for a higher degree.

Louise Saul

DrCalum D. Sutherland

## Abstract

PPARγ is the receptor for thiazolidinedione (TZD) anti-diabetes drugs, and a key regulator of adipose differentiation and insulin sensitivity. Increased heart failure associated with specific TZDs has reduced their clinical use. However recent work suggested that phosphorylation of PPARγ at Ser273 modified its response to TZDs, shifting the risk-benefit ratio of these drugs. Cyclin dependent kinase-5 (CDK5) which requires a non-cyclin partner (p35) for activity was proposed to phosphorylate Ser273, while obesity promoted cleavage of p35 to p25 thereby enhancing CDK5 phosphorylation of PPARγ (Choi *et al*2010). However the sequence surrounding Ser273 is not a CDK5 consensus, therefore I have analysed PPARγ phosphorylation more carefully. I mutated Ser273 on PPARγ to alanine and compared phosphorylation of mutant and wild-type by multiple protein kinases. I raised a phosphospecific antibody to Ser273 of PPARγ and used this to monitor phosphorylation of PPARγ isoforms.P35-CDK5 and p25-CDK5 phosphorylate wild-type and S273A PPARγ to similar levels *in vitro*. The phosphospecific Ser273 antibody did not detect phosphorylation of endogenous PPARγ in adipose tissue of rats (with or without obesity). I could not detect phosphorylation of Ser273 on recombinant PPARγ when over-expressed in HEK293 or 3t3-L1 cells (± differentiation). Finally, phospho-Ser273 was not present on PPARγimmunoprecipitated from adipose tissue (obese and non-obese), or from cell lines, as assessed by phosphopeptide analysis or immunoblot. I have tried multiple approaches to validate that CDK5 phosphorylates Ser273 of PPARγ but our data questions the clinical potential of targeting this modification.

# Chapter1 – Introduction

## 1.1 Glucose Homoeostasis

Homeostasis is the process by which the body maintains a constant internal environment by changing physiological responses (Barnett 2008). Glucose regulation is one of the many homeostatic processes that occurs within the body, with others including regulation of water concentration, temperature and pH.The liver, brain, pancreas, intestine, muscle and adipose tissue are the major organs involved in the management of energy metabolism; these organs communicate with each other to sense the energy status of the entire organism and coordinate their function (Feinglos and Bethal 2008).

It is important that glucose levels are maintained as glucose is the primary source of energy for the body's cells. Glucose is kept in a narrow range between 3mM after prolonged fasting or exercise, and maximum values of 9mMafter a meal. Homoeostasis of glucose is crucial so that hyperglycaemia and hypoglycaemia do not occur; hyperglycaemia is when there is a higher than normal amount of blood glucose present and hypoglycaemia is when blood sugar levels are too low. Hyperglycaemia can result in non-enzymatic glycosylation and thus the loss of protein function, as well as glucose induced oxidative damage. Hypoglycaemia leads to an under supply of glucose to tissues and can thus be a danger for neuronal cells, fibroblasts and erythrocytes, which use glucose as the main energydelivering fuel when under normal physiological conditions(König,Bulik and Holtzhütter 2012).

When food is consumed, also known as the fed state, the pancreatic beta cells secrete the hormone insulin, which instructs the body to store fuel. Insulin promotes the deposition of glycogen in the liver, activates glucose transport and glycogen synthesis in muscle and promotes triglyceride accumulation in the adipose tissue;it does this by inhibitingketogenesis in the liver, proteolysis in the muscle and lipolysis in adipose tissue (Taylor 1999).Insulin binds to its receptor, initiates a protein kinase cascade (see section 1.1.1) and stimulates glycogen synthesis via glycogenesis, as well as suppressing gluconeogenesis in the liver(Berg *et al* 2007).

When blood glucose levels begin to drop several hours after a meal, known as the fasting state, there is a decrease in insulin secretion and a rise in glucagon secretion;glucagon is secreted by the alpha cells of the pancreas in response to the low blood sugar levels, and it binds to the glucagon receptor within the plasma membrane. Glucagon mobilizes glycogen stores when there is no dietary intake of glucose, and the mobilized glycogen is broken down into glucose via a process known as glycogenolysis. Glucagon alsopromotes gluconeogenesisand suppresses glycolysis to increase the levels of glucose available (Berg *et al*2007). Another function of glucagon is that it promotes lipolysis, to break down the lipids stored as triglycerides in fat cells (Liljenquist*et al* 1974).Thus glucagon and insulin work as opposing factors but as their synthesis is reciprocally regulated by blood glucose they are generally not produced at the same time in healthy individuals.

### 1.1.1 Liver in glucose homeostasis

As described in section 1.1, the liverplays a crucial role in maintaining glucose and free fatty acid homeostasis. The liver buffers plasma glucose between net hepatic glucose utilization (HGU) and net hepatic glucose production (HGP), depending on if the plasma glucose levels have risen or fallen below the critical threshold value of 6mM. The switchbetween HGU and HGP is between a positive export of glucose and negative import of glucose to get a net hepatic glucose balance; in this process hepatic metabolism is altered from glucose production (glycogenolysisand gluconeogenesis)duringhypoglycaemia, to glucose utilization and storage(glycolysis and glycogen synthesis)duringhyperglycaemia.The hepatocytes are thus key for transient storage of glucose as glycogen, thesynthesis of glucose from glycerol, lactate and amino acids, and the conversion of excess glucose into triglycerides(König, Bulik and Holtzhütter 2012).

### 1.1.2 Muscles in glucose homeostasis

During exercise the uptake of glucose is required to provide a supply of fuel to the working muscles, and for after exercise it is needed for the replenishment of muscle glycogen stores (Sinacore and Gulve 1993).Skeletal muscle accountsfor

approximately 80–85% of peripheral glucose uptake, with the remaining proportion going to the rest of the body's cells (Feinglos and Bethal 2008).

Muscle lacks glucose 6-phosphatase, so glycogenolysis in muscle does not provide glucose for release into the blood. However in the fasting state, amino acids and other substrates are exported from the muscles to the liver,to generate glucose via hepaticgluconeogenesis (Taylor 1999).

The entry of glucose into muscle cells isachieved by a carrier-mediated system with protein transport molecules; the two most common are GLUT-1 and GLUT-4. GLUT-1 transporter is found in the sarcolemmalmembrane, and it is involved in glucose transportunder basal conditions. Upon insulin stimulation, glucose transport accelerates due to the translocation of GLUT-4from an intracellular pool out to thesarcolemmal membranes and T-tubule (Barnard and Youngren 1992).Experiments in mice with muscle-specific GLUT4 deficiency showed decreased insulin responsiveness in adipose tissue and liver (Zisman*et al* 2000), and those that were adipose-specific GLUT4 depleted showed muscle and liver insulin resistance (Abel *et al* 2001). The insulin resistance is thought to happen through elevated blood glucose levels occurring in the conditional knockout animals, which secondarily impairs insulin signalling (Kim *et al* 2001).

### 1.1.3 Adipocytes and adipose tissue in glucose homeostasis

Adipocytes are the major fat-containing component of adipose tissues. In mammals the two main types of adipose tissue are white adipose tissue and brown adipose tissue. White adipose tissue is present in many species, and is the main adipose tissue in humans. Brown adipose tissue functions primarily in thermogenesis, due tothe high number of iron-containing mitochondria present in the cells helping dissipate energy in the form of heat (Wu, Cohen and Spiegelman 2013).

Recent research has shown a third type of adipocyte known as beige or brite adipocytes; these are brown adipocytes that appear in white adipose tissue that derive from precursor cells that are different from those in classical brown adipose tissue. The beige adipocytes are thought to be involved in the trans-differentiation between white to brown adipocytes, and to play a role of

thebrowning process in protection against obesity (Giralt and Villarroya 2013). The thermogenic process of beige and brown and fat cells can increase whole-body energy expenditure and therefore is suggested they can protect against obesity and diabetes (Wu, Cohen and Spiegelman 2013).

Adipocytes in white adipose tissue are highly specialized, with the crucial function of storage, metabolism, and release of lipids (Lazar 1999).Most energy stores in healthy humans are contained within the adipose tissue (Rosen and Spiegelman 2006).Adipose tissue stores energy in the form of triglycerides during nutritional excess and this energy can be mobilized by lipolysis, releasing fatty acids and glycerol into the circulation when required (Feinglos and Bethal 2008).

Adipose tissue is also an endocrine organ, as it synthesizes and secretes the biologically active adipokines that affect various homeostatic systems; these include tumour necrosis factor alpha (TNF-α) and leptin, which are elevated during obesity (Gregoire, Smas and Sul 1998). In adipose tissue liopogenesis (lipid storage), and lipolysis (lipid utilization), are regulated by several hormones, whichrequire the presence of key transcription factors such as peroxisome proliferator-activated receptors, sterol regulatory element-binding proteins, and enzymes, such as fatty acid synthase and carnitinepalmitoyltransferase (Lee 2012).

Excess adipocyte mass is thedefining feature of obesity, a condition that is closely linked to other diseases such as hypertension, atherosclerosis, cancer, gallbladder disease, and type 2 diabetes (Gregoire, Smas and Sul 1998).Adipocytes derive from fibroblast-like precursor cells, which are differentiated by a timed cascade of transcriptional events, withperoxisome proliferator activated receptor gamma (PPARγ) central to this process. PPARγ is activated by natural fatty acid derivatives including eicosanoids, as well as compounds such as the anti-diabetic thiazolidinedione class of drugs (Lazar 1999 and see later).

### 1.1.4 Insulin signalling pathway

Insulin triggers the uptake of glucose, fatty acids and amino acids into liver, muscle an adipose tissue, as well as promoting the storage of these nutrients in the form of glycogen, proteins and lipids (Saltiel and Pessin 2007).It binds to its receptor and triggers the activation of a signalling pathway that stimulates the transport of nutrientsfrom the blood supply to tissues and promotes the conversion of these nutrients into storage macromolecules (Lizcano and Alessi

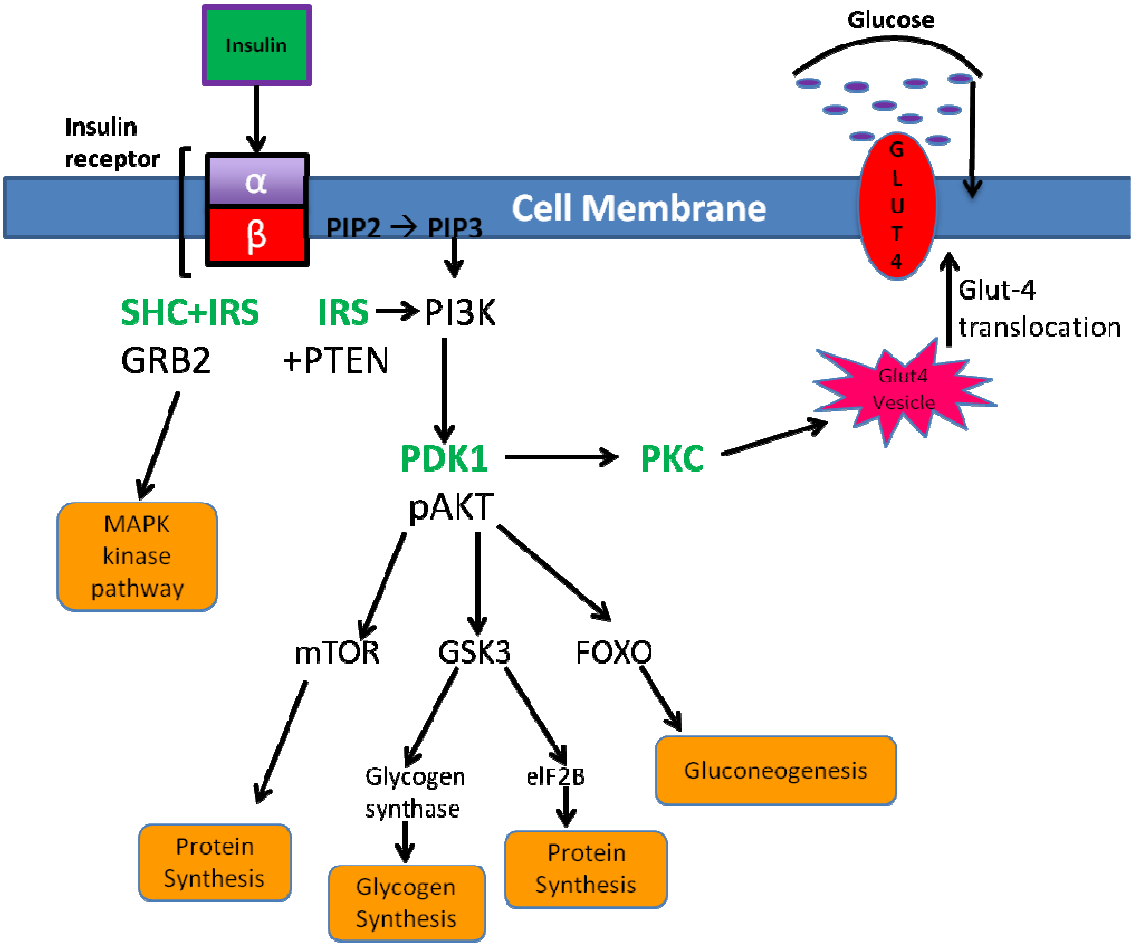


2002). A diagram of theinsulin signalling pathway is shown in figure 1.1, showing the key components and phosphorylation pathways

Figure 1.1- Diagram illustrating the different stages of the insulin signaling pathway

The insulin receptor is a complex that consists of two extracellular alphasubunits, which bind insulin, andtwo trans-membrane beta subunits that have tyrosine kinase activity. Insulin binding to the alpha subunit induces the phosphorylation of onebeta subunit by another on specific tyrosine residues in an activationloop; the receptor also undergoes auto-phosphorylation at othertyrosine residues in the juxta-membrane regions and intracellulartail (Chang, Chiang, Saltiel2004).

The activated insulin receptor can then phosphorylate tyrosine residues on intracellular substrates by recognition of the residues by the phospho-tyrosine binding domain of adaptor proteins; these include the insulin receptor substrate (IRS) family, Growth Factor Receptor-Bound Protein 2(GRB-2)and signal regulatory protein family members.The phospho-tyrosine residues in the proteins then interact via SrcHomology 2 (SH2) domains with adapter subunits of signalling intermediates, includingphosphatidylinositol 3-kinase (PI 3-kinase) (Chang, Chiang, Saltiel2004).

The catalytic subunit of PI 3-kinase then phosphorylates phosphatidylinositol (4,5) bisphosphate, which then leads to the formation of Ptd(3,4,5)$P_3$. A major downstream effector of Ptd(3,4,5)$P_3$ is AKT, which when activated requires the protein kinase 3-phosphoinositide-dependent protein kinase-1 (PDK1). Activated AKT can then enter the cytoplasm,where it phosphorylates and inactivates glycogen synthase kinase 3 (GSK3).Glycogen synthase is a major substrate of GSK3, and it is an enzyme that catalyses the final step in glycogen synthesis; therefore the inactivation of GSK3 by AKT promotes glucose storage as glycogen(Lizcano and Alessi 2002).Activation of the mitogen activated protein (MAP) kinase pathway occursthrough Ras activation, withSyp modulating the MAP kinase and other effector pathways(Holman and Kasuga 1997).

As well as promoting glucose storage, insulin inhibits the production and release of glucose by the liver by blocking gluconeogenesis and glycogenolysis (Saltiel and Kahn 2001). Insulin directly controls the activities of a set of metabolic enzymes by phosphorylation and dephosphorylation events, and by

regulating the expression of genes that encode for hepatic enzymes involved in gluconeogenesis (Schmoll*et al*2000).

Protein tyrosine Phosphatases (PTPases) catalyze the dephosphorylation of insulin receptor and its substrates, leading to a reduced effect of insulin action. PTPasesare linked to being negative regulators of insulin signaling, including protein-tyrosine phosphatase 1B (PTP1B), phosphatase and tensin homolog deleted on chromosome-10 (PTEN) and SH2-containing Inositol Phosphatase-2 (SHIP2).Over-expression of SHIP2 decreases insulin-stimulated Akt activation, GSK3 inactivation, and glycogen synthase activation (Wolf *et al* 1995).Any defects in the insulin signalling pathway can contribute towards diabetes, and due to there being so many stages within the insulin pathway that can go wrong, and there is a lot of research investigating these pathways for therapeutic potential for the treatment of type 2 diabetes.

## 1.2 Diabetes Mellitus

Diabetes Mellitus is described by Tuch, Dunlop and Proietto (2000),as a disorder ‘characterized by the presence of an excess of glucose in the blood and tissues of the body’. The history of diabetes dates back to the ancient Egyptians in 1550BC, with an Egyptian papyrus thought to be the first reference, mentioning a rare disease that caused a patient to lose weight quickly and urinate frequently. The first clinical description of diabetes was given by the Ancient Greek physician Aretaeus in 30-90CE, with symptoms recorded such as thirst, weight loss and frequent urination. In 131-201CE, Galen hypothesized that it was a disease of the kidney (DIABETES 2014).The origin of Diabetes Mellitus is a Greek and Latin phrase, which translates as diabetes being the Greek for siphon, referring to an excess quantity of urine being discharged, and mellitus being the Latin for honey; thus the literal meaning is the passage of large amounts of sweet urine (Tuch, Dunlop, and Proietto2000). When the body has an inability to produce insulin, or fails to uptake and store nutrients due to defects in the insulin signalling pathway (see section 1.14), diabetes (plasma hyperglycaemia) is the result.

The two main types of diabetes are type 1 and type 2. Type 1diabetes is an autoimmune disease, which results in almost complete loss of the pancreatic beta cells that are the sole site of insulin production in the body. Therefore hyperglycaemia in Type 1 diabetes is due to a lack of insulin production and is often referred to as insulin dependent. Type 2diabetes is a more complex multifactorial disorder primarily caused by the body’s ineffective response to insulin, or insulin resistance (WHO 2012); type 2 diabetes is the more common form, accounting for roughly 85% of the total diabetes burden. In the UK alone, there are currently 2.9 million people that have been diagnosed with diabetes, alongside an estimated 850,000 people who have the condition but are unaware of this fact (Diabetes UK 2012).

There are many signs and symptoms associated with diabetes, but the main symptoms are an increase in thirst, and an increase in the need to urinate; other symptoms may include weight loss, tiredness, mood swings and nausea. The symptoms of type 1 diabetes develop very quickly, over a matter of weeks,

whereas the symptoms of type 2 diabetes are harder to recognise as they develop slowly over time (Diabetes UK 2012). The diagnosis of diabetes requires two separate measures of fasting blood glucose being greater than 7mM, with fed blood glucose levels above 11mM.

There is no defined cause of diabetes, and this area is still under research, with many current theories. There are influences fromboth genetics, and environment (including lifestyle choices such as diet and exercise). While type 1 diabetes is due to loss of the pancreatic beta cells that produce insulin, the causes of type 2 diabetesare multi-factorial, including obesity, sedentary lifestyle and aging(Diabetes UK 2012). Type 2 diabetes Mellitus (T2DM) affects 5% of the population (Juresa and Metelko 2009),and is described as ‘an insidious chronic disease’, that has an increasing prevalence each year due to the global waistline expanding (Whitehead 2011).It is a heterogeneous disorder that is caused by concomitant impairment of insulin secretion by pancreatic beta cells, and of insulin action in peripheral target tissues (Fiume *et al* 2011).The disease itself is associated with disturbances of carbohydrate, fat and protein metabolism, and cardiovascular risk factors, such as insulin resistance, obesity, hypertension, dyslipidemia, and atherosclerosis (Tontonoz and Spiegelman 2008); therefore much focus is on understanding the connection between obesity, T2DM and cardiovascular disease.

It is possible to have diabetes without being obese, but there are very strong links between the 2 diseases. Under normal conditions, the pancreatic islet β-cells increase insulin release sufficiently to overcome the reduced efficiency of insulin action, therefore maintaining normal glucose tolerance. For obesity and insulin resistance to be associated with type 2 diabetes, the β-cells must be unable to compensate fully for decreased the insulin sensitivity. Some people can have β-cell dysfunction with normal glucose levels, due to them having a high risk ofdeveloping the disease (Kahn *et al* 2006).

In obese individuals, adipose tissue secretes increased amounts of non-esterified fatty acids, hormones, glycerol, pro-inflammatory cytokines and factors involved in the development of insulin resistance.

Excessive secretion(or reduced storage) of free fatty acids and altered production of adipokines from adipose tissue arelikely contributors to insulin resistance in the peripheral tissues (Steppan C. M *et al* 2001). Polypeptides such as leptin, adiponectin and tumour necrosis factor alpha (TNF-α), which are secreted by adipocytes, have been shown to affect insulin actionon other tissues. An increase in plasma free fatty acids (FFAs) causes lipotoxicity in the non-adipose tissues such as the liver, pancreas and skeletal muscle, and this reduces glucose disposal, increases gluconeogenesis and impairs insulin secretion (Gross and Staels 2007).

## 1.3 Treatment of Diabetes

There are many current treatments available for T2DM; these consist ofbiguanides, sulphonylureas, meglitindines, thiazolidinediones, alpha glucosidase inhibitors, incretinsand insulin therapy. One of the most common oral treatments is metformin, a biguanide drug, which seems toimprove insulin action and exert insulin dependent effects. Thesulphonylureas, incretins and meglitinides work by stimulating insulin secretion, whereas alpha glucosidase inhibitors slow down the rate of carbohydrate digestion. A new group has also emerged known as SGLT2 inhibitors, and these work by decreasing glucose absorption in the kidneys so more is excreted in the urine. The final group of drugs, thethiazolidinediones, improves insulin action via induction of the transcription factor peroxisome proliferator activated receptor gamma (PPARγ) which is a key regulator of adiposity(Barnett 2008, Lehmann 1995).Many of these drugs have side effects such as weight gain, or may not be suitable for each patient, so alternatives need to be sought, alongside an exercise and diet plan (Diabetes UK 2013). My project investigates regulation of PPARγ, and the mechanism of action of the thiazolidinedione drugs.

## 1.4 Peroxisome Proliferator-Activated Receptors

### 1.4.1 Background

Peroxisome proliferator-activated receptors (PPAR) are ligand activated transcription factors that are part of the nuclear receptor family. The name originates from the fact that ligandssuch as fibrates can induce the proliferation of intracellular peroxisomes; while their biological roles include control of differentiation, proliferation and metabolism of glucose, lipids and proteins(Juresa and Metelko 2009).They share a high degree of structural homology with the other members of the nuclear receptor family, especially in the DNA binding domain and ligand and cofactor binding domains (Michalik*et al* 2006).PPARs exist as heterodimers with a retinoid X receptor (Berger and Moller 2002), and upon ligand activation the dimer modulates transcription via binding to a specific DNA sequence element, the peroxisome proliferator response element (PPRE), in the promoter region of target genes (Michalik*et al* 2006).

There are three isoforms of PPAR, peroxisome proliferator-activated receptor alpha (PPARα), peroxisome proliferator-activated receptor beta(PPARβ), and peroxisome proliferator-activated receptor gamma (PPARγ); the first to be discovered was PPARα in 1990 (Evans, Barish and Wang 2004). Each PPAR isoform has a different set of target genes, ligands, biological functions, and different tissue expression profile(Juresa and Metelko 2009**,** Burns and Huvel2007). PPARα is highly expressed in hepatocytes, proximal tubes of the kidney, enterocytes and cardiomyocytes, all of which oxidise fatty acids. PPARβ, also known as PPARδ, is expressed ubiquitously, and PPARγ is predominantly expressed in adipose tissue.

PPARα plays a key role in energy homeostasis.During a fasting stage, fatty acids are released from adipose tissue and transported into the liver, where PPARα is robustly induced; this promotes hepatic fatty acid oxidation to generate ketone bodies and provides an energy source for peripheral tissues. Fibrates are PPARα selective agonists, and they are widely used to treat hypertriglyceridemia(Evans, Barish and Wang 2004). PPARβ also regulates energy homeostasis but also has an influence on placental and gut

development.PPARβ is the least understood of the PPARs, but PPARβ selective agonists have been found to increase HDL-C levels in diabetic mice (Berger, Akiyama andMeinke 2005). PPARγ is crucial for adipose tissue differentiation (Michalik*et al* 2006),and recent work has linked obesity and PPARγ phosphorylation to the regulation of PPARγ transcriptional activity and response to ligands (Choi et al 2010).

### 1.4.2PPARγ

PPARγ was initially characterized as the master regulator for the development of adipose cells(Tontonoz and Spiegelman 2008). It exists as two distinct isoforms, namely γ1 and γ2,which arise by differential transcription start sites and alternativesplicing (Burns and Huvel 2007); PPARγ2 is 30 amino acids longer at the N Terminus. The C-terminus of PPARγ contains the ligand binding pocket, which includes the AF2 domain that is important for the docking of co-activator proteins. The N terminus of PPARγ is the target for upstream regulatory pathways(Tontonoz and Spiegelman 2008). PPARγ2 is found at high levels in adipose tissues, while PPARγ1 is expressed more broadly, extending to the gut, brain, vascular cells, and specific kinds of immune and inflammatory cells(Michalik*et al* 2006).

### 1.4.3 Functions of PPARγ

#### *1.4.3.1 Upstream regulationof PPARγ*

The biological functions of PPARγ are wide ranging, but it is best known as a master transcriptional regulator of lipid metabolism, being required for adipocyte differentiation and modulating triglyceride accumulation in adipocytes (Distel*et al* 1987)(Ye 2011, Jones *et al* 2005). PPARγ expression is induced during the differentiation of pre-adipocytes into adipocytes (Lazar 1999), and its expression is enriched in both brown and white adipose tissue.Glucocorticoids will induce expression of C/EBP-δ promoting formation of C/EBP-δ -C/EBP-β heterodimers and transcriptional activation of the PPARγ gene (Gregoire, Smas and Sul 1998). Signalling pathways such as the hedgehog, Wnt pathways, C/EBPβ and -δ, and EBFs are upstream of PPARγ.Hormonal treatment of pre-adipose cells induces C/EBP-β and –δ, and this causes them to bind to thePPARγ promoter and induce PPARγ(Tontonoz and Spiegelman 2008).

PPARγ has many synthetic and biological ligands and modifiers.Thiazolidinediones (TZDs), or glitazones, comprise a class of compounds that reverse insulin resistance and improve the symptoms of type 2 diabetes, possiblythrough specific activation of PPARγ (Gross and Staels 2007, Lehmann 1995).However TZDs have side effects, such as oedema and weight gain; this restricts the use of TZDs, so alternativesto TZDwhich still induce PPARγ activity but with less side effects are being sought, (Gross and Staels 2007); these include regulators of SIRT1, CREB, nitrous oxide, p38, ERK and CDK5. The key endogenous ligands of PPARγ are not yet fully known (Tontonoz and Spiegelman 2008). Natural ligands including fatty acid and their derivatives, such as eicosanoids, fatty acids and eicosanoid derivatives,can activate PPARγ at micro-molar concentrations(Ye 2011).My project aimed todecipher how phosphorylation of PPARγ affects its regulation and/or activity.

*1.4.3.2 Downstream actions of PPARγ*

The activation of PPARγ promotes adipocyte differentiation through the induction of target genes that are involved in energy homeostasis (Kota, Huang and Roufogalis 2005); these include GLUT4 and PEPCK which are important for glucose and triglyceride uptake and storage (Tontonoz and Spiegelman 2008 and Kota, Huang and Roufogalis 2005), as well as many adipose specific genes.

Activation of PPARγ in adipose tissue improves its ability to store lipids and subsequently to reducelipotoxicity in muscle and liver. PPARγtarget genes encode molecules that promotelipogenesis and lipid storage; these include lipoprotein lipase(hydrolysis of lipoproteins), FATP-1 (fatty acid transporter), aP2 (fatty-acidbinding protein), CD36 (receptor for lipoproteins), glycerolkinase, and SCD-1 and SREBP-1 (regulators of sterol and fatty acidsynthesis and sterol). The lipid re-partitioningto increase the triglyceride contentof adipose tissuelowers free fatty acids and triglycerides in the circulation, liver and muscle; due to this there is an improved insulin sensitivity of these tissues (Evans, Barish and Wang 2004).

Drugs that target PPARγ alter the release of adipokines from fat, including TNF-α, leptin, resistin and adiponectin; these moleculeshave multiple metabolic

effects in other tissues in the body. TNF-α and resistin promote insulin resistance, but their expression is inhibited by PPARγ agonists. Concurrently, PPARγagonists stimulate the production of molecules such as adiponectin, which promotesfatty acid oxidation and insulin sensitivity in muscle and liver; as a result of this hepatic glucose production is reduced and muscle glucose use is increased. The PPARγ-adiponectinpathway can induce the activity of AMP-activated protein kinase, the energy sensor of the cell. This protein kinase may well be a key player in the beneficial effects of PPARγ agonists on glucose metabolism and as such represents a possible pharmacologic target for type 2 diabetes mellitus (Evans, Barish and Wang 2004).

## 1.5 Regulation of PPARγ Phosphorylation

### 1.5.1 Protein kinases

Protein kinases are enzymes that can transfer a phosphate group from a high-energy phosphate, usually adenosine triphosphate (ATP), to polypeptide, usually to serine, threonine or tyrosine residues (Daintith and Martin 2005). Protein phosphorylation mediatesa large partof signal transduction in eukaryotic cells and by modifyingkinase-substrate interactions hormones and growth factors control many cellular processes that include metabolism, transcription, cytoskeletal rearrangement, cell movement, cell cycle progression, differentiation and apoptosis.

There are eight main human protein kinase families as defined by their primary structure (Fig 1.2). The main groups linked to insulin and glucagon action are the AGC (contains PKA, PKG, PKC families), CMGC (contains CDK, MAPK, GSK3, CLK families)and CAMK (calcium/calmodulin-dependent protein kinases)families, while cell cycle, apoptosis and cell growth are associated with activity of the CMGC family; there is also a small group known as the atypical protein kinases that do not containsufficient sequence homology to the other protein kinases within the catalytic core to suggest they would code for an active enzyme. The CMGC kinases, which contain cyclin-dependent kinases (CDKs), CDK-like kinases, glycogen synthase kinases (GSK), and mitogen-activated protein kinases (MAP kinases) (Fig 1.1), were of particular interest to my work as certain members of this group have previously been proposed to phosphorylatePPARγ (Adams *et al* 1997 and see below).

AMPK has also been shown to be involved with PPARγ, being a key downstream target of the PPARs. It is an important regulator in energy metabolism, and overall, the effects of PPAR agonists on AMPK-mediated metabolic functions may contribute to the recovery of insulin sensitivity or treatment of metabolic syndrome (Lee and Kim 2010). AMPK plays a role in suppressing the expression of PPARγwhilst increasing adipocyte specific genes that are up-regulated by PPARγ;activation of PPARγimproves insulin sensitivity, whereasmoderate reduction of PPARγ activity also improves it. Fasting has been shown to cause an elevated AMP/ATP ratio and activatedAMPK activity

inadipose tissue, and AMPK shown to be involved in thefasting-induced gene regulation of adipocytes (Kajita*et al* 2008).

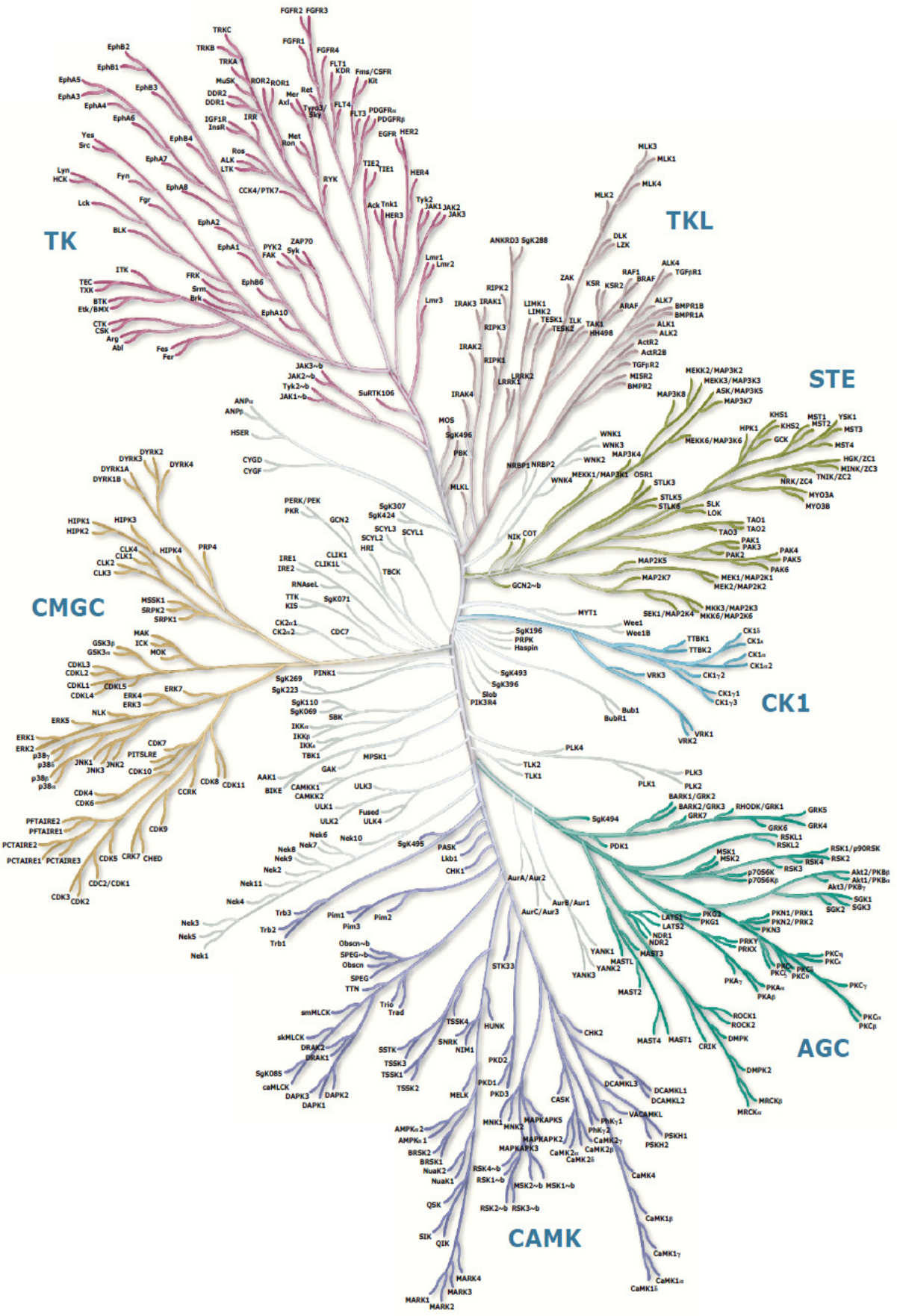


Figure 1.2 –Diagram showing the human kinome map and the known kinase families (Manning 2002)

1.5.2 PPARγ phosphorylation and function

PPARγ is a phospho-protein but as yet there are only a few reports of direct phosphorylation by specific protein kinases. Firstly,MAP kinaseswere found to phosphorylate PPARγ (Adams *et al* 1997), and this altered the transcriptional activity of both isoforms. ERK2 and JNK phosphorylated PPARγ1 at Ser84 and PPARγ2 at the homologous residue Ser112 (Adams *et al* 1997). PPARγ lacking this serine was transcriptionally enhanced both basally and in response to ligands, suggesting this phosphorylation was inhibitory. More recently the Pigment epithelium-derived factor (PEDF) induction of interleukin-10 expression in human macrophages was found to requirePPARγ and this regulation was blocked by an inhibitor of ERK (Yang *et al* 2010). In addition the ERK regulation of PPARγ was proposed as a therapeutic target in Alzheimer's Disease (Denner*et al*, 2012). However these latter studies did not establish a role for direct phosphorylation of PPARγ by a MAP kinase. In addition the connection is further complicated by the fact that ERK2 signalling may also lie downstream of PPARγ (Chen *et al* 2006). The ERK2 regulation of PPARγ clearly requires further clarification.In other work PPARγ was reported to be a CDK7 substrate and again the residue targeted was the Ser84/Ser112 (Compe*et al* 2005). These studies also demonstrated that mutation of Ser84/Ser112 altered the transcriptional activity of recombinant PPARγ, and its response to ligands.

More recently phosphorylation of PPARγ at Ser273 by CDK5 was reported by Choi *et al*(2011). They proposed that PPARγactivationwas controlled by CDK5 phosphorylation at Ser273 (PPARγ1 sequence numbering), although this sequence does not resemble the consensus sequence for phosphorylation by this kinase. Mutation of Ser273 to a non-phosphorylatable alanine did not alter the adipogenic capacity of PPARγ, but rather modified the target gene profile in obesity, including increases in adiponectin, resistin and leptin mRNA (Choi *et al* 2010). The authors showed that the phosphorylation of PPARγ by CDK5 in cells was blocked by PPARγ ligands, such as rosiglitazone and MRL24. PPARγ phosphorylation was induced by obesity associated factors (egTNFa, IL-6 and IL-10) at least in cultured 3t3-L1 cells, and this could be reduced by knockdown of CDK5 by RNAi. Moreover obesity was proposed to promote cleavage of the CDK5 regulatory subunit p35 to p25, which promotes movement of CDK5

fromthe membrane compartment to other parts of the cell including the nucleus (Fig 1.3), and increased PPARγ phosphorylation was reported in adipocytes from obese mice.Meanwhile preliminary evidence was presented to suggest that inhibition of PPARγ phosphorylation in obese patients by rosiglitazone was associated with the anti-diabetic effects of the drug; this data led the authors to propose that Cdk5-mediated phosphorylation of PPARγ may be involved in the pathogenesis of insulin-resistance, and that the CDK5 pathway provided an opportunity for an improved generation of anti-diabetic drugs that would act through regulation of PPARγ (Choi *et al* 2010). The same group has subsequently reported potent anti-diabetic actions of a novel non-agonist PPARγ ligand that works by interfering with Cdk5-mediated phosphorylation (Choi *et al* 2011). Importantly the authors indicate that their work provides an opportunity to develop ligands that would induce the insulin sensitizing actions of PPARγ without the unwanted side-effects of heart failure and oedema.

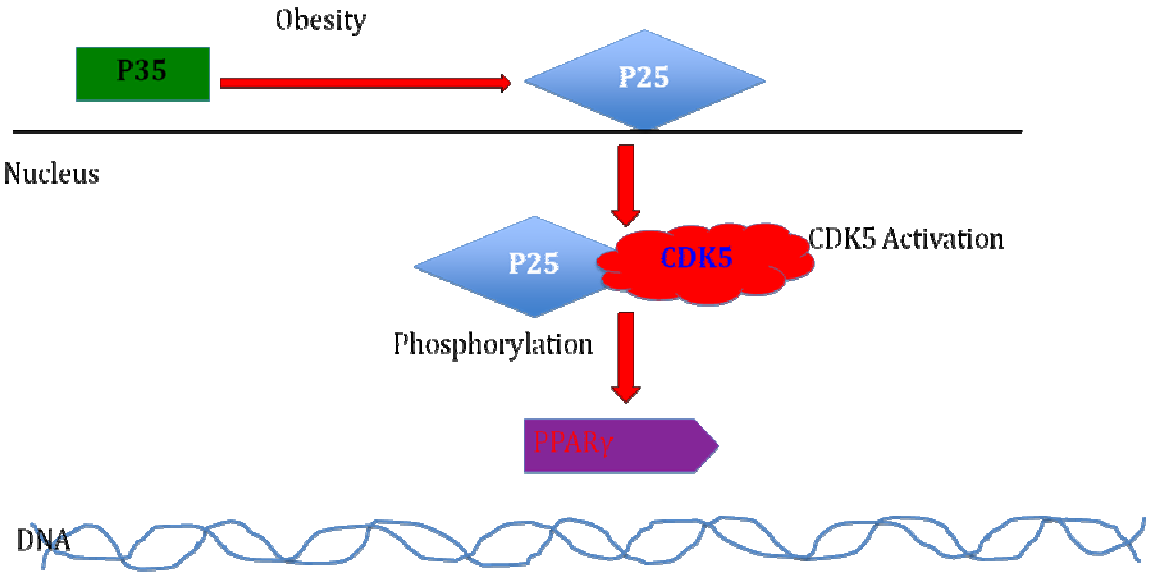


Figure 1.3– Proposed mechanism of phosphorylation of PPARγ by CDK5 and obesity, showing the cleavage of p35 to p25, the activation of CDK5 and phosphorylation of PPARγ

## 1.6 CyclinDependent Kinase 5, PPARγ and diabetes

Spiegelman and colleagues have proposed that PPARγ is regulated by cyclin-dependent kinase 5 (CDK5) during obesity to influence the development of diabetes (see above). Cyclin dependent kinases play an important role in the cell division cycle, and there are 21 genes encoding CDKs based on sequence similarity, with an additional five genes encoding for the more distant group of CDKL kinases(Malumbres*et al* 2009). These serine/threonine kinases share the unusual property of being inactive when not bound to a specificregulatory partner (Sharma *et al* 1999).

CDK5 is ubiquitously expressed in mammals (Ahmed and Sharma 2011). However it is enrichedin neurons and unlike its related kinases, it does not appear to have a role in cell-cycle control.This is because the CDK5 partner proteins p35 or p39 are notcyclins, and thus CDK5 activity does not cycle during cell division.However it has been proposed that these regulatory subunits are targeted by various cytokines and inflammatory signals that are increased in obesity and type 2 diabetes(Whitehead 2011).The details of these regulatory signals remain unclear and how they may influence the proposed neuronal functions of CDK5, including axon guidance, cell survival, regulation of synaptic spine density and neuronal migration are also not yet known. Interestingly CDK5 phosphorylates the Alzheimer's disease related protein tau and as such has been proposed as a potential drug target in neurodegeneration(Qu*et al* 2011).

CDK5 is a proline-directed kinase meaning that it will onlyphosphorylate aserineorthreonine immediately upstream of a proline residue (Dhavan and Tsai 2001). Studies using peptide substrates have suggested thatCDK5 also has a preference for a basic residue in the +3 position (ie consensus sequence (S/T)PX(K/H/R), where S/T isserine or threonine, X is any amino acid, and P is the proline in the +1 position (Songyang 1996).

CDK5 in the pancreatic islet is proposed to regulate both glucotoxicity and insulin release (Ahmedand Sharma 2011).When CDK5 activity isoverexpressed, the overall effects include decreased rates of insulin release,

reduced insulin production and diminished insulin gene expression. Insulin secretion starts whencalcium enters the beta cell through the L-VDCC in response to an enhanced level ofextracellular glucose.CDK5phosphorylates loop II and III of the *α*1c subunit of L-VDCC restraining channel activity, thereby inhibiting glucose stimulated insulin secretion(Ahmed and Sharma 2011).

## 1.7 Unanswered questions regarding regulation of PPARγby obesity and CDK5.

PPARγ2has five possible Ser/Thr-Pro phosphorylation sites within its sequence (Fig 1.4) that CDK5 could phosphorylate, but none of these are particularly close to theproposed consensus (Songyang 1996), including Ser273, the site proposed to influence obesity induced diabetes. None have the basic residues that enhance CDK5 phosphorylation, at least *in vitro*. In addition much of the data on PPARγ phosphorylation in cells was obtained using an antibody raised against a consensus CDK5 phosphorylation motif, so it remains possible that this antibody detects more than Ser273 phosphorylation. Importantly, Choi *et al* did not provide an assessment of phosphorylation stoichiometry or comparison of PPARγ phosphorylation with that of other CDK5 substrates, or by other CMGC kinases, such as ERK2 and CDK7 (see earlier). Studies with a Ser273Ala mutant PPARγ indicate changes in transcriptional function of this factor however this does not necessarily indicate that CDK5 is the only or even the major Ser273 kinase (or in fact that it is only loss of phosphorylation that mediates the difference in function of the mutant). Finally, it seems that if obesity altered CDK5 regulation that there would be many additional physiological effects on CDK5 function, since this is a relatively ubiquitous protein kinase and is known to regulate neuronal and pancreatic biology.

As such my project aimed to investigate the regulation of PPARγ by the CMGC protein kinase family in more detail, and in particular to obtain mechanistic insight into whether the obesity induction of diabetes involved both PPARγ isoforms, other CMGC kinases and required the generation of p25CDK5.

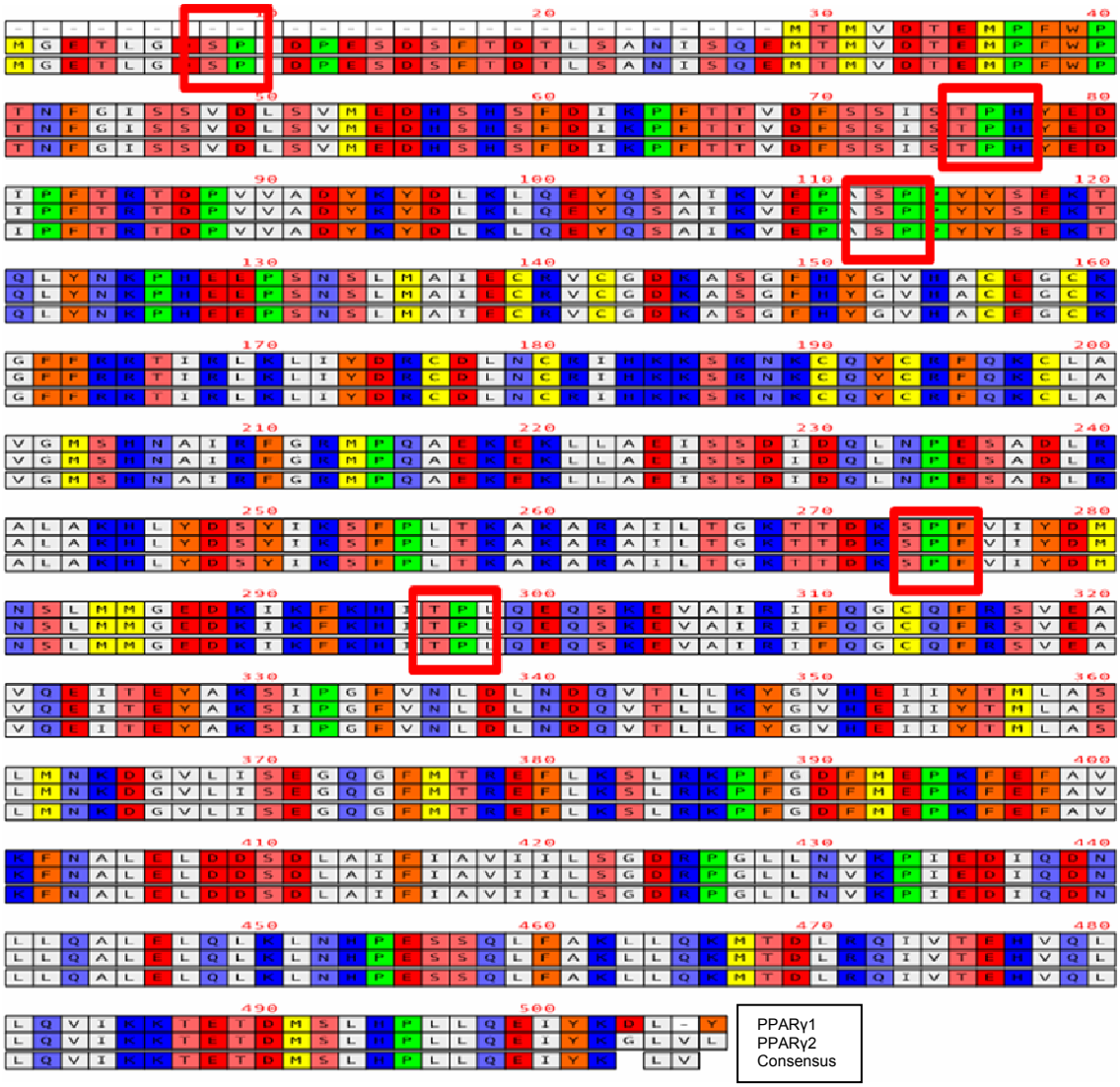


Figure 1.4- PPARγ1 and PPARγ2 sequence alignment

## 1.8 Aims of this thesis:

Overarching Aim: To establish the mechanism by whichCDK5,or a relatedCMGC kinase,links high fat and sugar diets, PPARγ and poor insulin action leading toT2DM.

Specific Objectives:

- To characterize and compare the phosphorylation of PPARγ isoforms by CMGC kinases in more detail.
- To elucidate whether Ser273 is abnormally phosphorylated in obesity
- To establish whether Ser273 is the only residue on PPARγ that is regulated by obesity
- To investigate how p35 is converted to p25 by obesity.

# Chapter 2- Materials and Methods

## 2.1 Materials:

### 2.1.1 Reagents

Listed below are the most commonly used reagents bought commercially, prepared in the lab or obtained in house during my project.

Commercial reagents

Site directed mutagenesis kit and competent cells (Agilent), nuclease free water (Ambion), precast TGX SDS-PAGE gels 10 well and 15 well, precision plus protein marker, Bradford reagent, Laemmli 4x sample buffer (Biorad), roscovitineand purvalanolA (Cal Biotech), 10x RIPA buffer, 10x TRIS lysis buffer and U0126 inhibitor (Cell Signaling), enhanced chemiluminescence (ECL) kit (G.E. Healthcare), Fetal Bovine Serum (Gibco), penicillin/streptomycin (100x), trypsin/EDTA, Topo 2.1 cloning kit and competent cells, lipofectamine 2000 reagent, plasmid mini purification kits and Simply Blue Coomassie stain (Invitrogen), autoradiography film and cassettes (Kodak), Dulbecco's Modified Eagle Medium (Life Technologies), DNA gel purification kit (Machery Nagel), CDK5/p35 14-477 and CDK5/p25 14-516 his tagged (Merck Millipore), Skimmed Milk powder (Marvel), KOD hot start polymerase chain reaction (PCR) kit (Novagen), DNA maxi-prep kit (Omega Biotek), [$\gamma$-32P]adenosinetriphosphate (ATP) and scintillation fluid (Perkin Elmer), nitrocellulose membrane, bicinchoninic acid (BCA) assay kit, subcellular protein fractionation kit (Pierce), restriction enzymes and buffers, 1kb DNA ladder, 6x loading dye, T4 ligase and buffer (Promega), protease inhibitor tablets (Roche), general laboratory chemicals, harmine, harmane inhibitor and primers for PCR (Sigma Aldrich), orthophosphoric Acid, DNA maxi purification kit (VWR), p81 paper (Whatman).

In house reagents:

*Division of Signal Transduction Therapy (DSTT)*

CDK5/p35, CDK9 his tagged, CDK7, DYRK2 GST tagged, DYRK1A GST tagged, DYRK 1B GST tagged, ERK2, ERK8, JNK1, JNK3, CLK2, HIPK1, SRPK1, GSK3$\beta$, SAPK2$\beta$, SAPK4, PCTAIRE.

Rat adipose tissue from standard chow and high fat fed was a kind gift from Dr Alison McNeilly, University of Dundee. cDNA for PPARγ1 and PPARγ2 were gifts from Professor Colin Palmer, CVDM, University of Dundee. TNFα was a gift from Dr Graham Rena, CVDM, University of Dundee

*Media Kitchen Services*

Liquid broth, agar, sterile water, phosphate buffered saline (PBS)

2.1.2 Recombinant proteins

Bacterially expressed proteins were manufactured in house by the DSTT pGEX-PPARγ and pGEX-PPARγ mutated constructs were provided to the protein production service in the DSTT. This service generated large quantities of purified PPARγ wild type and mutant protein fused to GST. In addition they produced purified PPARγ proteins lacking the GST by incubation with precision protease.

2.1.3 Antibodies

In house

PPARγ1 and PPARγ2 were both rabbit polyclonal and were gifts from Professor Colin Palmer, CVDM, University of Dundee. P-Ser273 was produced in-house and was raised against amino acid peptides based around the Ser273 residue, from the 268-278 residues, of human PPARγ where the Ser273 was chemically phosphorylated. This peptide was injected into sheep and then subsequent bleeds isolated after 3 months for 3 weeks, antibodies were purified against the antigenic peptide by DSTT.

Commercial primary

Phospho-112 rabbit polyclonal (Abcam ab60953)

Phospho-Erk rabbit monoclonal (Cell Signaling 4370)

CDK Substrate rabbit monoclonal (Cell Signaling 9477)

PPARγ mouse monoclonal (SCBT sc-7273), CDK5 rabbit polyclonal (SCBT sc-173), P35 rabbit polyclonal (SCBT sc-820), FABP rabbit polyclonal (Abcam ab-7847), actin mouse monoclonal (Sigma A8353), flag mouse monoclonal (Sigma F3165)

Commercial secondary

Goat anti-rabbitIgG IR-dye800 (Rockland Biosciences 611-132-002), donkey anti-mouseIgGAlexa-Flur 350 (Invitrogen A10035), rabbit anti-sheepIgG IR-dye800 (Rockland Biosciences 613-432-002), goat anti-rabbit IgGHRP(Thermo), rabbit anti-sheep IgG HRP (Thermo)

## 2.2 Methods:

### 2.2.1 Buffers and solutions

Table 2.1 includes the most commonly used buffers for my project and the materials they contained.

Table 2.1: Table of most commonly used buffers and solutions

| Buffer | Ingredients |
|---|---|
| Lysis Buffer (Tris) | 50mM Tris-HCl pH 7.4, 0.1mM EGTA, 1% (v/v) Triton X-100, 1mM EDTA, 1mM $Na_3VO_4$, 50mM NaF, 5mM $Na_4P_2O_7$, 0.27M sucrose, 0.1% (v/v) β-mercaptoethanol and protease inhibitor cocktail tablet |
| Hepes Buffer | 50mM HEPES, 150mM NaCl, 10% (v/v) glycerol, 1% (v/v) Triton X-100 pH 7.5 |
| NaCl buffer | 50 mMTris-HCl pH 7.4, 150 mMNaCl, 0.2 mM EDTA, and protease inhibitor cocktail tablet |
| Ripa Buffer | 20 mMTris-HCl pH 7.5, 150 mMNaCl, 1 mM $Na_2EDTA$, 1 mM EGTA , 1% NP-40, 1% sodium deoxycholate, 2.5 mM$Na_4P_2O_7$, 1 mMβ – glycerophosphate, 1 mM $Na_3VO_4$, 1 µg/ml leupeptinand protease inhibitor cocktail tablet |
| Kinase Buffer | 20mM MOPS at pH7, 1mM EDTA, 5% (v/v) glycerol , 0.01% (v/v) Brij-35, 0.1% (v/v) β-mercaptoethanol and 1mg/ml BSA |
| Tris-HCL buffered saline tween (TBST) | 50mM Tris-HCl at pH 7.5, 150mM NaCl, 0.1% (v/v) Tween 20 |
| SDS Running Buffer | 250mM Tris-HCl at pH 8.3, 1.92M glycine, 1% (w/v) SDS |
| Transfer Buffer | 48mM Tris, 39mM Glycine, 20% (v/v) methanol |
| TBST Blocking Buffer | 50mM Tris-HCl at pH 7.5, 150mM NaCl, 0.1% (v/v) Tween 20 and 5% (w/v) milk |
| Tris-HCl acetate EDTA (TAE) | 40mM Tris-HCl-acetate pH8, 100mM EDTA |
| 2 x BES | 50mM N.N-bis(2-hydoxyethyl)-2-aminoethanesulfonic acid (BES), 280mM NaCl, 1.5mM $NaH_2PO_4$ at pH 6.95 |

| | |
|---|---|
| 10 x Mg ATP | 100mM magnesium chloride and 1mM ATP |

2.2.2 Molecular Biology

*2.2.2.1 Agarose gel electrophoresis*

Agarose gel electrophoresis was a technique used to separate DNA based on molecular size. 0.8% (w/v) agarose gels were prepared by boiling 0.4g in 50ml 1xTAE buffer or 0.8g in 100ml 1xTAE buffer in a microwave oven. After cooling, 2μg/ml of intercalating ethidium bromide was added. The solution was then poured into a gel cast with separating combs and left to set at room temperature. The gel was then placed into a gel-tank and submerged in 1x TAE buffer. The 1kb DNA ladder and the samples containing 6x DNA loading dye were loaded onto the gel and the gel run for 40-60minutes at 100v. The gel was then placed under ultraviolet light to visualise the DNA/ethidium bromide complexes.

*2.2.2.2 DNA purification from agarose gel fragments*

DNA molecules (plasmids or oligonucleotides) separated by agarose gel electrophoresis were cut out of the gel and the DNA purified using the Macherey Nagel gel extraction kit according to the manufacturer's protocol.

*2.2.2.3 Polymerase chain reaction*

KOD polymerase is thermostable and possesses 3' to 5' exonuclease proofreading activity, and is used to generate PCR fragments with sticky ends. The standard PCR components and reaction cycles for each PCR reaction are listed in table 2.2 and table 2.3. The primers used for each reaction are listed in table 2.4. and they include the restriction sites needed for cloning, a flag tag for the ease of detection of PPARγ, and a Kozac sequence and ATG to initiate translation; these are all highlighted in bold at the start of each primer sequence. PPARγ2 is the product of an alternative transcription start site to PPARγ1, so a different 5' primer is needed, and different restriction enzymes were used to clone into vectors for expression in bacteria (pGEX) or mammalian cells (pCMV5). The primers to clone cDNA into pGEX contained no Kozac sequence or ATG as this vector introduces a 5'primed GST tag.

Table 2.2: Reaction Components for KOD PCR

| Component | Volume (μl) | Final Concentration |
|---|---|---|
| 10x KOD Buffer | 5 | 1x |
| 25mM MgSO4 | 4.5 | 1.5mM |
| dNTPs | 5 | 0.2mM |
| PCR grade water | 30.5 | - |
| Sense (5') Primer @ 10μM | 1.5 | 0.3μM |
| Antisense (3') Primer @ 10μM | 1.5 | 0.3μM |
| DNA | 1 | 0.22ng/μl |
| KOD Hot Start DNA Polymerase | 1 | 0.02U/μl |
| **Total Reaction Volume** | **50** | |

Table 2.3: Reaction cycles for KOD PCR

| Step | Temperature and Time |
|---|---|
| 1. Polymerase Activation | 95°C for 2 minutes |
| 2. Denature | 95°C for 20 sec |
| 3. Annealing | 60°C for 4 cycles, 70°C for 30 more for 10sec |
| 4. Extension | 70°C 30 sec |
| 5. Repeat steps 2-4 | 34x (changing annealing after 4) |
| 6. Hold | 4°C |

Table 2.4: Primers used in wild type KOD PCR reactions (non-PPARγ sequence is shown in bold, Kozac sequence is underlined and the FLAG tag is in italic)

| Template | Forward/Reverse |
|---|---|
| PPAR γ1 - CMV | 5- **GGTACCGCCACCATG*GACTACAAGGACGACGATGAC***ACCATGGTTGACAC |
| | 3-TCTAGACTAGTACAAGTCCTTGTAGATCTCCTGC |
| PPAR γ1 - PGEX | 5- **GTAGTCGACTC*GACTACAAGGACGACGATGAC***ACCATGGTTGACAC |
| | 3- CAAGCGGCCGCCTAGTACAAGTCCTTGTAGATCTCCTGC |
| PPAR γ2 - CMV | 5- **GGTACCGCCACCATG*GACTACAAGGACGACGATGAC***GGTGAAACTCTGGG |
| PPAR γ2- PGEX | 5- **GTCGACTC*GACTACAAGGACGACGATGAC***GGTGAAACTCTGGG |

*2.2.2.4 Restriction enzyme digests of PCR products and plasmid DNA*

A standard restriction enzyme digest contained 1unit of endonuclease enzyme, 1μl of 10x compatible buffer and 5μl of the DNA or PCR product to be digested with a final volume of 10μl. The solution was then incubated at 37°C for the amount of time specified by the manufacturers of the restriction enzyme being used.

*2.2.2.5 TOPO cloning*

The TOPO system is used to ligate DNA into the TOPO vector using topoisomerase I in place of DNA ligase. The topoisomerase is covalently linked to the vector and allows for a quick ligation. Using the TOPO system introduces multiple cloning sites on the vector as well as a way for the DNA to be sequenced easily. 4μl of PCR product was mixed with 1μl of salt solution (containing 0.06M $MgCl_2$ and 1.2M NaCL) and 1μl of TOPO vector and left for 20minutes at room temperature before transformation into TOP10 competent cells according to the manufacturer's instructions.

*2.2.2.6 Shrimp Alkaline Phosphatase (SAP) treatment*

DNA digested with a single enzyme needs to be treated with SAP to stop the 'sticky' overhanging stretch of unpaired nucleotides produced during digestion re-annealing with their complementary base pair and regenerating the parent DNA plasmid with no insert. Sticky ends occur due to the fact restriction enzymes digest DNA between the deoxyribose and phosphate groups, leaving a phosphate group of the 5' end and hydroxyl group on the 3' end of the DNA strands. SAP removes the phosphate overhang at the 5' end to prevent self re-ligation of linearized plasmid DNA. The plasmid DNA was incubated with 1 unit of SAP and SAP buffer for 37°C for 30minutes, and then the reaction stopped by heat inactivation of the phosphatase at 65°C for 10minutes.

*2.2.2.7 Bacterial transformations*

DH5α or XL1-Blue competent cells were thawed on ice and 50μl was aliquoted into 1.5ml eppendorf tubes. 3-5μl of DNA was added and the mixture gently flicked and placed on ice for 30minutes. The cells are then heat-shocked at 42°C for 1 minute and placed on ice. Cells then had 500μl of liquid broth added to them and they were incubated at 37°C for 1 hour. 50μl of the transformation

was spread across agar plates impregnated with ampicillin (50μg/ml) and the plates were left overnight at 37°C to allow ampicillin resistant colonies (cells containing the vector) to form.

*2.2.2.8 Ligations*

Various vector to insert ratios (for example 7μl insert, 1μl vector, 1μl 10X buffer, 1μl ligase) were tried for the ligation of wild type and mutant PPARγ1 and PPARγ2cDNA inserts into both pCMV5 and pGEX vectors. The DNA fragment and vector of choice were cut with compatible restriction enzymes and incubated together with 1 unit of T4 DNA ligase and ligase buffer in a final volume of 10μl, and the reaction left overnight at 4°C or at room temperature for 3 hours. Ligation reactions were then transformed as described in section 2.2.2.7.

*2.2.2.9 PCR Site Directed Mutagenesis (SDM)*

Site directed mutagenesis allows the incorporation of a base change into a DNA sequence to alter the amino acid in the protein sequence. The primers (shown in table 2.5) were designed to mutate specific Ser or Thr residues to a non-phosphorylatable Ala. They were identical to the wild type DNA sequence of PPARγ, except for the desired mutation around the middle of the primer. The primers were designed to be 25-45 base pairs in length, with a melting temperature of greater than 78°C with 10-15 base pairs either side of the mutation. The primers did not contain more than 40% GC content which would increase the risk of secondary structure. The standard reaction contained 5μl of 10x SDM buffer, 1μl template DNA (miniprep), 1.5μl (150ng) of each primer, 1μl of dNTPs and 1μl of PfuUltra HF DNA polymerase (2.5 U/μl) in a final volume of 50μl, and was placed in a themocyclerwith the reaction carried out according to table 2.6. Post reaction, 1μl ofDpn I restriction enzyme (10U/μl) was added and the reaction incubated at 37°C for 1 hour to digest parental doubled stranded DNA. The final product was then transformed into XL1-Blue competent cells. I generated the Ser273Ala mutant PPARγ, while constructs containing each of the other four individual phosphorylation sites for the CMGC family (proline-directed) were generated by Dundee Cell Products.

Table 2.5: Primers used for site directed mutagenesis reactions of PPARγ1 and PPARγ2

| Template | Forward/Reverse | Primer Sequence |
|---|---|---|
| PPAR γ2 - CMV | 5-GACGGGTGAAACTCTGGGAGAT**GCT**CCTATTGACC | ser8 |
| | 3-GGTCAATAGG**AGC**ATCTCCCAGAGTTTCACCCGTC | ser8 |
| | 5-TTGACTTCTCCAGCATTTCT**GCT**CCACATTACGAAGGAC | thr75 |
| | 3-GTCTTCGTAATGTGG**AGC**AGAAATGCTGGAGAAGTCAA | thr75 |
| | 5-ATCAAAGTGGAGCCTGCA**GCT**CCACCTTATTATTCTG | ser112 |
| | 3-CAGAATAATAAGGTGGA**GCT**GCAGGCTCCACTTTGAT | ser112 |
| | 5-GACAACAGACAAG**GCCCC**CATTCGTTATC | ser273 |
| | 3-GATAACGAA**TGGGGC**CTTGTCTGTTGTC | ser273 |
| | 5-CAAGTTCAAACACATC**GCC**CCCCTGCAGGAG | thr296 |
| | 3-CTCCTGCAGGGG**GGC**GATGTGTTTGAACTTG | thr296 |

Table 2.6: Themocycler steps for mutagenesis of ser273 to alanine

| Step | Cycle | Temperature and Time |
|---|---|---|
| 1. Polymerase Activation | 1 | 95°C for 30 seconds (initial denature) |
| 2. Denature | 2-16 | 95°C for 30 seconds (denature) |
| | | 55°C for 1 minute (primer annealing) |
| | | 68°C for 1 minute/kb of plasmid length (extensions) |
| 3. Final Extension | | 72°C for 7minutes |
| 4. Hold | | 4°C |

*2.2.2.10 DNA purification*

Small scale mini-preparations of DNA were produced from individual transformed bacterial colonies picked from agar plates. The colonies were transferred to 5ml of liquid broth with 50μg/ml ampicillin and grown overnight. The cells were pelleted by centrifugation at 4000g and DNA extracted as per instructions given in the Invitrogen mini-prep kit. For larger scale DNA preparations the transformed colonies were grown for 6hours in 5ml of liquid broth with 50μg/ml ampicillin, and then transferred to 200ml of liquid broth containing 50μg/ml ampicillin and shaken at 37°C overnight. The DNA was then extracted from the pelleted cells following instructions of an Omega Biotek maxi-prep kit.

*2.2.2.11 Measurement of DNA concentration*

DNA concentration was measured by absorbance at 260nm using the nanodrop (Nanodrop NP8000). Absorbance readings are performed by pipetting 2μl of the DNA solution or dilution thereof onto the NanoDrop measurement pedestals. The baseline is automatically corrected at 320nm for any baseline offsets attributable to light scattering artifacts.

*2.2.2.12 DNA sequencing and analysis*

Sequencing was carried out by The Sequencing Service, Ninewells Hospital. Macvector software was used to align and analyse DNA sequences.

2.2.3 Cell Culture

*2.2.3.1 Cell maintenance and passage*

Human embryonic kidney cells (HEK-293), HeLa cells and 3T3-L1 cells were cultured in Dulbecco's modified Eagle's medium high glucose (DMEM) with 10% fetal bovine serum (FBS) and 5% penicillin streptomycin and split when confluent with trypsin, phosphate buffered saline (PBS) and media pre-warmed to 37°C before use. The Flp-In T-Rex-293 cells were grown and treated as described in section 2.2.4.3

*2.2.3.2 3T3-L1 Cell Differentiation*

Cells were split into 6 well plates. Once confluent (day 0) the cells were placed in fresh basal medium for 2 more days (day 2) and then incubated with insulin (167nM), IBMX (0.115mg/ml) and dexamethasone (10μM) for a further 2 days. Finally the cells were incubated in insulin (167n for 2-3 days prior to placing in basal medium again for a further 2 days. The media was removed and cells either stained for lipid (Oil Red O) or lysed for measuring protein concentration and identification of proteins of interest by western blotting.

2.2.4 DNA Transfections

2.2.4.1 *Calcium-phosphate DNA precipitation inBES buffer*

Table 2.7:BES transfection protocol method

| Plate/dish | 6 well plate | 6cm dish | 10cm dish |
|---|---|---|---|
| 2x BES | 150 μl | 200 μl | 250 μl |
| Nuclease free water | up to 135μl | up to 177.5μl | up to 220 μl |
| DNA | 1 μg | 2 μg | 3 μg |
| 2.5M $CaCl_2$ | 15 μl | 22.5 μl | 30 μl |
| Volume per dish/well | 300 μl | 400 μl | 500 μl |

Nuclease free water and 2x BES buffer were combined in a 14 ml polypropylene tube as described in table 2.7 and gently flicked. The DNA to be transfected was then added to the tube with the tube being gently flicked during addition. Fresh $CaCl_2$ was added according to the volume in table 2.7 drop-wise and the tube left at room temperature for 20minutes, with gentlemixing every 2-3 minutes to allow an even precipitate to form. The precipitate was then pipetted drop-wise all over the cellswhich were thenincubated at 37°C with 5% CO2. After 4 hours fresh media was added to the cells and the plates left in the incubator for 12-20hrs.

2.2.4.2 *Lipofectamine*

DNA was introduced into cells using Lipofectamine 2000 (Invitrogen) as per manufacturer's instructions. Briefly, the DNA and lipofectamine solution were mixed together with basal media before adding this mixture to the cells. For 6 wells plates, 4μg DNA in 150μl DMEM and 6μllipofectamine in 150ml DMEM were combined and left for 10 minutes at room temperature whilst antibiotic free

media was added to the cells. The solution was then added to the cells and left for 4 hours at 37°C, prior to addition of growth media and incubation at 37°C for 12-20hrs.

2.2.4.3 *Production of a cell line with inducible PPARγ expression (FT-PPARγ)*

The Flp-In T-Rex-293 cell line can be used as a host to generate a tetracycline-inducible Flp-In T-Rex expression cell line by co-transfecting the FRT expression vector containing PPARγ(FRT-PPAR*γ*), and the Flprecombinase expression plasmid, pOG44 (O'Gorman et al., 1991). The pOG44 mediates integration of the FRT vectorcontaining PPARγ into the genome via Flp Recombination Target (FRT) sites. Flp-In T-Rex 293 cells are grown in zeocin selection media (DMEM + 10% FBS + 5% penicillin streptomycin + 100μg/ml zeocin + 15μg/ml blasticidin) and then plated in complete media (DMEM high glucose + 10% FBS + 5% penicillin streptomycin). Zeocin is used as a selective agent forthe FRT-PPARγ plasmid and blastacidin is used as a selection agent for the pOG44 plasmid. FT-PPARγ was transfected into the cells with pOG44 at a 1:5 ratio in serum free media with lipofectamine and grown in complete media overnight. Cells were passaged and media changed to HSM media (DMEM high glucose + 10% FBS + 5% penicillin streptomycin + 75μg/ml hygromycin + 15μg/ml blastacidin).Following co-transfection, the Flp-In T-Rex-293 expression clones become sensitive to zeocin,therefore the selection medium cannot contain zeocin, and instead the stable transfectants are selected using hygromycin B. The medium should still contain blasticidin for selection for the pOG44 plasmid. 24 hours before harvest, cells were treated with 1μg/ml tetracyclineto induce PPARγ expression.

*2.2.4.4 Treatment of cells with inhibitors and stimulants*

To try to induce and to inhibit PPARγ phosphorylation in cells, various stimulants and inhibitors were tried. Media was removed and the cells were incubated for 3-12hrs in pre-warmed serum free DMEM containing penicillin/streptomycin to serum-starve cells. Inhibitors and stimulants were added at the concentrations and for the times stated in the figure legends prior to cell lysis and immunoblot to measure protein phosphorylation.

## 2.2.5 Protein Isolation and Purification

### *2.2.5.1 Lysis of cells*

To harvest protein from the cells the plates were placed on ice and the media aspirated prior to wash with ice-cold PBS. Between 200μl and 1ml of freshly prepared ice-cold lysis buffer (either TRIS or RIPA, see Table 2.1) was added (depending on number of cells being harvested) and left for 5 minutes on ice. Cells were then scraped into pre-chilled eppendorf tubes, pippetted up and down and spun at 13,000g at 4°C for 10 minutes. The supernatant contained cellular protein; this was measured by the method of Bradford or BCA (see later), was snap frozen on liquid nitrogen and kept at -20°C until required.

### *2.2.5.2 Lysis of tissues –lysis buffer*

Rat adipose tissue was weighed out under liquid nitrogen. The frozen tissue was ground with a pestle and mortar under liquid nitrogen prior to addition of an equal volume of lysis buffer (TRIS, RIPA - see Table 2.1) and pippetting up and down. Alternatively, tissue was homogenized in HEPES buffer, with a hand held douncehomogeniser on ice instead of pestle and mortar. The samples were further homogenized using a sonicator for 10 minutes, and then spun at 13000g at 4°C for 30 minutes. The fat layer was removed and the protein containing supernatant was placed in a fresh eppendorf tube and spun for a further 10 minutes and any remaining lipid layer removed. Protein was measured in the samples, they were snap frozen on liquid nitrogen, and placed in a -20°C freezer until required.

### *2.2.5.3 Lysis of tissues – solvent extraction*

Rat adipose tissue was weighed out under liquid nitrogen. The tissue was pulverized under liquid nitrogen using a 2:1 solution of chloroform and methanol in a pestle and mortar. The lysate was then placed into a 15ml falcon tube and left on ice for 15minutes. A 1:1 ratio of chloroform:water was added to the lysate and solution mixed. The lysate was then spun at 800g for 5minutes at 4°C and both upper aqueous phase and protein disc collected in eppendorf tubes. 3 volumes of 10% TCA in water was added to each tube and left overnight at 4°C to precipitate protein. The pellets were then washed in acetone

to remove the TCA and left to air dry before the addition of SDS containing sample buffer for analysis by immunoblot.

*2.2.5.4 GST Purification of pGEX PPARγ*

The pGEX-PPARγ and pGEX-PPARγ mutant constructs were provided to the protein production service in the DSTT, CLS. This service generated large quantities of purified PPARγwild type and mutant protein fused to GST. In addition they produced purified PPARγ proteins lacking the GST by incubation with precision protease.

*2.2.5.5 Protein immunoprecipitation*

Antibodies that are raised against an endogenous target protein or a recombinant tag can be coupled to protein G sepharose or agarose beads; this is then used to isolate the protein of interest from cell or tissue lysates. Protein G Beads were washed in 500μlPBS and spun in a centrifuge at 2000g twice to remove ethanol. After the second spin, beads were left in a 50/50 slurry of PBS/beads. The antibody of choice was then added to the 50/50 slurry of beads (1μg antibody per 10μl beads) and incubated shaking for 1 hour at room temperature. The beads were then washed with PBS at 2000g twice. 100-500μg of sample was added to 20μl of 50/50 antibody beads and left overnight at 4°C shaking. The following day the solution was spun to pellet the beads-antibody and any associated protein and then washed with lysis buffer twice. 40μl of 1x SDS sample buffer was added to the beads and heated at 70°C for 10minutes to release protein into the sample buffer. The samples were then centrifuged at 13000g for 1 minute and the supernatant kept at -20°C.

*2.2.5.6 Covalent linkage of antibodies*

Antibody-coupled beads were prepared as described in section 2.2.5.5. The beads were then washed and spun in 500μl pH9 0.1M sodium borate twice. The beads were then re-suspended in 500μl fresh 20mM DMP in 0.1M sodium borate and shaken for 30minutes at room temperature. The tubes were then spun at 2000g and supernatant removed. The beads were re-suspended in 500μl 20mM DMP in 0.1M sodium borate and shaken for a further 30minutes at room temperature. The beads were then washed at 2000g twice with 500μl

pH2.5 50mM glycine. The beads were then washed 3x with PBS and once with 500μl lysis buffer, before re-suspension as a 50/50 slurry in lysis buffer; these beads were then used to immunoprecipitate proteins as described in section 2.2.5.5.

*2.2.5.7 Measuring protein concentration using Bradford*

Protein concentrations were measured using the Bradford method (Bradford, 1976), or using bicinchoninic acid (BCA) assay (see section 2.2.5.7). The Coomassie G-250 dye in the Bradford reagent binds to protein inan acidic environment, resulting in a spectral shift from red 465nm to blue 595nm. The more protein there is present, the darker blue the colour. A calibration curve covering 0-5mg/ml bovine serum albumin (BSA) standard was performed in triplicate in a 96well plate. Samples of unknown protein concentration were added to the plate in 200μl of Bradford reagent. After incubation at room temperature for 10minutes the absorbance at 595nm was obtained and a standard curve plotted (Fig 2.1).

Figure 2.1 - An example of a standard curve from a Bradford assay used to measure protein concentration in mg/ml

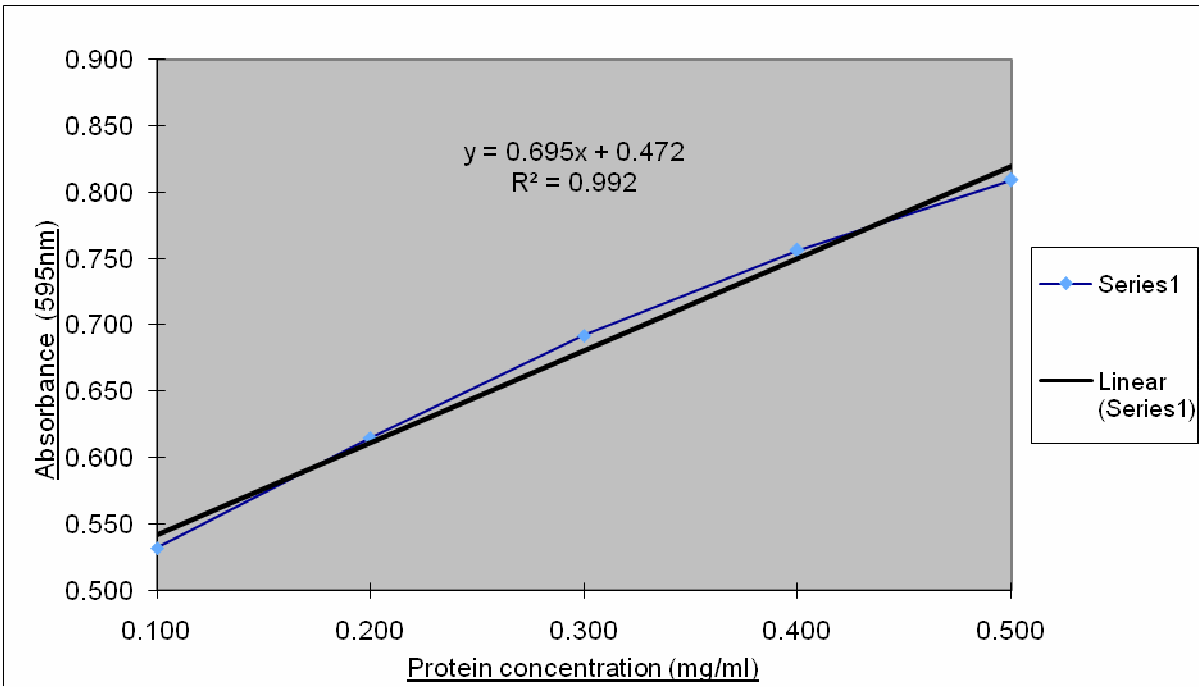

*2.2.5.8 Measuring protein concentration using BCA*

A BCA assay was needed to measure protein concentration when RIPA lysis buffer was used; this is due to incompatibility ofthe Bradford assay with the sodium dodecyl-sulphate (SDS) present in RIPA buffer. The BCA assay consists of 2 reactions. Firstly peptide bonds in any protein present in a sample cause $Cu^{2+}$in the BCA reagent to be reduced to $Cu^{+}$. Secondly, two molecules of BCAchelate with each $Cu^{+}$ion to form a purple product that absorb at 562nm. As with the Bradford assay a calibration curve of 0-2mg/ml BCA was performed along with the samples of interest. 200µl of the working reagent provided was added to each standard and sample and incubated at 37°C for 30minutes. The plate was cooled and then absorbance values read on a spectrophotometer at 562nm.

2.2.6 SDS polyacrylamide gel electrophoresis (SDS-PAGE)

SDS-PAGE is a technique used to separate proteins according to their molecular weight using an electrical current (Laemmli 1970). SDS or lithium dodecyl-sulphate (LDS) sample buffer is added to the samples to denature any protein present and to coat them with a negative charge in a uniform mass to charge ratio. The SDS buffer added to the sample also contains DTT to reduced disulphide bonds between cysteine residues, in addition to the negatively charged sulphate groups disrupting the hydrophobic amino acid interactions. After the addition of the sample buffer the samples are heated at 70-95°C for 10 minutes for further denaturing of the proteins before being loaded onto a pre-cast 4-15% Biorad gel. A molecular weight marker was also loaded onto the gel for use as an internal standard curve. The gels were then run at 120-160V with 1x SDS running buffer, with the negative charge causing the sample to move towards the positively charged electrode. Smaller proteins travel further down the gel due to their ability to diffuse through the gel pores faster.

2.2.7 Coomassie staining

Proteins present on the SDS-PAGE gels were visualised using Coomassie staining, unless they were to be transferred to nitrocellulose for western blotting (section 2.2.8). The gel was washed 3 times for 5 minutes with deionized water on a shaking platform; and then immersed in Simply Blue stain for 1 hour at

room temperature. The gel was then de-stained with water on a shaker for 1 hour at room temperature, or overnight if a more thorough de-stain was required. The coomassie dye binds to protein in the acidic environment allowing them to be visualised under visible light.

### 2.2.8 Western Blots

#### *2.2.8.1 Transfer of proteins onto a nitrocellulose membrane*

To transfer protein samples from the gel to a 0.45mm nitrocellulose membrane (Hybond C-Extra, GE Healthcare), after SDS-Page, the gel and membrane are pre-soaked in transfer buffer and a current of 35V applied for 2 hours to allow the negatively charged proteins to transfer from the gel to the membrane by moving towards the positive cathode.

#### *2.2.8.2 Immunoblotting*

Immunoblotting allows the visualization of specific proteins of interest via interaction with specific antibodies. Firstly the nitrocellulose membrane containing the transferred proteins from the SDS-PAGE above was blocked for 1 hour at room temperature in TBST blocking buffer to prevent any non-specific binding of the primary antibodies to the membrane. The blocked membrane was then incubated overnight at 4°C with the primary antibody of choice (diluted in the blocking agent) on a rolling mixer. The following day the membranes were rinsed 3 times for 10 minutes in TBST at room temperature, to remove any unbound antibody. The membrane was then incubated for 1 hour at room temperature on a shaker with the secondary antibody of interest (diluted in the blocking agent), before being washed 3 times for 10 minutes in TBST to remove any unbound secondary antibody. The membrane was then left in TBST covered at 4°C until visualisation.

#### *2.2.8.3 Visualisation*

Membranes were either visualised using the Licor Odyssey infrared detection system, or by chemilluminesence (ECL). If the secondary antibody is conjugated with horse radish peroxidase then this enzyme will generate chemiluminescent light when incubated with luminol (ECL reagent), and this can be detected on photographic film. Alternatively, if the secondary antibody is

conjugated to infrared emitting dyes the light emission can be detected directly using the Licor Odyssey scanner.

2.2.9 Preliminary Characterisation of Phosphospecific Antibody

Peptides (0.5-10ng) based around the PPARγ sequence surrounding Ser273, one with the Ser273 chemically phosphorylated were dotted onto nitrocellulose membranes. The membranes were blocked in 5% milk in TBST and incubated overnight with the phospho-specific Ser273 antibody at dilutions of 1 in 200 or 1 in 1000, followed by secondary antibody linked to HRP (Fig 2.2). The blots were then developed by ECL as described in section 2.2.8.3.

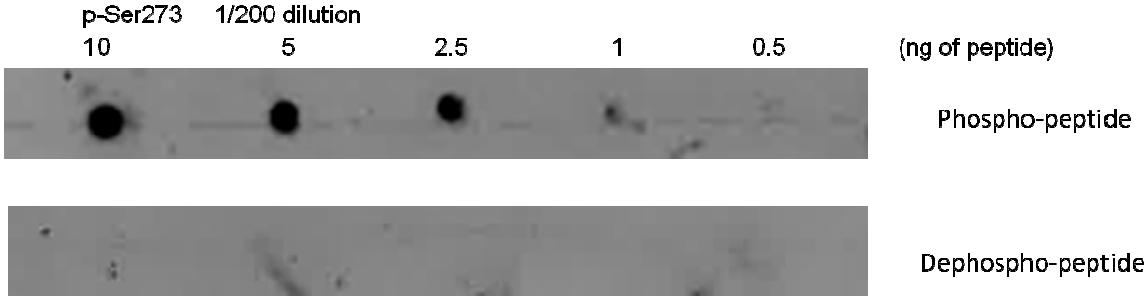


Figure 2.2 - Dot blot characterising p-Ser273 antibody using a) phosphopetide to ser273 and b) dephospho peptide to ser273

2.2.10 Kinase Assays

*2.2.10.1 Myelin Basic Protein Assay*

To measure the specific activity of a kinase before use in an *in-vitro* kinase assay, it was measured against myelin basic protein activity by incubation at 30°C with Mg[γ-32P]ATP for 10 minutes. The kinase reaction was stopped after 10 minutes by adsorption of 40μl (50μl total assay volume) onto squares of phospho-cellulose p81 paper, followed by dropping the squares immediately into 75mM phosphoric acid. The squares were then washed 3x in the phosphoric acid to remove any unincorporated Mg[γ-32P]ATP. A final wash in acetone dried the squares before they were placed in a scintillation vial for counting as described in section 2.2.10.2

*2.2.10.2 In-vitro kinase assay*

Active CDK5/p25 and active CDK5/p35 were purchased from Milllipore. GST and cleaved wild type and Ser273Ala PPARγ1 and PPARγ2(5μM) were incubated (60μl assay) with each CDK5 complex plus Mg[γ-32P]ATP (10mM

MgCl2, 0.1mM ATP, approx 0.5 x $10^6$ CPM/nmole) or non-radioactive MgATP, in kinase assay buffer (20 mM Mops, 1mM EDTA, 5% glycerol, 0.01% Brij-35, 0.1% β-mercaptoethanol, and 1mg/ml BSA). After10, 30, 60 and 180 minutes at 30°C equal aliquots of the sample were taken and the reaction stopped with appropriate amounts of 4x SDS sample buffer and heating for 10 minutes at 95°C. CDK5 was added at the activity indicated in the figure legends. When other CMGC kinases were used, the specific activities were matched using myelin basic protein (MBP) as a common substrate and an equal amount of units of MBP kinase activity used in the assay but in a 30μl assay volume for 30 minutes. The [Ser8Ala]PPARγ, [Thr75Ala]PPARγ, [Ser112Ala]PPARγ, and [Thr296Ala]PPARγ proteins were all incubated with the CMGC kinases at 5μM.

*2.2.10.3 Phosphorylation measurements*

The reactions from above were loaded on a precast Biorad 4-12% SDS-PAGE system to separate the phosphorylated substrate from other assay constituents. Gels were Coomassie stained, dried and visualised by autoradiography and phospho-image analysis. Phosphorylation was quantified by carefully cutting gel pieces containing the stained PPARγ and counting in 2ml of scintillation fluid. The number of nanomoles of ATP transferred into protein was calculated from the specific activity of the ATP used in the reaction and this was used to establish the mole per mole incorporation or the specific activity of the kinase toward the substrate. One unit of activity is defined as 1 nanomole of phosphate incorporated into substrate per minute. The [Ser8Ala]PPARγ, [Thr75Ala]PPARγ, [Ser112Ala]PPARγ, and [Thr296Ala]PPARγ mutant proteins were analysed for degradation by SDS-PAGE and Coomassie staining. Densitometry was used to correct for variations in degradation between the mutant proteins. Briefly, 2μg of each protein was loaded onto a precast Biorad 4-12% SDS-PAGE system in duplicate, and the gels Coomassie stained and scanned on the Odyssey system. The CB signal ratios of the upper (full length protein) to lower bands (degradation products), total signals and ratios relative to the wild type PPARγ were calculated, and counts normalized to the wild type; this was repeated to get an average result for the normalization across three separate gels.

2.2.11 Statistics

The statistics throughout this thesis were based on the range, rather than standard deviation and the coefficient of variance,due to the availability and stability of the CMGC kinases. The error bars were based on a range of n=2.

# Chapter 3 -*In vitro* Assessment of PPARγPhosphorylation

## 3.1 Introduction

Previous work implicated the phosphorylation of PPARγ at Ser273 by CDK5 as a molecular link between obesity and diabetes, as well as the response to glitazone therapy (Choi *et al*). However this work raised multiple questions including how obesity regulated CDK5, and indeed why CDK5 would phosphorylate Ser273, which did not fit a consensus sequence for this kinase.Others have shown that additional CMGC kinases can phosphorylate PPARγ (Camp and Tafuri 1997); albeitthese are likely to phosphorylate PPARγ at ser112 (Adams *et al* 1997).

In order to fully establish whether PPARγ was truly a target for CDK5 or a related kinase in this Chapter I have performed a series of in vitro experiment to address the following aims:

- To establish whether CDK5 phosphorylates PPARγ*in vitro*
- To identify the residues phosphorylated by CDK5
- To compare the rates of PPARγ phosphorylation between each CDK5 complex
- To compare PPARγisoforms phosphorylation
- To establish whether other CMGC kinases phosphorylate PPARγ*in vitro* and if so at what residues

## 3.2 Results

### 3.2.1.CDK5 phosphorylation of wild type PPARγ1 and PPARγ2

To investigate the potential for PPARγ to act as a substrate for CDK5 complexes *in vitro* I measured phosphate incorporation into bacterially expressed PPARγ1 when it was incubated with either CDK5/p35 or CDK5/p25 (after activities were matched against histone) and [γ-32P]-ATP. CDK5/p35 phosphorylated a GST-PPARγ1 fusion protein faster and to greater extent than CDK5/p25 (Fig 3.1). In order to ensure that this difference was not due to the presence of the GST I repeated the experiment using a PPARγ1 protein after the GST was removed by proteolytic cleavage. Once more CDK5/p35 phosphorylated PPARγ1 faster and to greater extent than CDK5/p25 (Fig 3.1). Phosphorylation reached around 0.1 to 0.2 mole/mole within 10 to 30 minutes, and the GST tag did not seem to alter overall phosphorylation.

Next I compared phosphorylation of GST-PPARγ1 to that of GST-PPARγ2 with both CDK5 complexes (Fig 3.2). CDK5 phosphorylated each GST-PPARγ to a similar extent (0.1 to 0.2 mol/mol within 30 mins) and as with PPARγ1 CDK5/p35 phosphorylated GST-PPARγ2 to a greater extent than CDK5/p25 (Fig 3.2).

Figure 3.1:*In vitro* phosphorylation of PPARγ by CDK5 complexes (1006mU, n=2). WT; wild type PPARγ, 35; CDK5/p35 complex, 25; CDK5/p25 complex, error bars represent the range.

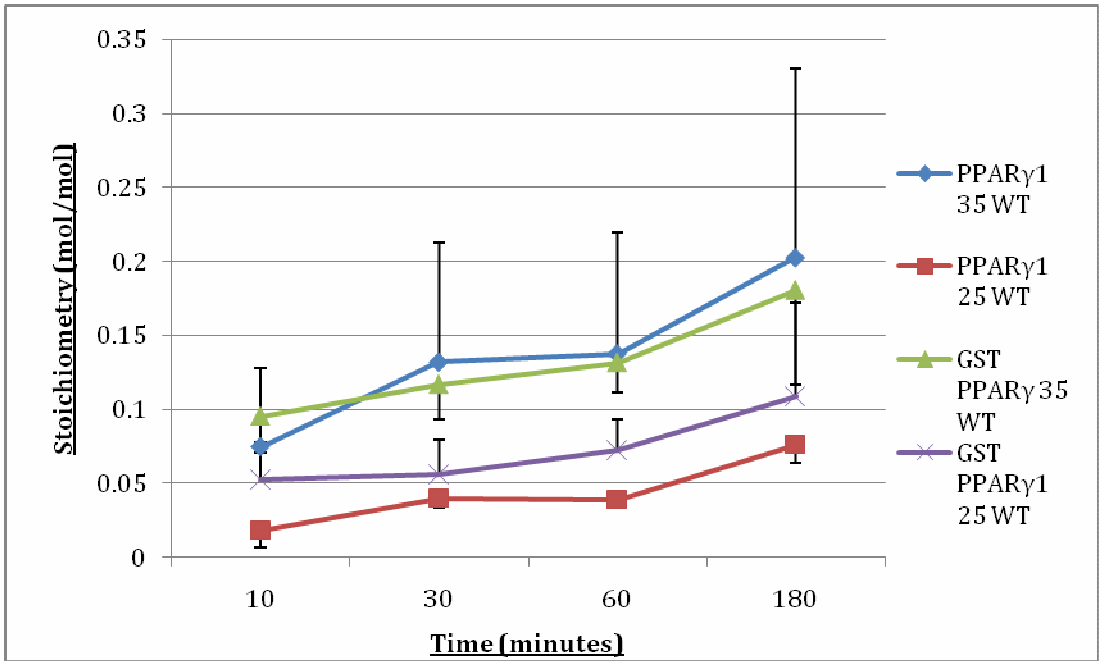

Figure 3.2:*In vitro* phosphorylation ofGST PPARγ1 and PPARγ2 by CDK5 complexes for 30 minutes (1006mU, n=2) p35; CDK5/p35 complex, p25; CDK5/p25 complex, error bars represent the range

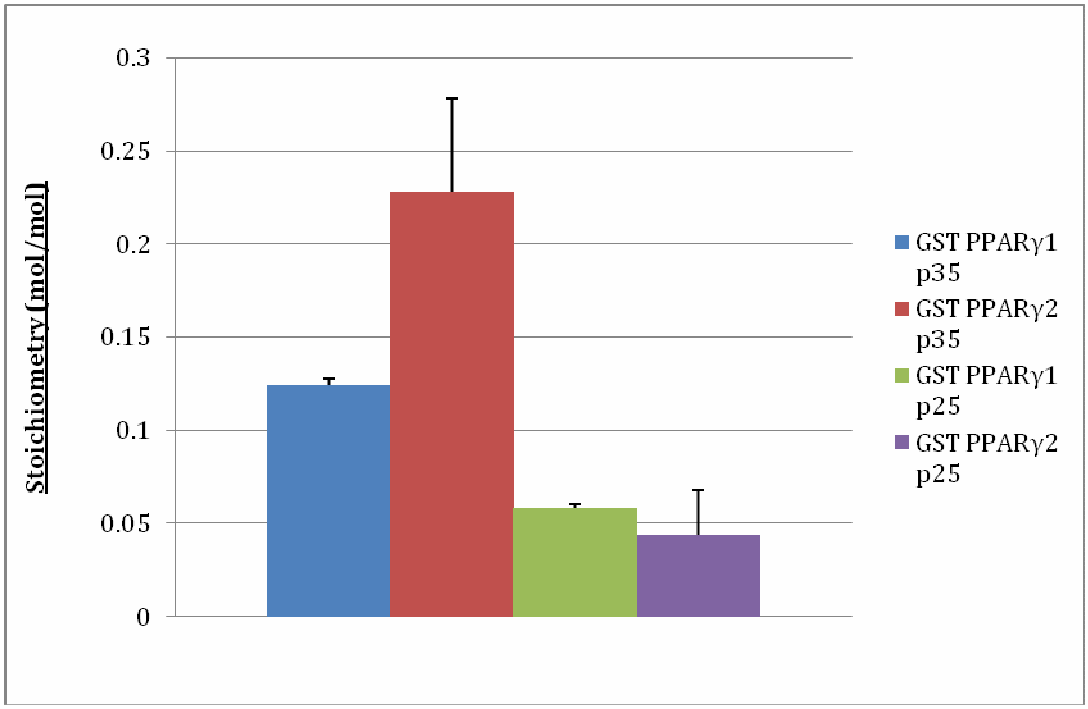


### 3.2.2 Investigation into CDK5 phosphorylation of Ser273

Next I investigated how much of the phosphate incorporated into PPARγ by CDK5 was going into Ser273. I compared the phosphorylation of wild type PPARγ1 to that of the [Ser273Ala]PPARγ1 mutant, by both CDK5/p35 and CDK5/p25, for both GST and cleaved PPARγ1; to confirm the mutation was present, the mutated protein was sequenced and compared to the wild type. Once more CDK5/p35 phosphorylated PPARγ1 to a greater extent than CDK5/p25 (Fig 3.3, Fig 3.4). There was no greatdifference in phosphorylation of GST-PPARγ1 and GST-[Ser273Ala] PPARγ1 by either CDK5 (Fig 3.3 and Fig 3.4). CDK5/p35 phosphorylation of the GST-[Ser273Ala] PPARγ1 was lower than that of GST-PPARγ1, but the decrease did not show a statistical trend. In addition phosphorylation of PPARγ1 wild type and [Ser273Ala]PPARγ1 lacking the GST tags (cleaved) was identical with both CDK5/p25 and CDK5/p35 (Fig 3.4). The fact mutation of Ser273 to an alanine has no great effect on phosphorylation of the PPARγ1 suggests this is not a target for CDK5, at least *in vitro*.

Figure 3.3: *In vitro* phosphorylation of GST-PPARγ1 wild type and [Ser273Ala] PPARγ1 mutant by CDK5 complexes (1006mU, n=2) WT; wild type, Mut; Ser273Ala, p35; CDK5/p35 complex, p25; CDK5/p25 complex, error bars represent the range

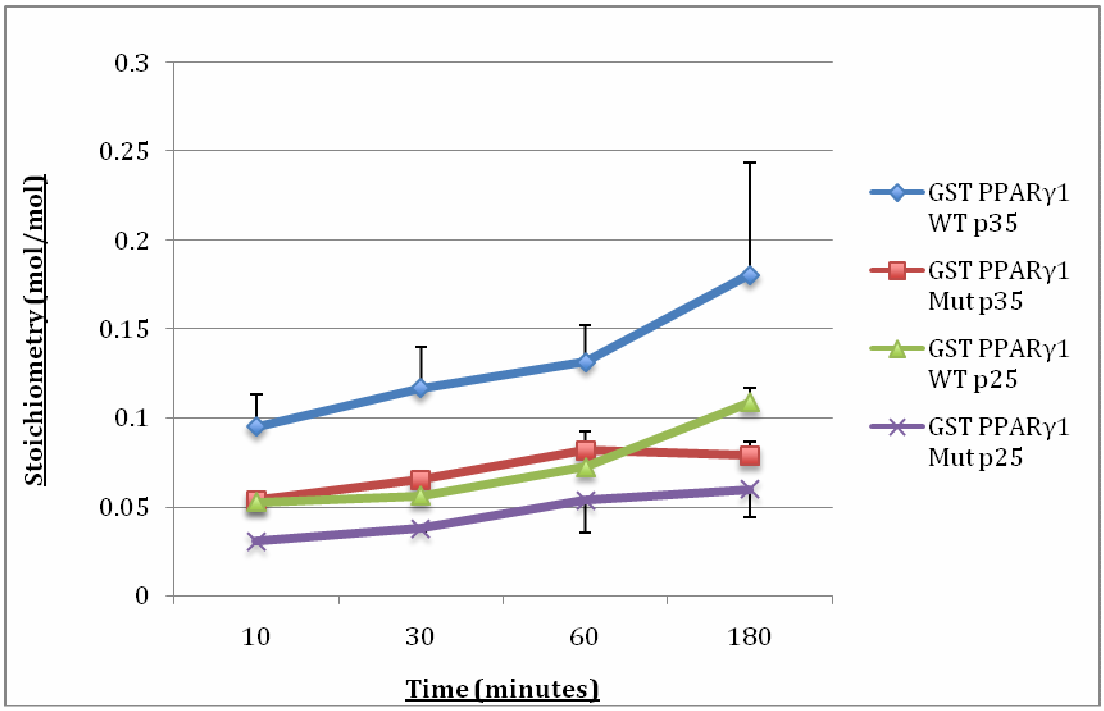


Figure 3.4: *In vitro* phosphorylation of cleaved PPARγ1 wild type and [Ser273Ala] PPARγ1 mutant by CDK5 complexes (1006mU, n=2). WT; wild type, Mut; Ser273Ala, 35; CDK5/p35 complex, 25; CDK5/p25 complex, error bars represent the range

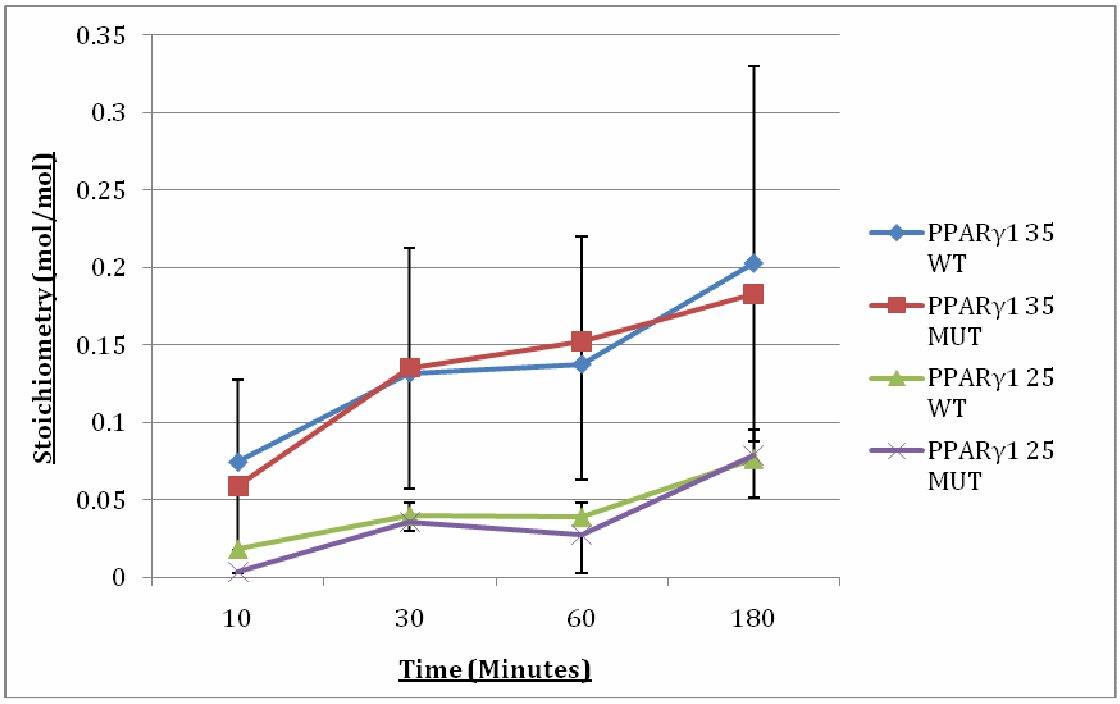

To further confirm this I incubated FLAG-tagged PPARγ1 and PPARγ2 with non-radioactive ATP and either CDK5/p25, CDK5/p35, or ERK2. ERK2 is reported to phosphorylate PPARγ at Ser112 (Adams *et al* 1997). These incubations were probed by immunoblot using antibodies to FLAG (for loading), phospho-Ser122 and phospho-Ser273. As expected, incubation with ERK2 induced phosphorylation of Ser112 in both PPARγ isoforms (Fig 3.5). Incubation of PPARγ1 and PPARγ2 with either CDK5/p25 or CDK5/p35 did not increase phosphorylation of either Ser112 or Ser273, providing further evidence that CDK5 does not phosphorylate PPARγ at Ser273 and that the phosphate incorporation by CDK5 is also unlikely to occur at Ser112. Similarly ERK2 does not phosphorylate Ser273 of PPARγ (Fig 3.5). The caveat to this experiment is that we have not yet obtained a positive control of phosphoSer273 PPARγ to validate the phospho specific antibody. The antibody has, however, been tested with phospho and non phospho peptide incubations as shown in the dot blots (fig 2.2); any signal picked up might be non-specific background due to the lack of positive control.

Figure 3.5: Immunoblot of GST-Flag-PPARγ1 and PPARγ2, following incubation with CDK5/p35, CDK5/p25 or ERK2 using antibodies as indicated (MW ~80KD). Control is PPARγ1 or PPARγ2 alone.

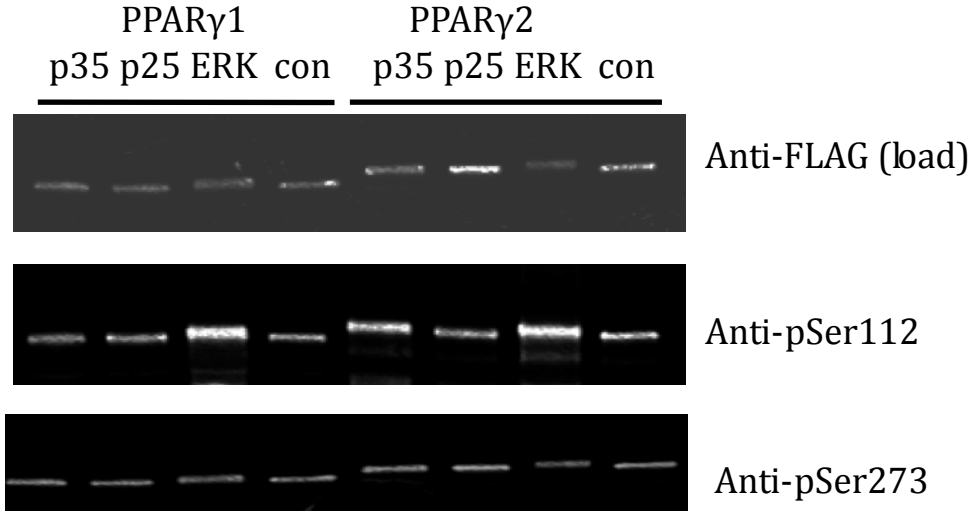

3.2.3 Phosphorylation of PPARγ2 by other CMGC kinases

Although my data above indicated that CDK5 did not phosphorylate Ser273 of PPARγ it remained possible that the reported regulation of this site was actually by a related kinase. Therefore I investigated whether other GMGC kinases could phosphorylate GST-PPARγ2 and GST-[Ser273Ala]PPARγ2*in vitro*. PPARγ2 was chosen for the kinase screen as it contains all of the proline directed sites (potential targets of this family of kinases) present in PPARγ1, plus an additional site within the N-terminal extension. This allowed me to investigate whether any of the CMGC kinases phosphorylated any of the 5 potential proline-directed residues in PPARγ (see Fig 1.3). I was able to source a range of CMGC family members, and tried to include at least one from each major subgroup of the CMGC kinases (unfortunately the SRK group were not available). Of the 17 kinases investigated (Fig 3.6) eight phosphorylated PPARγ2, namely ERK2, ERK8, DYRK1A, DYRK1B, DYRK2, SAPK4, CDK9 and CDK5. However all of the kinases phosphorylated [Ser273Ala]PPARγ2 to a similar extent to the wild type PPARγ2 (Fig 3.6). It should be noted that for some of the kinases the inherent autophosphorylation meant that accurate assessment of PPARγ2 phosphorylation was difficult; for example compare – lanes with + lanes for DYRK2, ERK2 and ERK8 (Fig 3.7). In all cases the radioactivity in the – lane (in the PPARγ2 gel piece) was subtracted from the + lane to account for background due to autophosphorylation of the kinase.

Each of the CMGC kinases that radiolabelledPPARγ2was then incubated with GST-Flag-PPARγ2 and non radioactive MgATP, followed by western blot with PPARγ, CDK substrate, p-Ser273and p-Ser112 antibodies; in order to examine whether any of the kinases phosphorylate either of these residues, while anti-PPARγwas used as the loading control. The results confirmed that ERK2 phosphorylates PPARγat Ser112, while DYRK2 and SAPK4 also phosphorylated Ser112 (Fig 3.8). ERK8, DYRK1A, DYRK1B and CDK9 did not phosphorylate PPARγ at Ser112 (Fig 3.8). None of the kinases appeared to induce phosphorylation at Ser273 to a great amount, at least as detected by this phosphospecific antibody. In addition, PPARγ incubated with ERK2 or the DYRKs was detected weakly by the cdk-substrate antibody(Fig 3.8), but as it

did not detect PPARγ incubated with SAPK4 it seems unlikely this antibody detects Ser112 phosphorylation.

Figure 3.6: CMGC Kinase Screen with activity matched to myelin basic protein and incubated with PPARγ2 wild type and [Ser273Ala]PPARγ2(x, n=2)

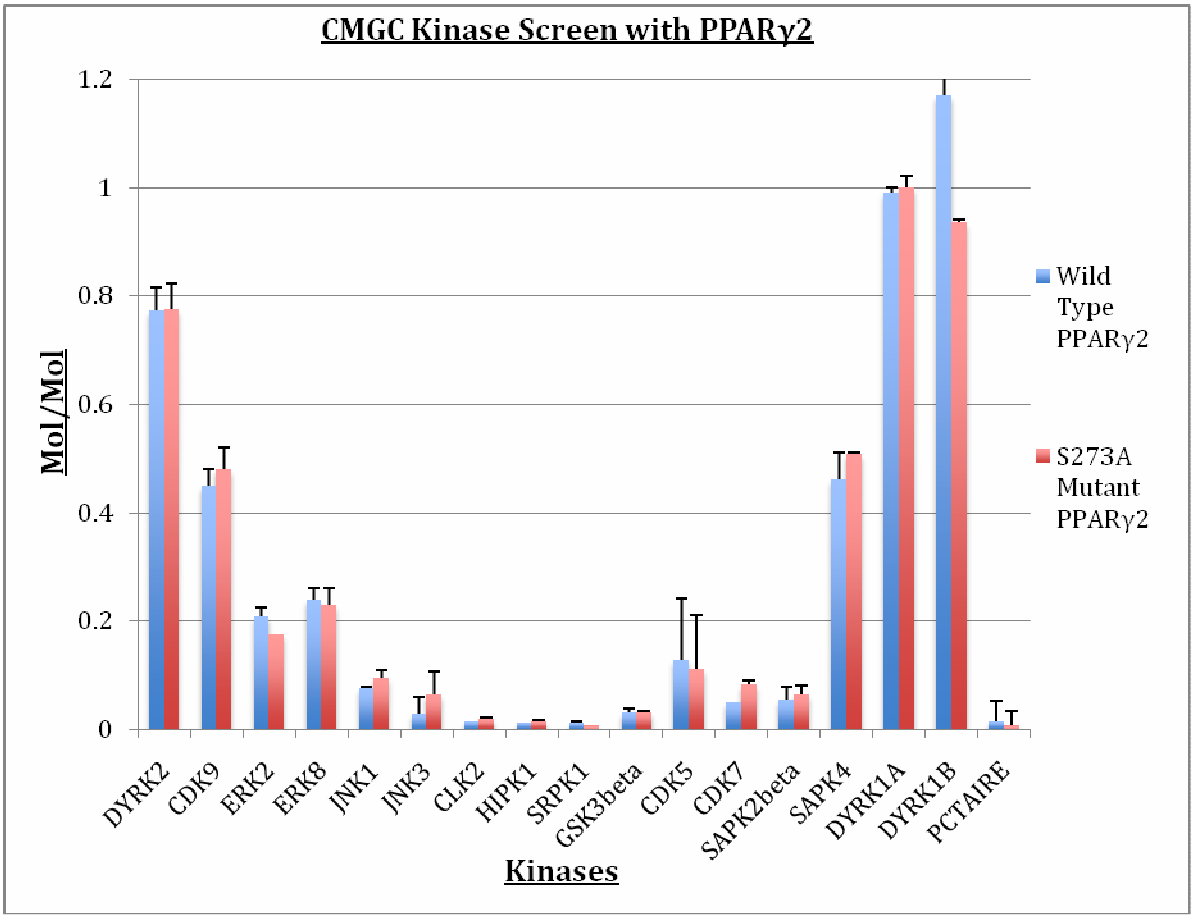


Figure 3.7: Autoradiograph showing examples of the data used to generate Fig 3.6. Incubationswere Mg[32P]ATP plus kinase alone (-) orkinase + PPARγ2 (+) as indicated.

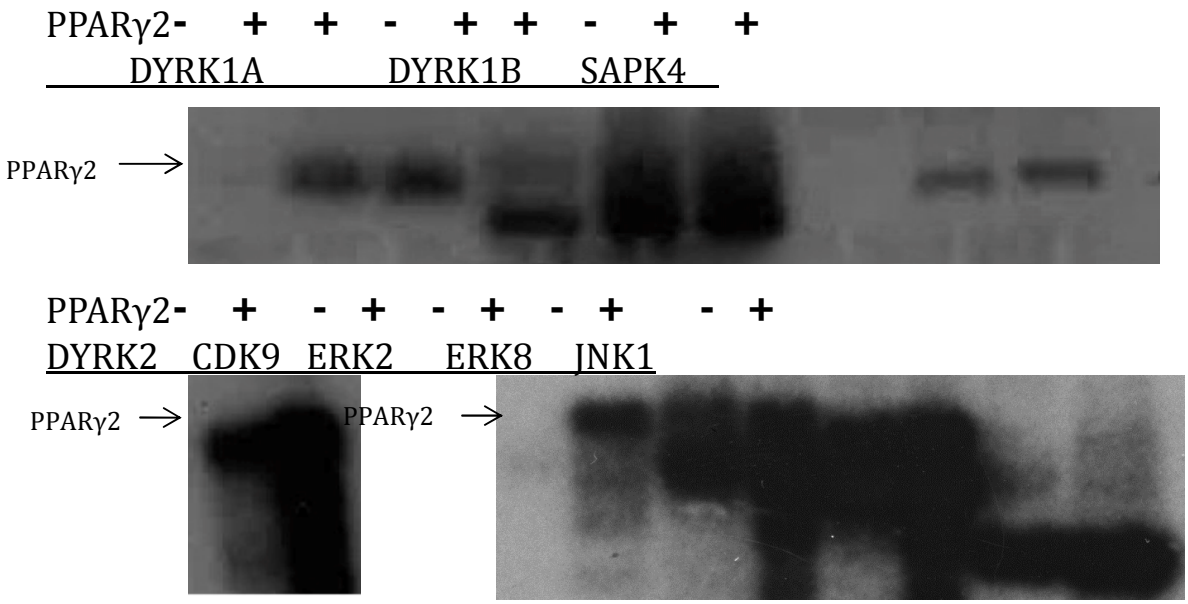

Figure 3.8: CMGC kinases that phosphorylatedPPARγ2were incubated with non radioactive MgATP and GST-Flag-PPARγ2 followed by western blot with PPARγ, CDK substrate, p-Ser273 and p-Ser112 antibodies as indicated (MW ~80KD). Control is PPARγ2 alone and band intensity is compared with control to see any increase in phosphorylation

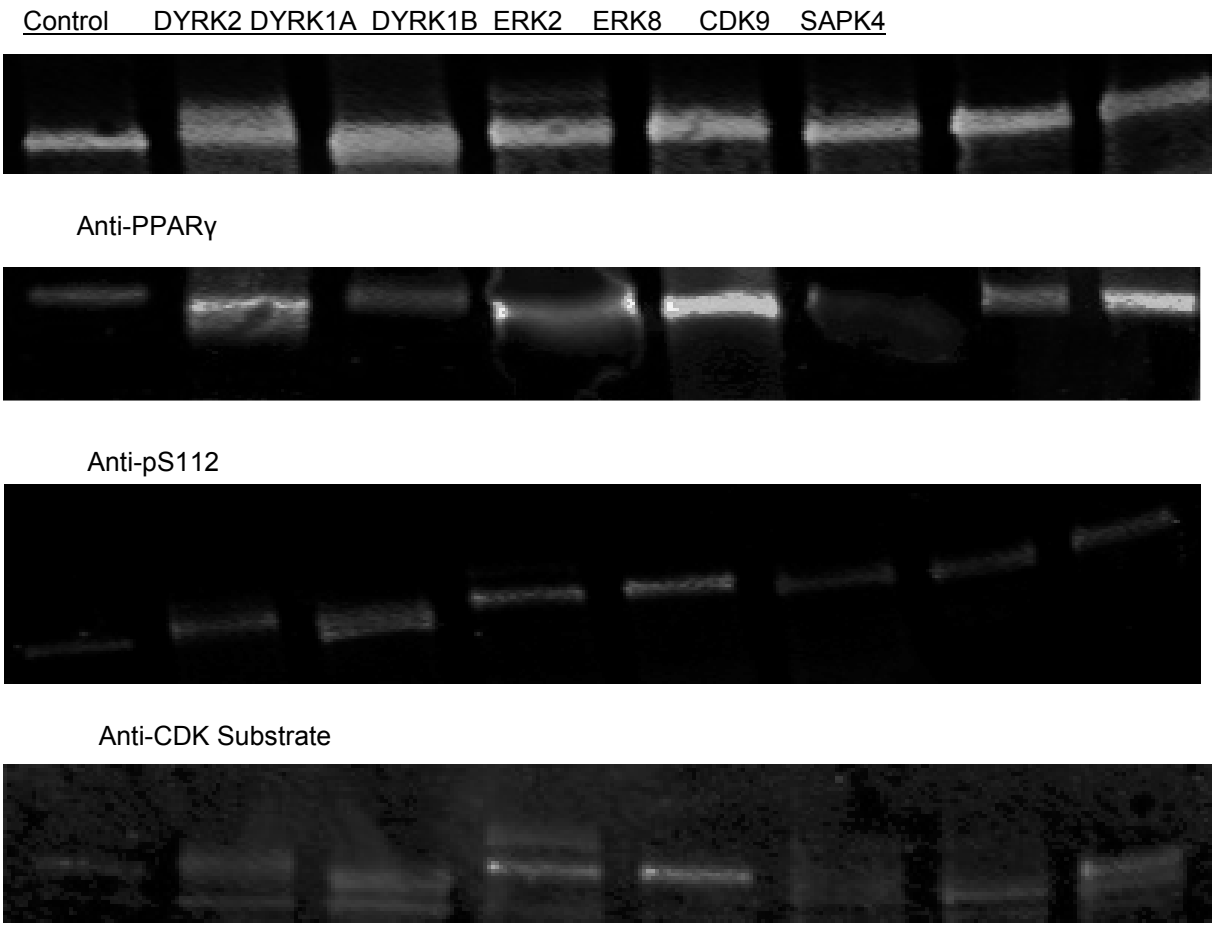

### 3.2.4 Proline Directed Phosphorylation of PPARγ2

There are five sequences within human PPARγ that conform to a minimum consensus for the CMGC family of protein kinases, namely a Ser or Thr residue immediately followed by a Pro (Fig 1.3). These lie at Ser8, Thr75, Ser112, Thr296 and Ser273. We generated PPARγ2 mutants with each of these five Ser/Thr residues changed to a non-phosphorylatableAla residue and incubated them (only [Ser8Ala]PPARγ, [Thr75Ala]PPARγ, [Ser112Ala]PPARγ, and [Thr296Ala]PPARγ as Ser273Ala PPARγ was investigated earlier),with the CMGC kinases from section 3.2.3.

Unfortunately, there was variable degradation of the recombinant proteins during the purification process, (as visualised by Coomassie stain, Fig 3.9) thus I had to perform a normalisation to correct for the presence of different amounts of full length protein in each sample (Fig 3.9 and Table 3.1). The degradation was calculated by looking at the averages of the signals of PPARγfrom the Odyssey, the total signal of the upper (full length PPARγ) and lower (degraded PPARγ) bands, the ratio of the upper bands to lower bands and the ration of 1 to the upper band.The [Thr75Ala]PPARγ mutant protein in particular had relatively low levels of full length protein thus data with this mutant is treated with caution. The degradation was easily accounted for on the autorads, as the PPARγ2bands seen further down the Coomassie stain with lower molecular weights than full length PPARγ2, were also visible on the autorad after incubation with the various CMGC kinases.

After correction for relative amount of full length PPARγ2 there was no indication that phosphorylation of any mutant varied from that of wild-type following incubation with CDK5/p35 (Fig 3.10A). There is less radioactivity incorporated into the [Thr75Ala]PPARγ, [Ser112Ala]PPARγ, and [Thr296Ala]PPARγ mutants compared with wild type PPARγ2 (Fig 3.10B), however after accounting for the variability in degradation of the substrates there was no evidence that these mutations significantly prevented phosphorylation (mole/mole). It is possible that further investigation of Thr296 is merited as in one of the two experiments (Fig 3.10B) there appeared to be lower phosphorylation (levels of full length Thr296Ala are similar to Ser8Ala,

compare phosphate incorporation of these two mutants), but this was not seen in the second experiment. Similarly the only PPARγ2 mutant that appeared poorly phosphorylated by CDK9, was [Thr296Ala]PPARγ (compared to wild type and Ser8Ala phosphorylation, Fig 3.11A and B).

Mutation of Ser112 of PPARγ2 to an Alagreatly reducedphosphorylation by ERK2 (Fig 3.12A and B) consistent with the data in section 3.2 and published data (Adams *et al* 1997) indicating that ERK2 phosphorylates PPARγ at Ser112. However the phosphorylation of PPARγ was not completely depleted by this mutation, suggesting some phosphorylation of alternative site(s) and combinatorial mutations would be required to assess this.

Phosphorylation by ERK8 is relatively weak compared to the other kinases studied here, making it very difficult to interpret the result of the point mutations (Fig 3.13A and B). The molecular weight of the ERK8 used was relatively close to that of PPARγ2, as is seen on the autorad in figure 3.13B, so the ERK8 might be interfering with PPARγ2 bands analysed.The Ser112Ala mutation appeared to reduce phosphorylation in one experiment but this was not seen consistently and earlier data using immunoblot had indicated this is unlikely to be a major target for ERK8 (Fig 3.8).

Confusingly, phosphorylation of both [Ser112Ala]PPARγand [Thr296Ala]PPARγby SAPK4 was reduced compared to the wild type (Fig 3.14A and B); this could be dues to issues with the degradation of the mutated PPARγ2. The immunoblot work from section 3.1.3 also suggested SAPK4 could phosphorylate Ser112, thus this seems to be a likely target for SAPK4. However it remains feasible that SAPK4 may also phosphorylate Thr296, or this region is involved in the interaction with SAPK4.

Auto-phosphorylation of DYRK2 resulted in high background radioactivity in the region of the gels used to assess the phosphorylation of PPARγ2 (Fig 3.15).Another issue with DYRK is that it lies very closely in molecular weight to PPARγ2, making it hard to distinguish from PPARγ2 on an autorad. To try to solve the auto-phosphorylation problem, I pre-incubated DYRK2 with non-radioactive ATP for 30minutes in an attempt to induce non-radioactive auto-

phosphorylation and thus decrease background radioactivity in these incubations. Subsequent phosphorylation of the [Ser112Ala]PPARγby DYRK2 appeared lower than wild type protein (Fig 3.16A and B), again agreeing with the immunoblot data in section 3.1.2. In contrast DYRK1B seemed to phosphorylate all of the PPARγ2 mutants, making it hard to establish which site may be targeted by these kinases (Fig 3.17A and B), and combinations of mutants may be needed to fully characterize this phosphorylation. DYRK1A incubation with the PPARγ2 mutants proved hard to get consistent results due to the high level of auto-phosphorylation, so the data is not included.

Figure 3.9: Coomassiestained SDS-PAGE gelof the GST-PPARγ2 mutants (upper gel), with lower gel showing areas quantified to generate the normalization ratios in Table 3.1. WTPPARγ2Ser8AlaThr75AlaSer112AlaThr296Ala

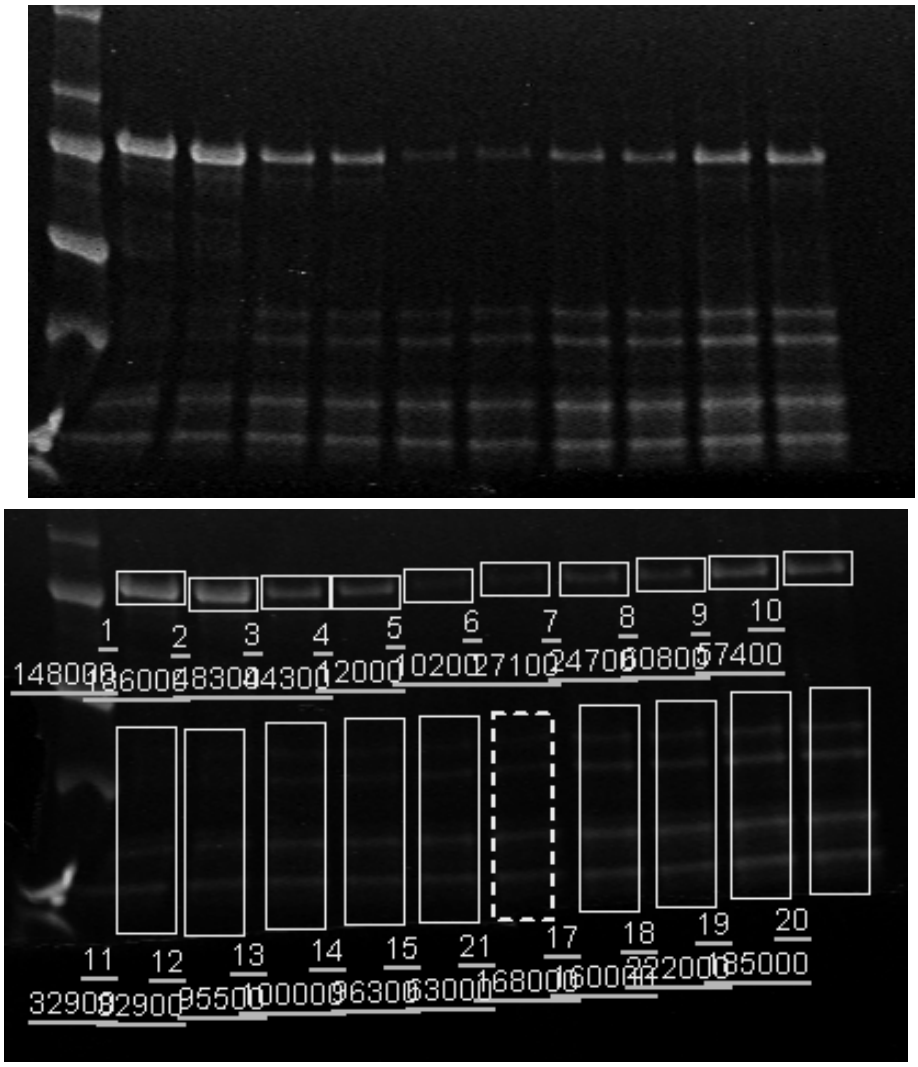


**Table 3.1: Normalization ratios to account for variable degradation of the GST-PPARγ2 mutants**

| Protein | Normalisation for degradation |
|---|---|
| Wild Type PPARγ2 | 1 |
| S8A PPARγ2 | 2.8 |
| T75A PPARγ2 | 11.1 |
| S112A PPARγ2 | 5.3 |
| T296A PPARγ2 | 3.5 |

Figure 3.10: (A) Graphical representation ofmol/mol stoichiometry of PPARγ2 mutants byCDK5 and (B) arepresentative autoradiograph of phosphorylation of PPARγ2 mutants, including control CDK5 alone lane (no PPARγ2 present)

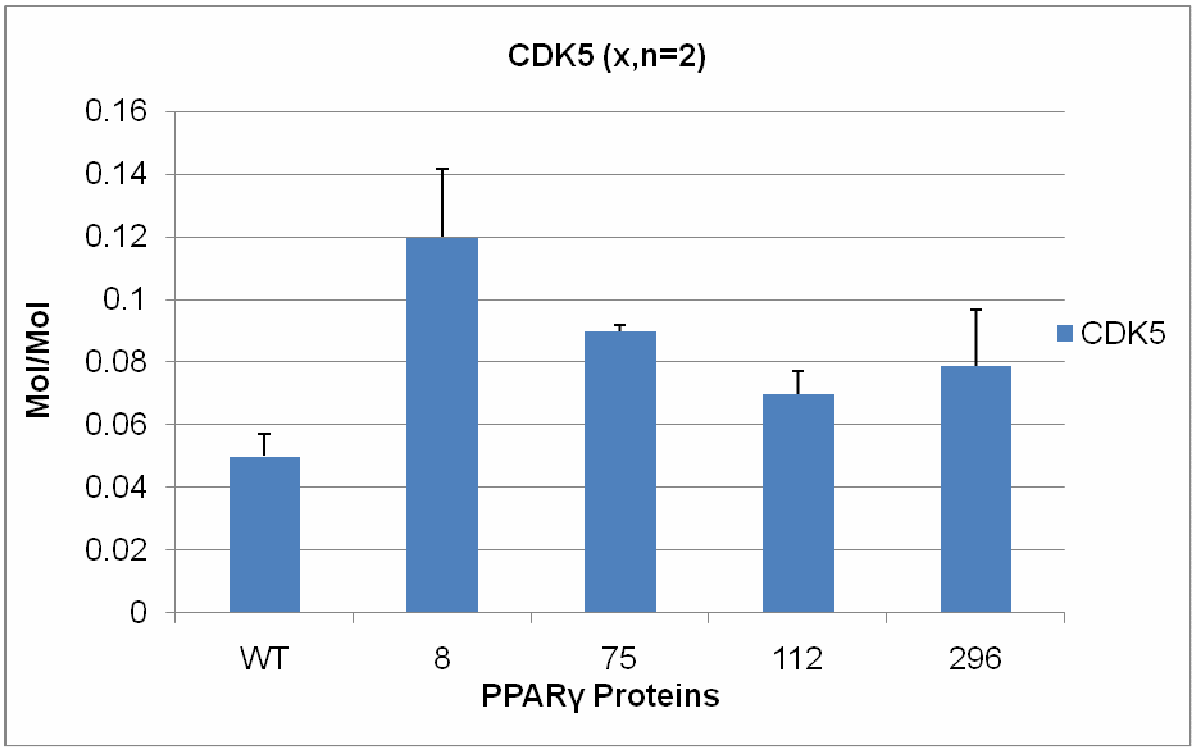


A

B

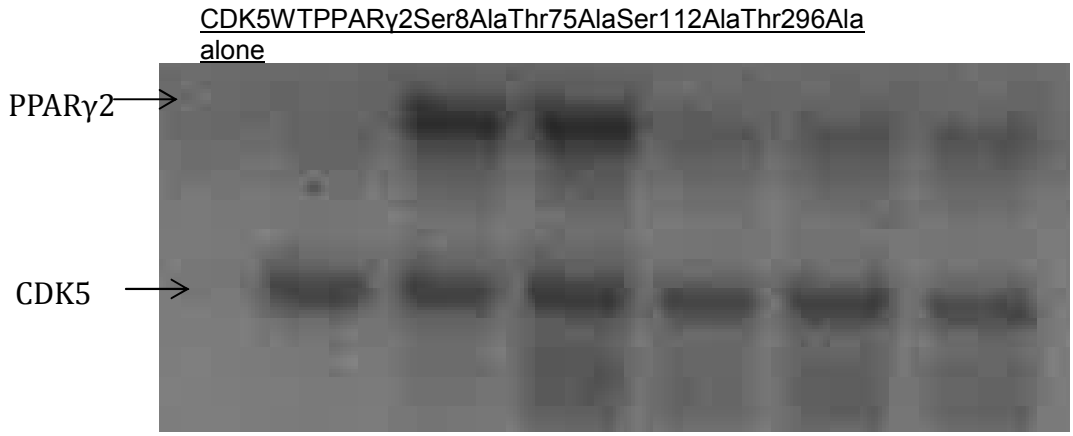

Figure 3.11: Graph (A) representing mol/mol stoichiometry of the phosphorylation of PPARγ2 mutants byCDK9 and autorad (B) showing phosphorylation of PPARγ2 mutants, including control CDK9 alone lane (no PPARγ2 present)

A

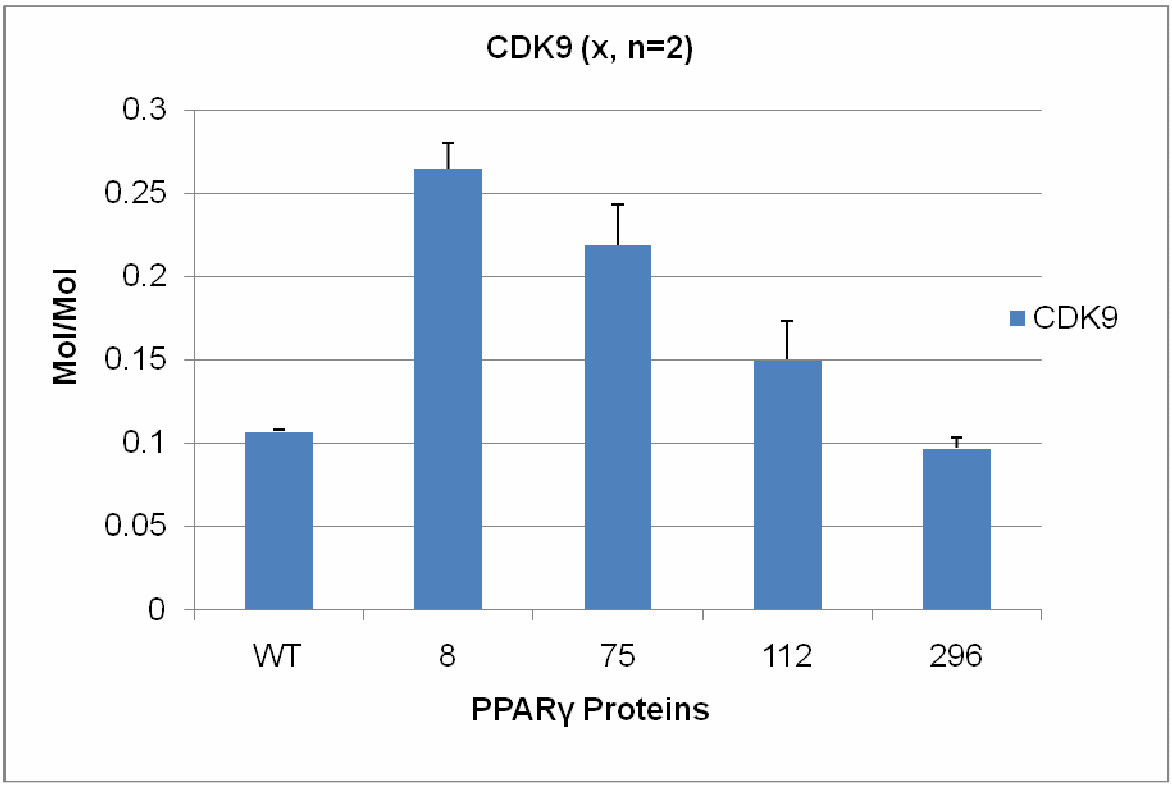


B

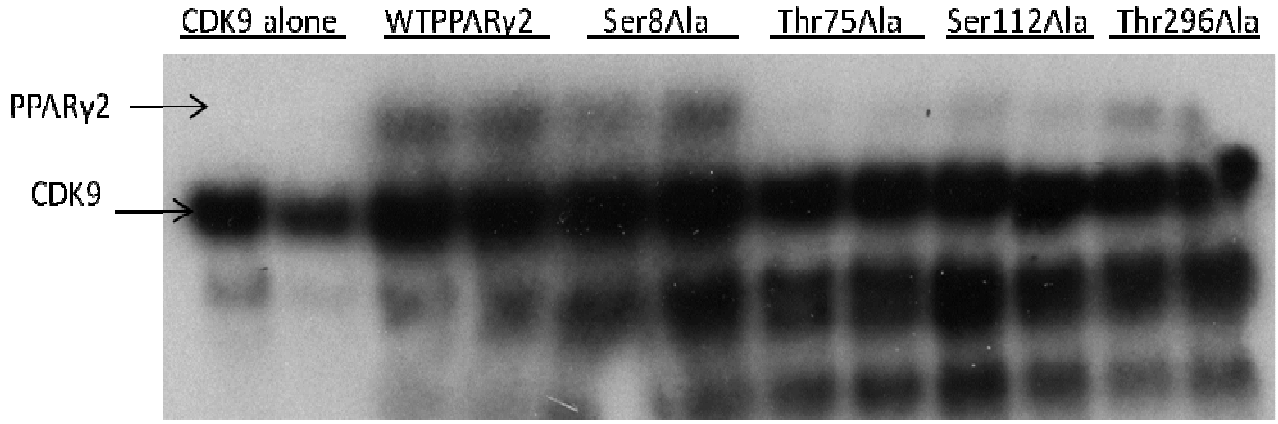

Figure 3.12: Graph (A) representing mol/mol stoichiometry of the phosphorylation of PPARγ2 mutants byERK2 and autorad (B) showing phosphorylation of PPARγ2 mutants, including control ERK2 alone lane (no PPARγ2 present)

**A**

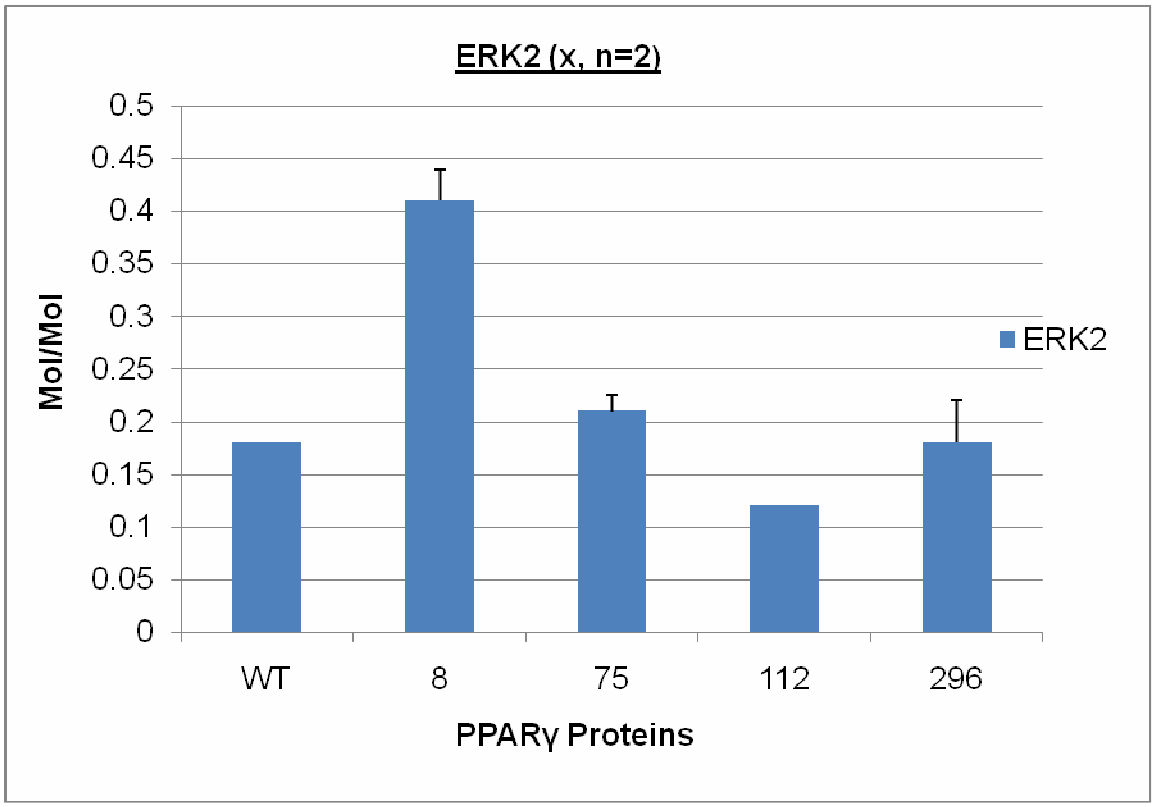


**B**

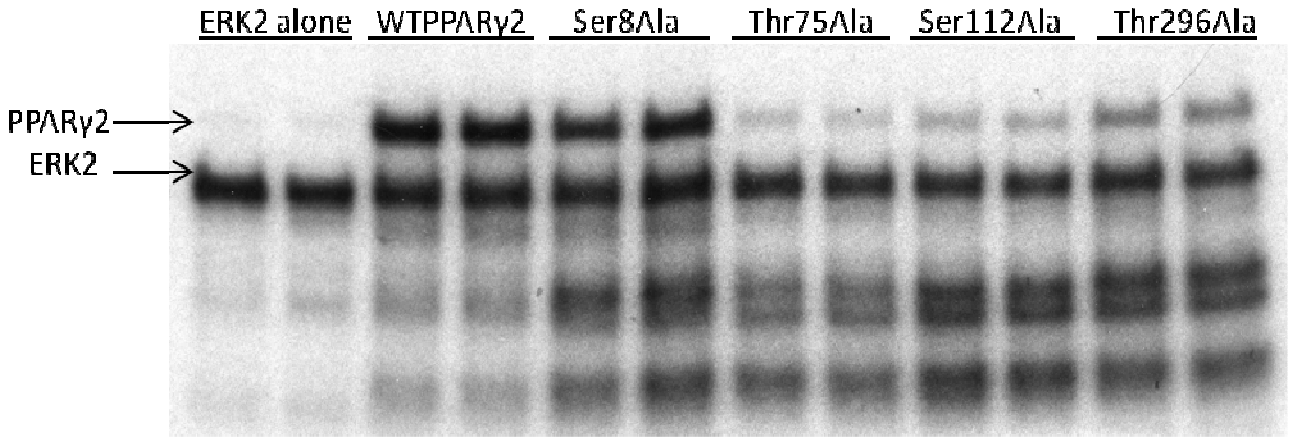

Figure 3.13: Graph (A) representing mol/mol stoichiometry of the phosphorylation of PPARγ2 mutants byERK8 and autorad (B) showing phosphorylation of PPARγ2 mutants, including control ERK8 alone lane (no PPARγ2 present)

**A**

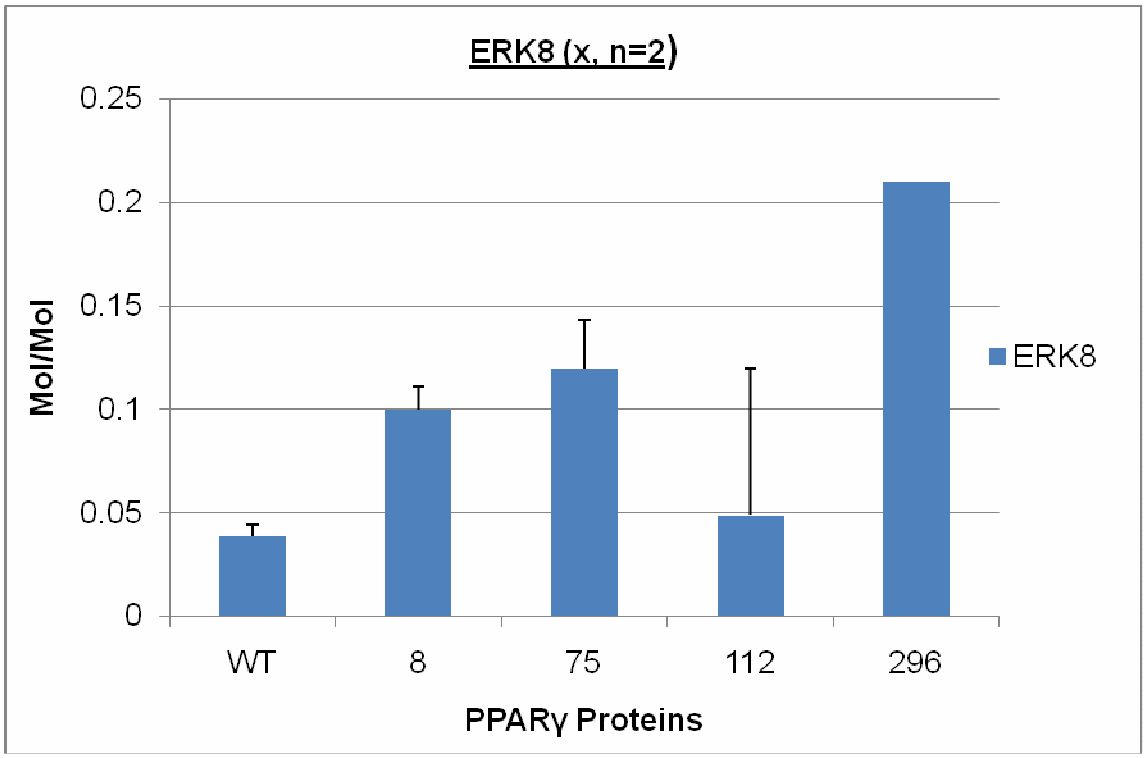


**B**

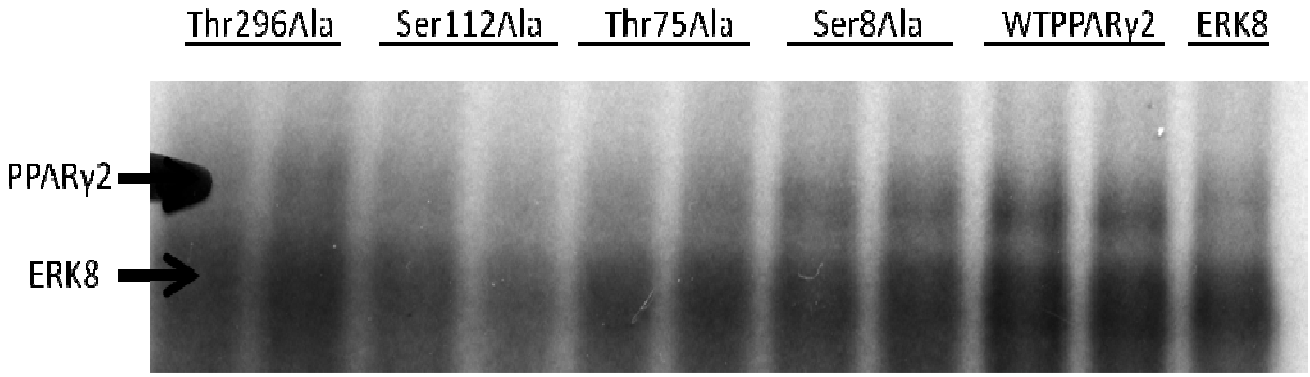

Figure 3.14: Graph (A) representing mol/mol stoichiometry of the phosphorylation of PPARγ2 mutants bySAPK4 and autorad (B) showing phosphorylation of PPARγ2 mutants, including control SAPK4 alone lane (no PPARγ2 present)

**A**

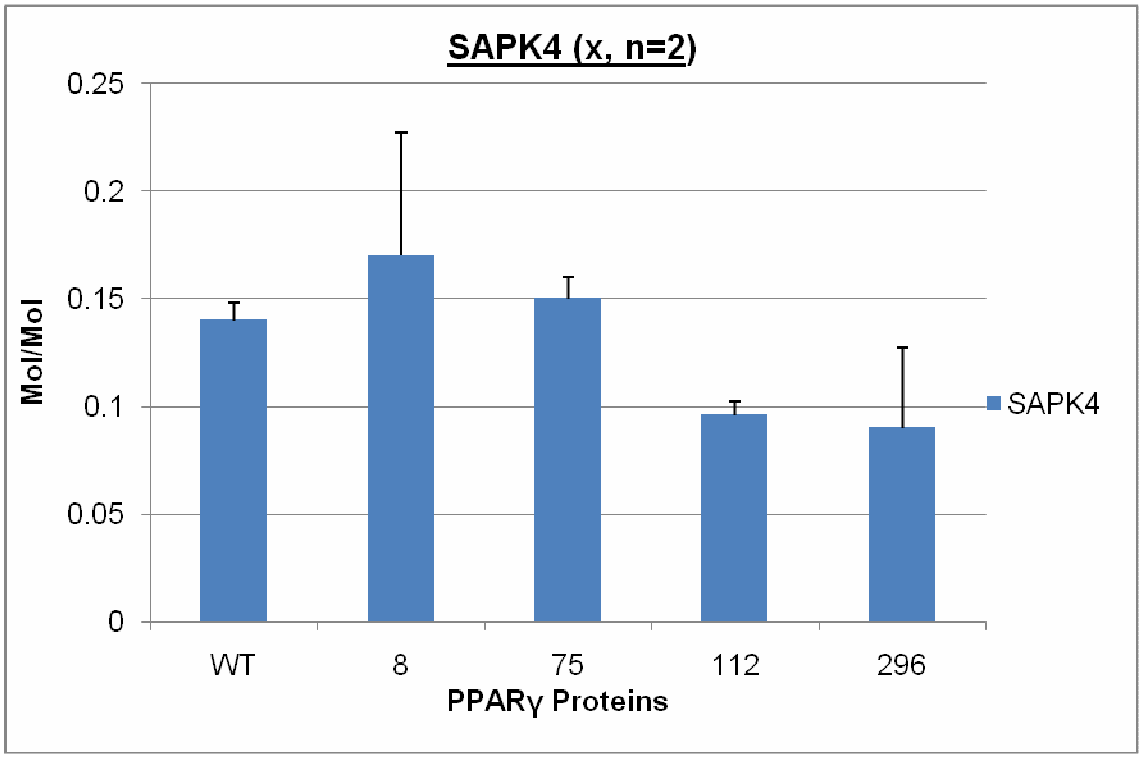


**B**

SAPK4 aloneWTPPARγ2 Ser8AlaThr75AlaSer112AlaThr296Ala

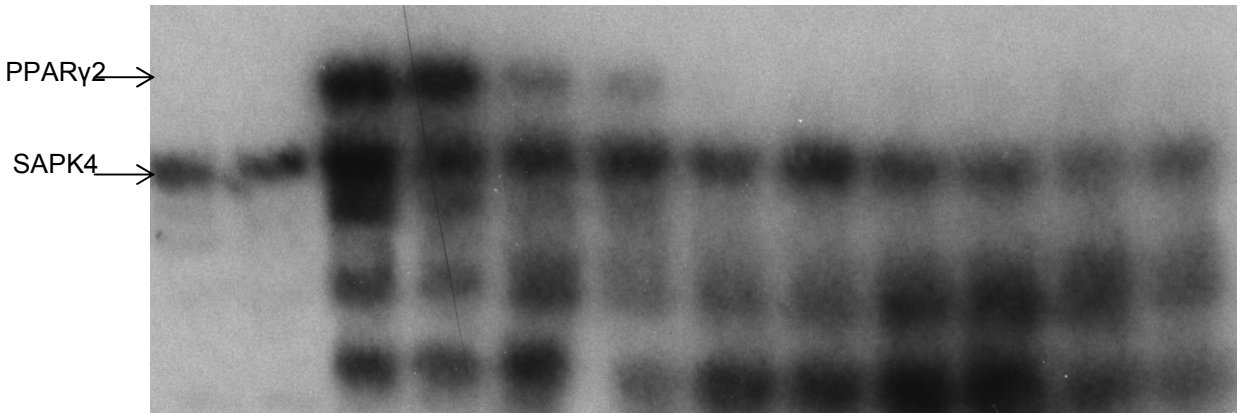

Figure 3.15: Graph (A) representing mol/mol stoichiometry of the phosphorylation of PPARγ2 mutants byDYRK2 without pre-incubation and autorad (B) showing phosphorylation of PPARγ2 mutants,including control DYRK2 alone lane (no PPARγ2 present)

A

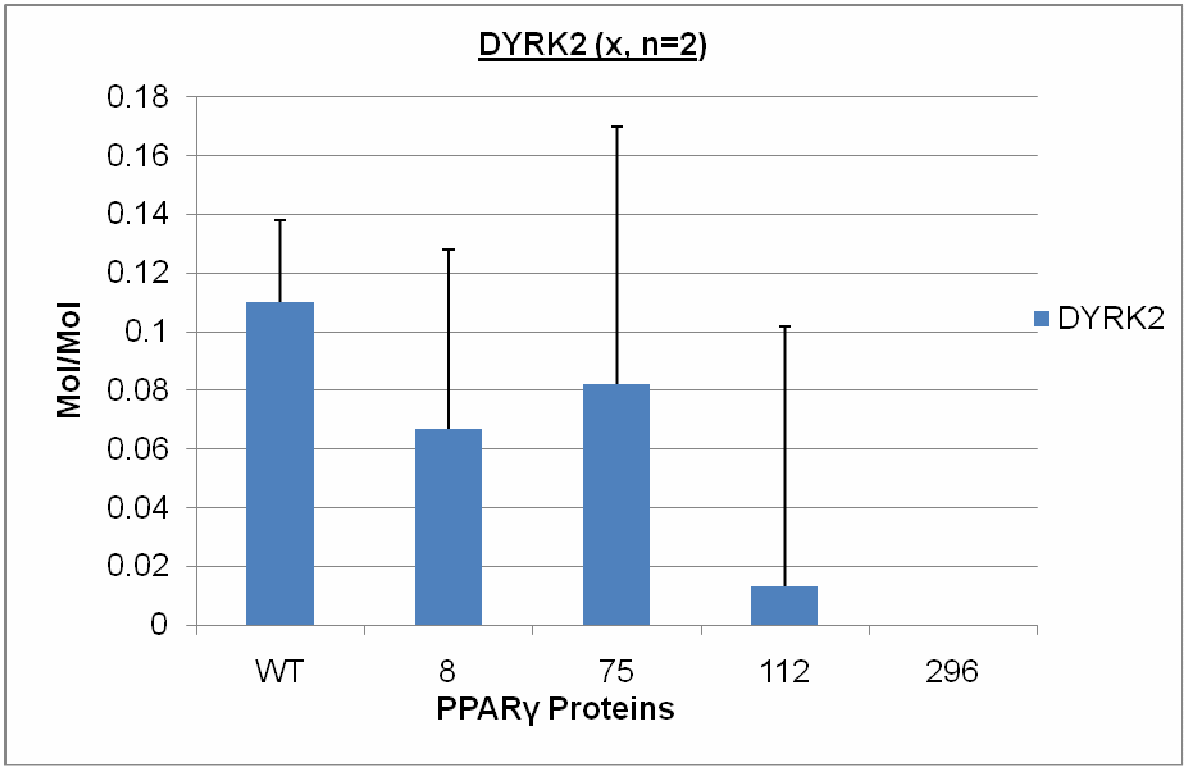


B

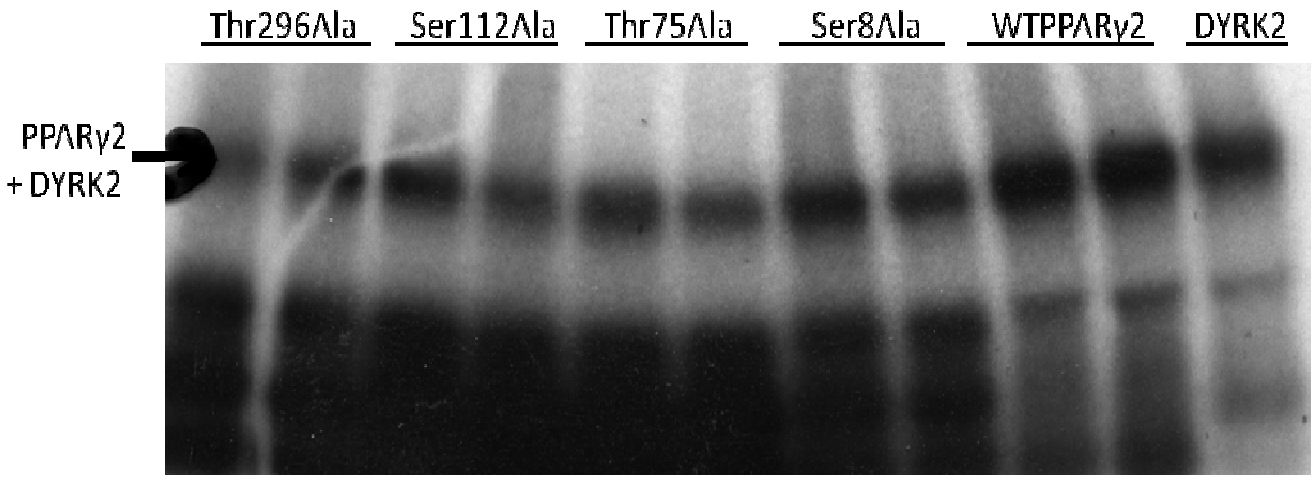

Figure 3.16: Graph (A) representing mol/mol stoichiometry of the phosphorylation of PPARγ2 mutants byDYRK2 pre-incubated with cold ATP prior to the radiolabeling reaction, and autorad (B) showing phosphorylation of PPARγ2 mutants

**A**

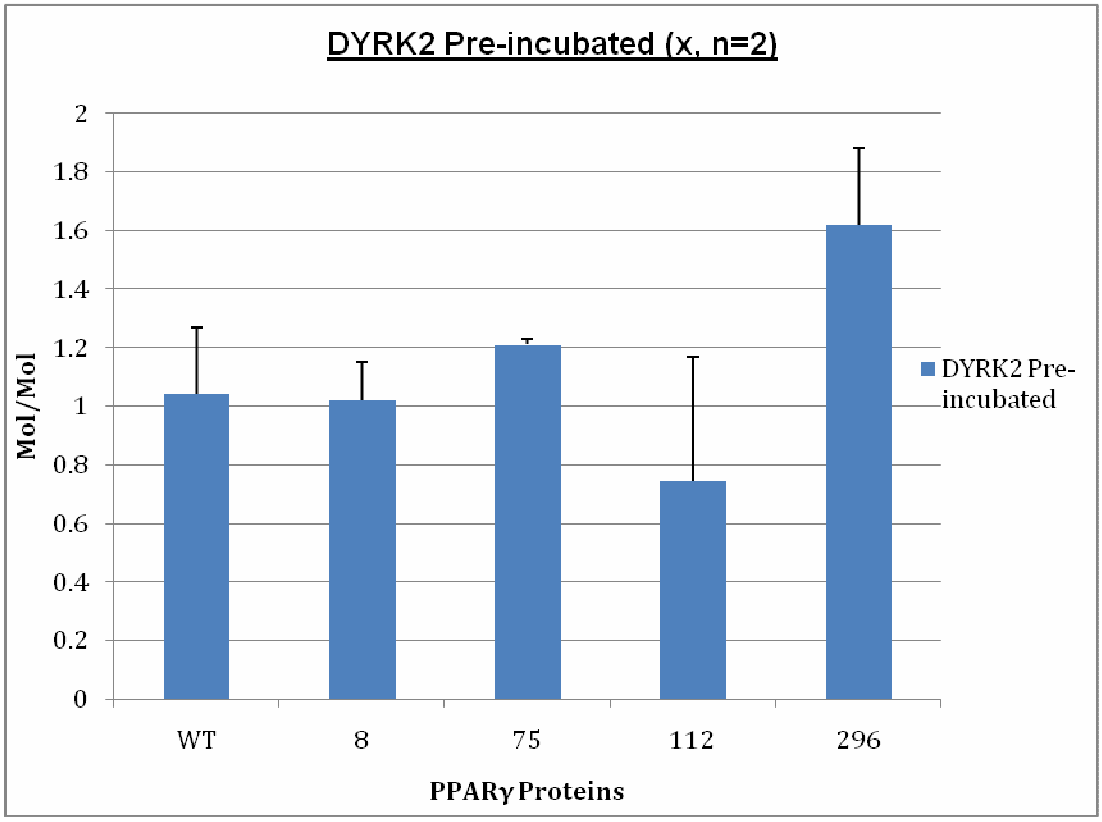


**B**

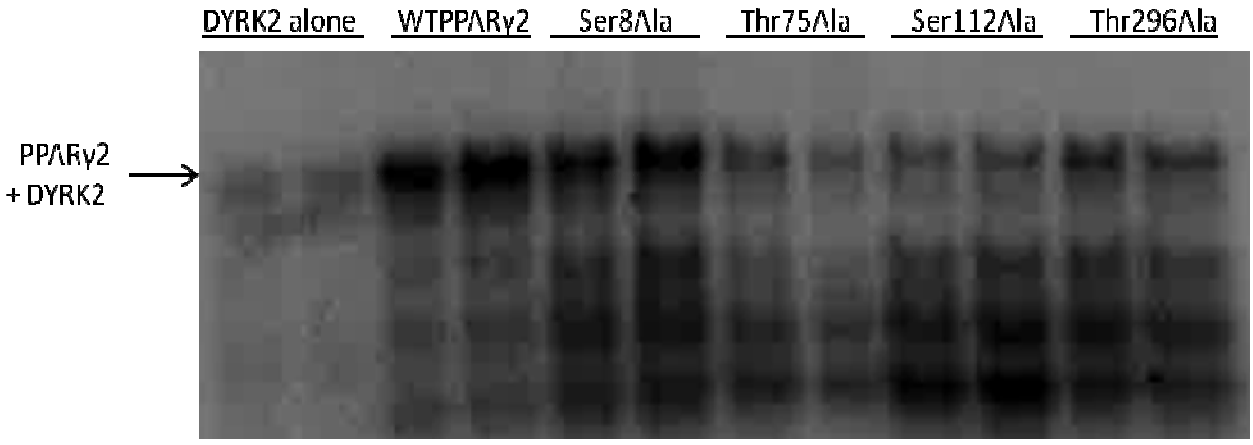

Figure 3.17: Graph (A) representing mol/mol stoichiometry of the phosphorylation of PPARγ2 mutants byDYRK1B and autorad (B) showing phosphorylationof PPARγ2 mutants

**A**

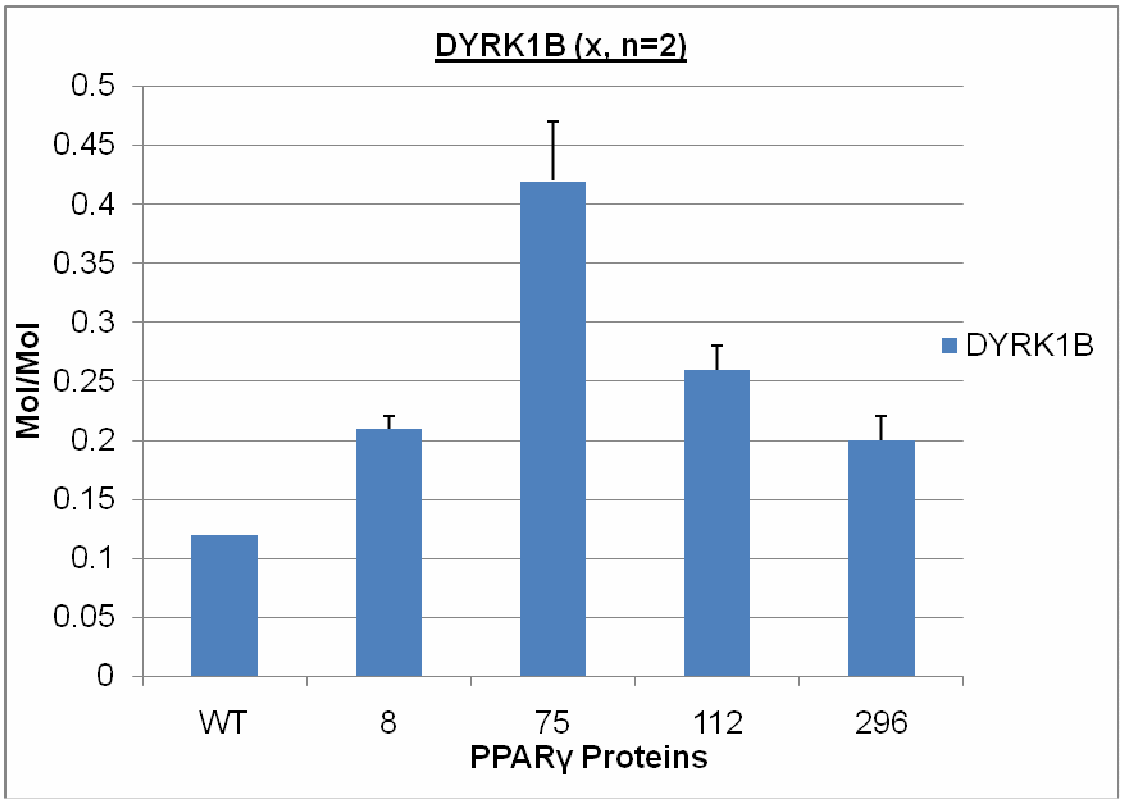


**B**

DYRK1B aloneWTPPARγ2Ser8AlaThr75AlaSer112AlaThr296Ala

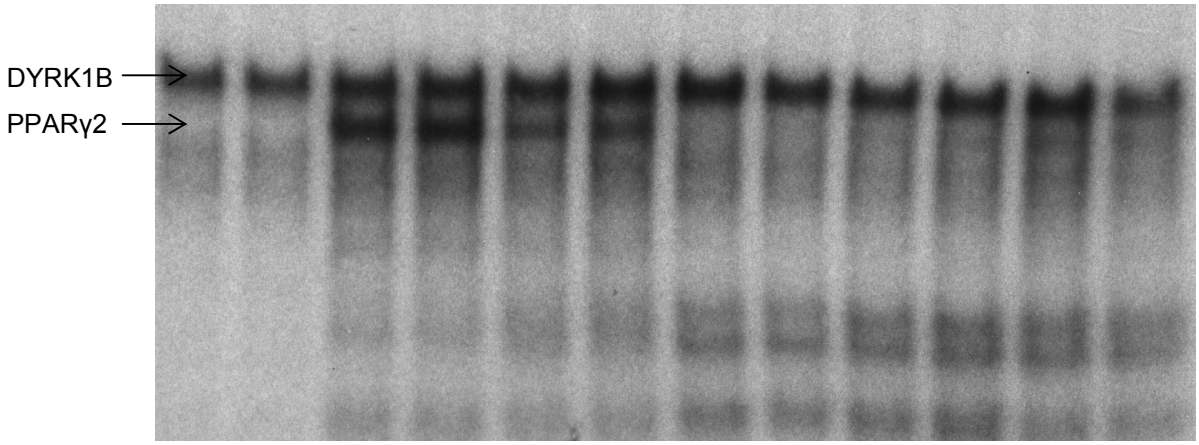

## 3.3 Discussion

The phosphorylation of PPARγat Ser273 was reported to regulate the response of PPARγ to TZD treatment, and that it may be possible to use this property to design improved TZDs lacking the unwanted side effects of these drugs but maintaining beneficial therapeutic properties (Choi *et al* 2011). Alternatively manipulating CDK5 in adipose could have direct therapeutic benefits in diabetes. However, the sequence surrounding Ser273 of PPARγ is not a classical consensus for CDK5 targeting (Fig. 1.3). It lacks key basic residues, in particular at positions +2 and +3 relative to the phosphorylated serine (Dhavan and Tsai 2001). In addition, the evidence provided that phosphorylation of Ser273 was performed by CDK5 *in vivo* was relatively weak (Choi *et al* 2011) and thus required more detailed examination;the data presented in the paper used a generic CDK substrate antibody for most of the ser273data instead of a ser273 phospho-specific antibody, and the blots shown were not clear, with many bands present.

My data suggests that PPARγ is a substrate for CDK5 *in vitro*, when it is complexed with p35 or p25, but that it is a better substrate for CDK5/p35 than CDK5/p25. Importantly, mutation of Ser273 to alanine did not affect the level of phosphorylation by either CDK5, indicating that this site was not a major phosphorylation siteforCDK5, at least *in vitro*. Mutation of each of the other serine or threonine phosphorylation sites on PPARγ (see Fig 1.3) did not cause a decrease in phosphorylation by CDK5, which may mean that CDK5 weakly phosphorylates more than one site, and this would require generation of PPARγ proteins with combinations of mutations to fully investigate. Alternatively phosphorylation site mapping by Mass Spectroscopy could identify which sites CDK5 phosphorylated *in vitro*, and development of phospho-specific antibodies to the different potential sites would allow quantification of relative phosphorylation in initial rate experiments. However a key finding from my phosphorylation analysis is that Ser273 seems not to be a major target for CDK5 *in vitro*.

In order to develop a means to phosphorylate Ser273 to allow characterization of a phosphoSer273 antibody and analyse the effect of phosphorylation of this

site on PPARγ function I investigated whether any CDK5 related kinases could phosphorylate PPARγ *in vitro.*Any kinase that phosphorylates Ser273 would be potential 'obesity regulated' kinases and would regulate TZD efficacy. I found that DYRK1A, DYRK1B, DYRK2, ERK2, ERK8 and SAPK4 could phosphorylate PPARγ, although none of these kinases phosphorylated PPARγ at Ser273.

ERK2 and ERK8 both phosphorylate PPARγ, but they appeared to do so at different sites. ERK2 has been previously documented to phosphorylate PPARγ at Ser112 (Adams *et al* 1997), but the site at which ERK8 phosphorylates PPARγremains unknown. ERK8 has a greater molecular mass than ERK2 and it is considered a distinct member of the ERK family (Abe *et al* 2002). Knowledge about the function of ERK8 is still limited (Strambi*et al* 2013), therefore it may interesting to investigate whether the PPARγsignalling cascade if truly a physiological target for this kinase (Gelman*et al* 2005).

DYRK2, DYRK1A and DYRK1B were all found to phosphorylate wild type PPARγ, and my preliminary data would suggest that DYRK2 can phosphorylate Ser112. The DYRK kinases prefer different consensus phosphorylation sequences, with DYRK2 preferring RXS/TP(Aranda, Laguna and Luna 2011); however it is also known that there are exceptions to the rule. Altered function of the DYRK family is linked to human disease, with DYRK1A expression being high in Downs Syndrome due to it lying on chromosome 21, DYRK1B being over-expressed in various types of cancer and DYRK2 expression being decreased in cancer (Aranda, Laguna and Luna 2011). This family has never previously been linked to the regulation of PPARγ however whether they regulate this transcription factor in vivoremains to be proven.

SAPK2β is also known as p38β, and SAPK4 as p38δ. The p38 kinases were already reported to phosphorylate PPARγ at Ser112 (Adams *et al* 1998). I found that SAPK2β phosphorylates PPARγrelatively poorly, compared to SAPK4. Experiments with the PPARγ mutants and using the phospho-specific antibodies suggested that phosphorylation by SAPK4 was most likely at Ser112, which agrees with the previously published data (Adams *et al).*Interestingly mutation of Thr296 to Ala also decreased phosphorylation by SAPK4which may suggest an additional novel regulation of PPARγ by this

kinase. However we cannot rule out that mutation of Thr296 interferes with phosphorylation of Ser112, either through hierarchical phosphorylation or by altering PPARγ interaction with SAPK4. This requires further investigation.

As discussed earlier in this chapter, calculations for the degradation of the proteins had to be made for accurate stoichiometry of the incubation of the PPARγ mutant protein with the CMGC kinases shown to phosphorylate PPARγ. Having to account for degradation might not portray the results as accurately as full length mutated PPARγ protein incubations. If there was more time on the project, the mutations of the PPARγ could be retried for a better yield of full length protein.

The thesis lacks statistical power due to the availability and stability of the kinases, meaning that most experiments were only done twice, so instead statistical trends are talked about based on the range of the results. Had it been possible, an n=3 would have been used for the kinase assays so that standard deviation and the coefficient of variance could have been carried out. To improve statistical analysis and totest the null hypothesis if more data had been available, one way analysis of variance (ANOVA) could have been carried out, written with F stat [variance] with probability of result (P value), using SPSS or similar stats software to conduct tests.A post-hoc test could also have been done, as well as Tukey to test the mean difference, and chi-squared test to test whether the results happened by chance.

For statistical analysis, sample size could have been used to detect any hypothetical difference. The larger a sample size, the more sure it can be that results are scientifically accurate and statistically significant.Aconfidence level, used in the sample size calculation shown below,reflects how sure you can be that the data lies within the confidence interval and is expressed as a percentage.The confidence interval is a plus or minus figure that shows quantification of the precision, represented as a margin of error. A 95% confidence level means you can be 95% certain of the data, and a 99% confidence level means you can be 99% certain; most laboratories use the 95% confidence level. For a given confidence level, the larger the sample size, the

smaller the confidence interval; however, the relationship is not linear, such that doubling the sample size does not halve the confidence interval.

An example of an equation that calculates sample size and could have been used for statistical analysis includes:

$$ss = \frac{Z^2 * (p) * (1-p)}{c^2}$$

Where
Z = Z value for confidence level (e.g. 1.96 for 95% confidence level)
p = percentage picking a choice, expressed as decimal (0.5 used for sample size needed, in the case of a yes or no survey)
c = confidence interval, expressed as decimal (e.g. .04 = ±4)

In terms of this thesis, a 95% confidence level would be used for the Z value and therefore a Z value of 1.96; the Z value is also known as the Z score and can be found using a Z score table. For the p value, 0.5 would be used as, similar to a yes or no survey, there is a yes or no answer with regards to is there a biological effect happening or not; in this case does phosphorylation of PPARγ get stopped by mutating it, or does phosphorylation still occur. The confidence interval is normally the standard deviation value, but as only the range was used due to n=2 results, the range would be used for the confidence interval.

In summary, the work in this chapter questioned whether CDK5 would phosphorylate Ser273 of PPARγ, but as this work was entirely performed *in vitro* I decided to further investigate phosphorylation of PPARγ in cells and tissues and this forms the basis of the work presented in Chapter 4.

# Chapter 4 - Analysis of PPARγ Phosphorylation in Cells and Tissues

## 4.1 Introduction and aims

Although protein phosphorylation in vitro is a useful starting point for establishing kinase-substrate interactions it is always important to validate potential interactions in intact cells. Equally, there are mechanisms by which a 'bona fide' target protein may not be a good substrate in vitro for a given kinase. For example if an additional protein or molecule was required to facilitate the interaction this would not be present in and in vitro assay and thus phosphorylation would not occur. Protein kinase B only becomes a substrate for PDK1 in the presence of the lipid phosphatidylinositol 3,4,5 trisphosphate and most protein kinase C isoforms require calcium and DAG to be active in vitro. Similarly, GSK3 requires its substrates to be pre-phosphorylated (primed) by an alternative kinase. Thus to investigate whether the phosphorylation of PPARγ by CDK5 required an unknown component I investigated the phosphorylation of PPARγ isoforms in intact cells and tissues. This required developing systems where I could express specific PPARγ isoforms along with the different CDK5 complexes andalso the use of cell systems or tissues that were reported to express both of these enzymes or could be induced to express them.

Aims of this Chapter:

- To investigate phosphorylation of PPARγ isoforms when co-expressed with p35/CDK5 and p25/CDK5
- To investigate phosphorylation of endogenous PPARγ in cells with or without CDK5 activity, and after exposure to stimuli related to obesity
- To develop an inducible cell system to study the effect of phosphorylation of PPARγ on its function.
- To investigate phosphorylation of PPARγ in rat adipose tissue isolated from animals fed normal chow or a high fat diet

## 4.2 Results

### 4.2.1 Phosphorylation of PPARγ after expression in HEK-293 and HeLa cells

As endogenous PPARγ is expressed at relatively low levels I attempted to develop a cell based recombinant system to study the phosphorylation of Ser273 of PPARγ. I was able to expressPPARγ (both isoforms and the S273A mutants) in the HEK-293 cells (Fig 4.1). However the recombinant PPARγ was not phosphorylated at Ser273, at least as assessed using our phospho-Ser273 antibody or the commercial anti-Cdk substrate antibody (data not shown). Therefore I attempted to co-transfect the HEK-293 cells with PPARγ, CDK5 and either p35 or p25 (Fig 4.1). Multiple conditionsusing both calcium phosphate and lipofectamineprotocols failed to achieve triple transfections of CDK5, PPARγ and p25 or p35. Although FLAG-PPARγ expressed well in the HEK-293 cells when co-transfected with CDK5 and p35 or p25 the expression of PPARγ (wild type or Ser273A) was lost; this made it impossible to establish whether co-transfection of either CDK5 complex induced Ser273 phosphorylation of PPARγ in this system.

HeLa cells are reported to contain endogenous CDK5(Lenstra and Bloemendal 1982) so these cells provided an opportunity to compare the effect of recombinant p35 and p25 expression on PPARγ phosphorylation, and they would potentially only require a double transfection of PPARγ with p25 or p35. However, althougheach protein expressed in these cells (Fig 4.2), this did not induce phosphorylation of PPARγ as measured by immunoblot using our phospho-Ser273 antibody or the commercial anti-Cdk substrate antibody (data not shown). Therefore these cell systems did not provide a model system to allow analysis of PPARγ phosphorylation and comparison of p35 with p25.

Figure 4.1: Expression of FLAG-PPARγ1 and PPARγ2, wild type and ser273a mutant, in HEK-293 cells is antagonized by co-transfection with CDK5 and p35.

HEK-293 cells were co-transfected with 3 μg of pCMVvectors designed to express either wild type or S273A PPARγ with or without vectors designed to express CDK5, p25 and p35 as indicated. After 24h the cells were lysed and analysed by western blot with anti-FLAG (4.1A), anti-CDK5 and anti-p35 antibodies (4.1B).

**(4.1A)**

PPARγ1 PPARγ2 S273Aγ1 S273Aγ2 PPARγ1 +CDK5 + p35 PPARγ2 +CDK5 + p35 S273Aγ1 +CDK5 + p35 S273Aγ2 +CDK5 + p35

p35 antibody (MW ~35KD) cdk5 antibody (MW ~35KD) **(4.1B)**

cdk5/p35 cdk5/p25 cdk5 cdk5/p35 cdk5/p25

Figure 4.2: Expression of FLAG-PPARγ1 and PPARγ2 wild type and ser273a PPARγ alone, and co-transfection with p35 in HeLa cells

PPARγ1 PPARγ2 S273Aγ1 S273Aγ2 PPARγ1 + p35 PPARγ2 + p35 S273Aγ1 + p35 S273Aγ2 + p35

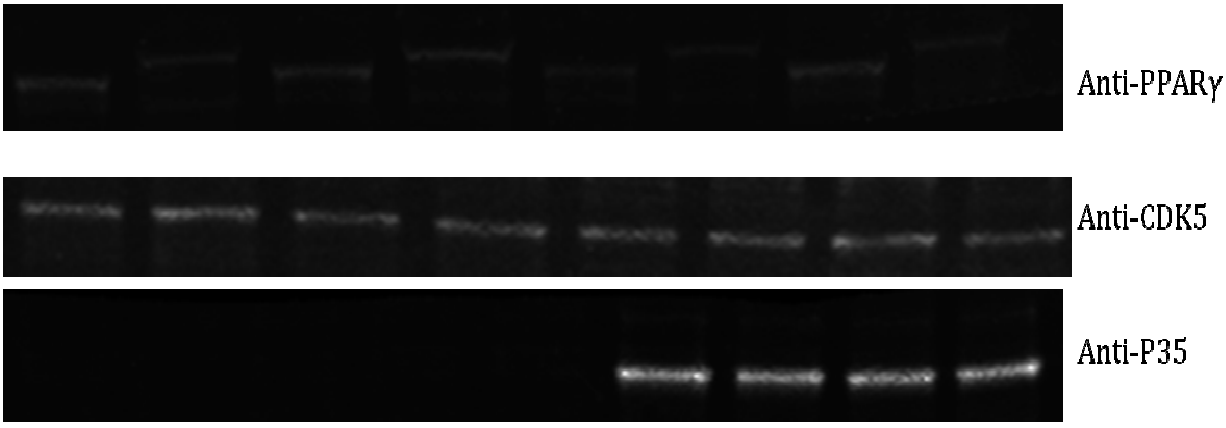

4.2.2. Stable inducible expression of PPARγ in HEK-293 cells.

In an attempt to overcome the technical issues with transient transfection detailed above I stably inserted the cDNA for FLAG-PPARγ2 into the FT-293 cell line (see Methods section). This cell system is designed to allow inducible expression of proteins of interest. I generated three clones of FT-293 cells containing PPARγ2 cDNA, namely LS1, LS2 and LS3. FT-293 LS1 showed the most consistent and robust expression of PPARγ as judged by immunoblot of lysates following induction (Fig 4.3) using both the flag antibody and PPARγ antibody; the FT-293LS1 cell line was used for all future experiments.

During these initial expression tests, the samples were also probed with the PPARγ phospho-specific antibodies by immunoblot. Both the anti-pSer112 and anti-CDK substrate detected PPARγ2, but the anti-pSer273 antibody did not detect anything at the appropriate molecular weight after induction of PPARγ expression (Fig 4.3).

The *in vitro* phosphorylation data (Chapter 3) indicated that DYRK and ERK2 could phosphorylate PPARγ2 at Ser112. In an attempt to establish if either of these kinases was responsible for the observed phosphorylation of Ser112 in the FT293 LS1 cells they were incubated with harmine (DYRK inhibitor) or U0126 (inhibitor of ERK2 activation). The phosphorylation of PPARγ2 at Ser112 was not altered by either inhibitor treatment, as judged using immunoblot with either the pSer112 or the Cdk substrate antibodies. U0126 efficacy was assessed by phosphorylation of ERK2 by immunoblot (Fig 4.4), but there are no good readouts for DYRK inhibition.

Figure 4.3: Analysis of lysates from the FT-PPARγ stable cell line by immunoblotwith PPARγ, flag, p-112, cdksubstate and p-Ser273 antibodies (MW ~58KD).

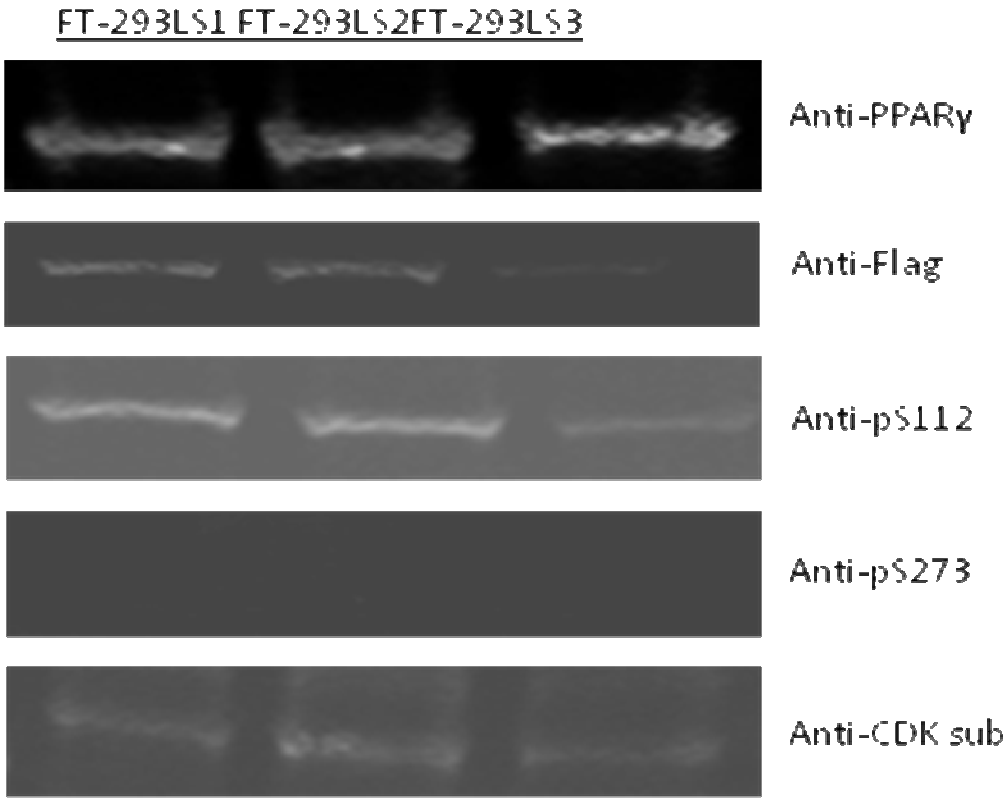


Figure 4.4: Analysis of PPARγ phosphorylation in FT-293LS1cellstreated with harmine and U0126, UI=uninduced, DMSO as a control (MW ~58KD).

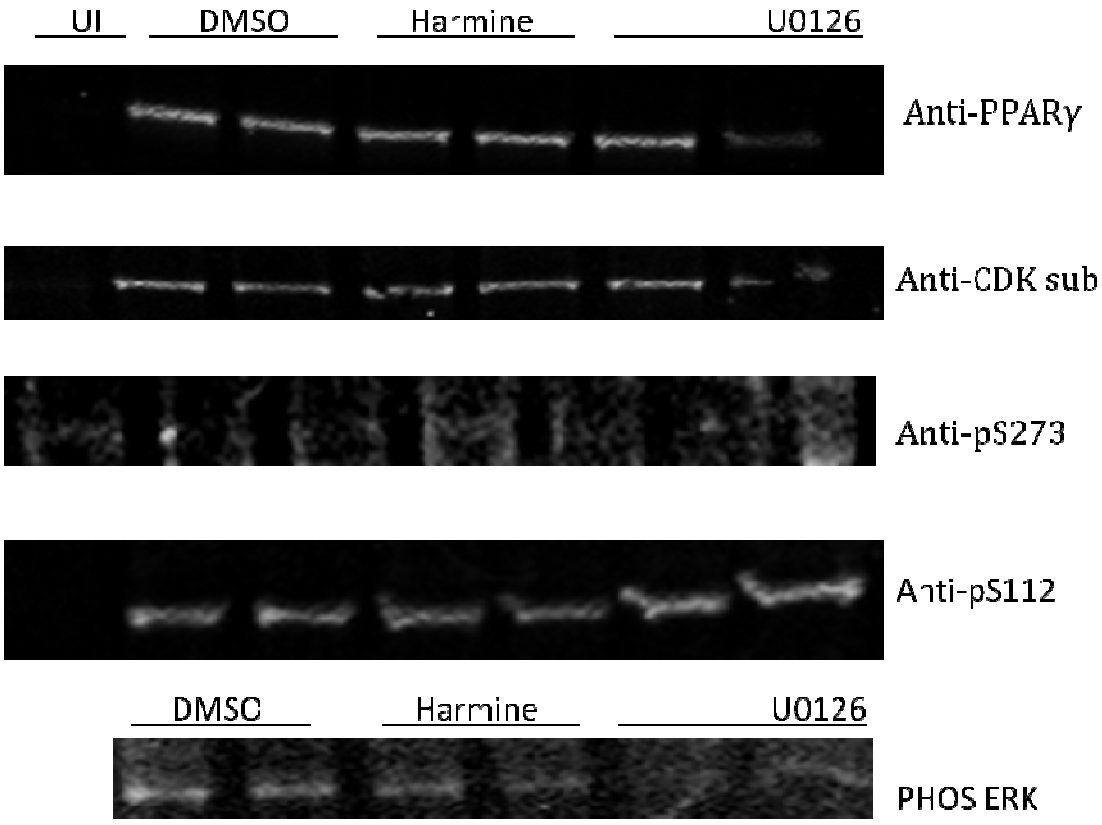

## 4.2.3 Analysis of PPARγ in differentiated 3T3-L1s

PPARγ expression is key to the differentiation of 3t3-L1 fibroblasts into adipocytes. Incubation of 3t3-L1 fibrobalsts with IBMX, dexamethasone and insulin over several days (see Methods section for details) promotes differentiation into adipocytes (Fig 4.5). This process can be monitored by Oil Red O staining of fat droplets (Figs 4.5 and 4.6).

Figure 4.5: Images of 3t3L1 fibroblasts at different stages of differentiation into adipocyte like cellsstained with oil red O.

Control Undifferentiated | Mid Differentiation IBMX, Dex, Insulin | Differentiated Post Insulin

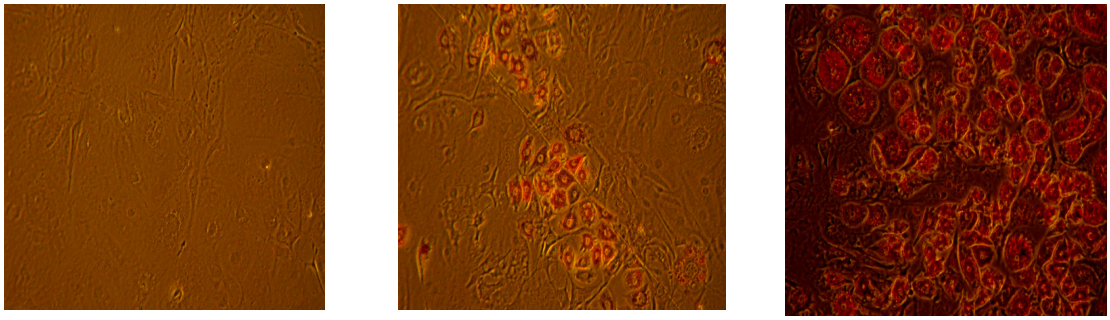

Figure 4.6: Images of 3t3L1 fibroblasts at different stages of induction to differentiate into adipocyte like cellsunder low and high light microscopy magnification.

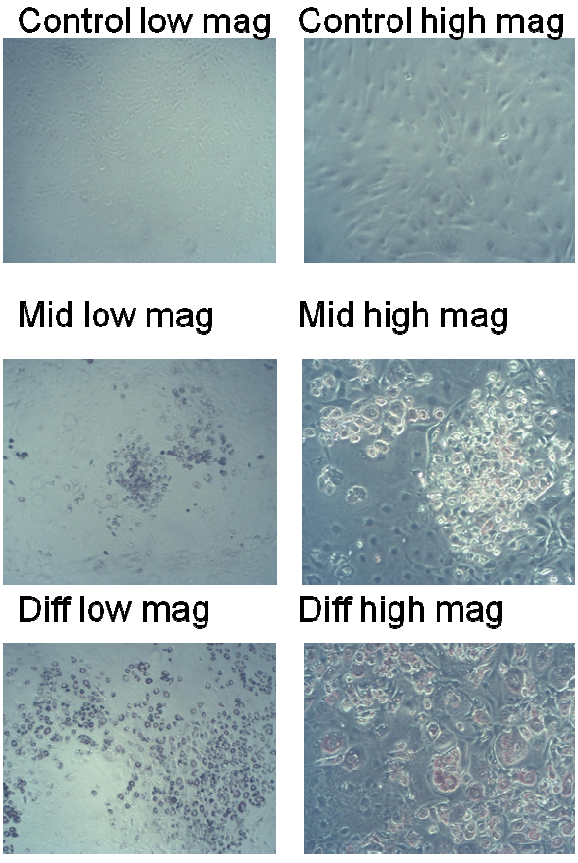

PPARγ (both isoforms) and fatty acid binding protein (FABP) are both induced during differentiation and can be detected by immunoblot of cell lysates isolated during the process (Fig 4.7). I detected CDK5 in undifferentiated and differentiated 3T3-L1 cells however I could not detect any p35 even after differentiation (Fig 4.7).

I was unable to detect any phosphorylation of PPARγ, using immunoblot and the p-Ser112 and p-Ser273 antibodies (Fig 4.8). I also failed to detect any sign of phosphorylation using the Cdk5 substrate antibody, even after immunoprecipitation of PPARγ (Fig 4.9).

Figure 4.7 Expression of PPARγ, FABP, p35 and CDK5 during differentiation of 3T3-L1 cells (control = undifferentiated, Mid Diff =day 2, ibmx+insulin, diff= differentiated, +ve control is recombinant PPARγ2)

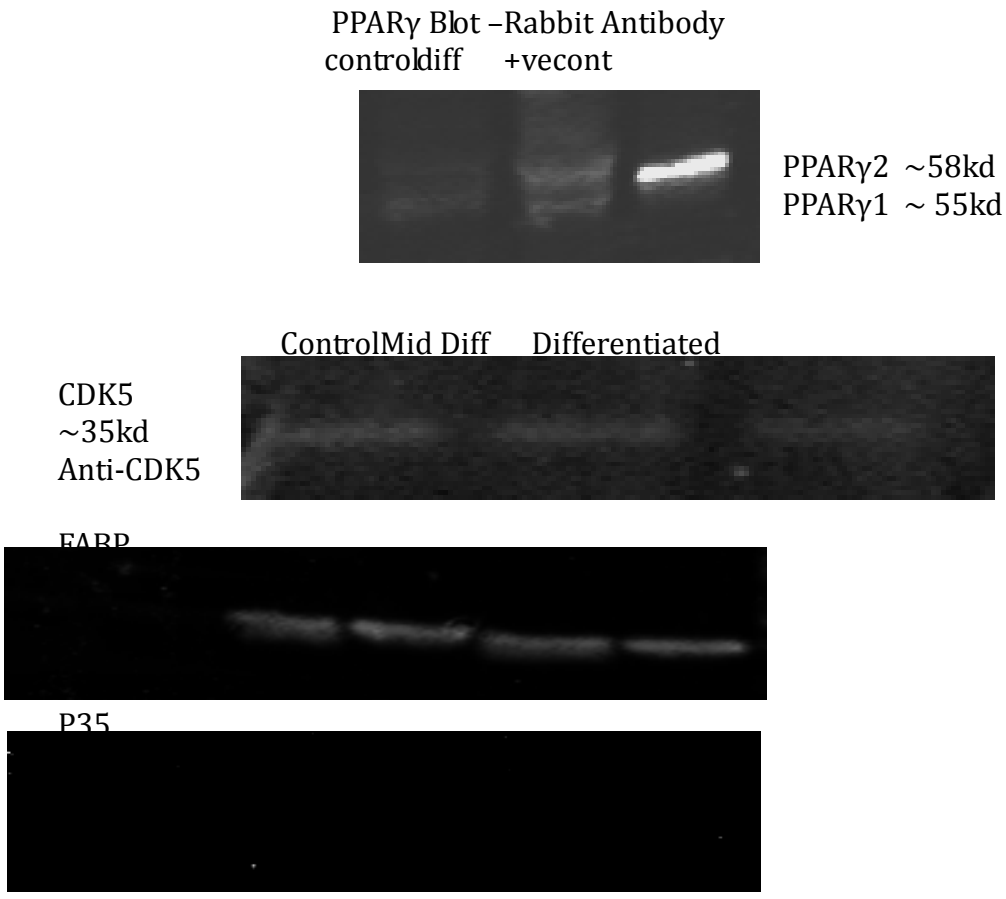

Figure 4.8: Analysisof PPARγ phosphorylation by immunoblot before and after differentiation of 3T3-L1 cells, with PPARγ p-Ser112 and p-Ser273 antibodies(control = undifferentiated, Day 2=ibmx+insulin, Day4= insulin, Diff= differentiated)

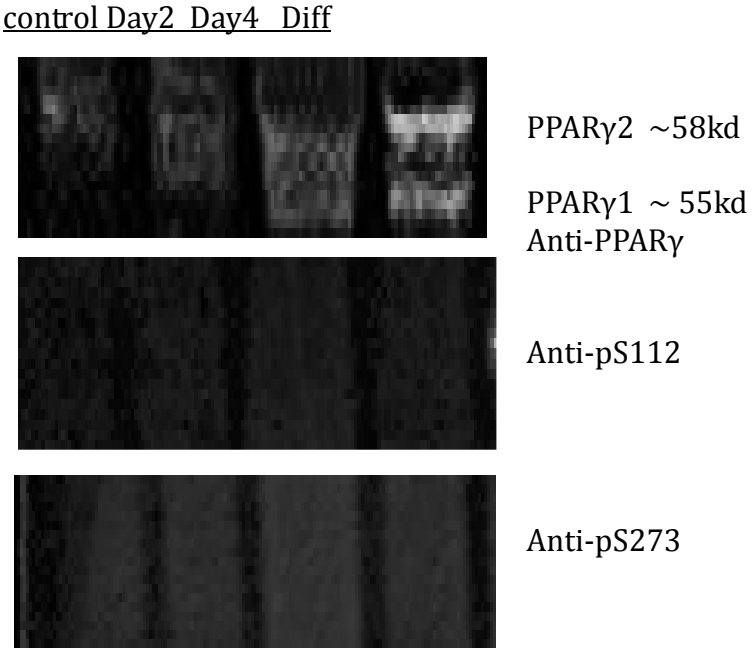


Figure 4.9: PPARγ was immunoprecipitatedfrom differentiated 3T3-L1 cells and analysed by immunoblot using a second PPARγ antibody and the anti-CDK substrate antibody. (+ve control= recombinant PPARγ1)

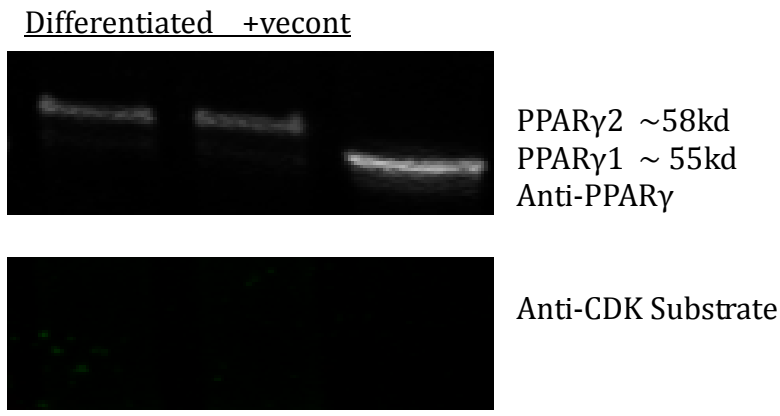

It remained possible that phosphorylation of Ser273 or Ser112 would only become apparent after specific cell stimuli (e.g. following hormone or nutrient challenge). Therefore I incubated differentiated 3T3-L1 cells with 500nM of palmitate to mimic obesity (Fig 4.10), 50ng of TNF-α, to mimic inflammation and 157nM insulin to mimic the fed state (Fig 4.11). The concentrations of these agents were based on previously published studies (Choi *et al* 2011 and Kakri*et al* 2011). However there was no phosphorylation of PPARγ seen with any of these treatments of my cells (using any of the phosphospecific antibodies), although TNF-α treatment reduced IkB levels while insulin treatment induced the phosphorylation of ERK (Fig 4.11); if this was to be investigated further, a total ERK antibody would be used to interpret total ERK phosphorylation.

Figure 4.10: Analysis of PPARγ phosphorylation by immunoblot, in differentiated 3T3 cells treated with 500nM palmitate, with PPARγ p-Ser112, p-Ser273 and CDK-substrate antibodies

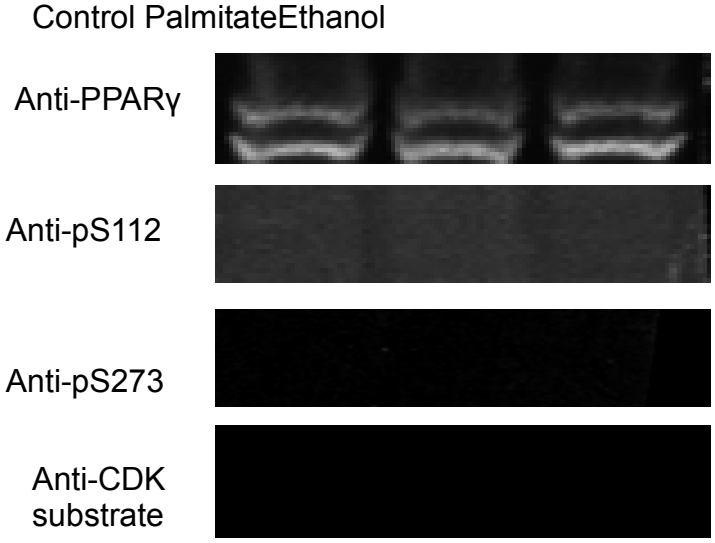

Figure 4.11: Analysis of PPARγphosphorylation by immunoblot in differentiated 3T3 cells treated with 50ng TNF-α or 167nm insulin for 1 hour, with PPARγ, p-Ser112, p-Ser273, CDK-substrate, IKB and p-ERK antibodies (MW PPARγ1 ~55 and PPARγ2 ~58kd, control- vehicle treated)

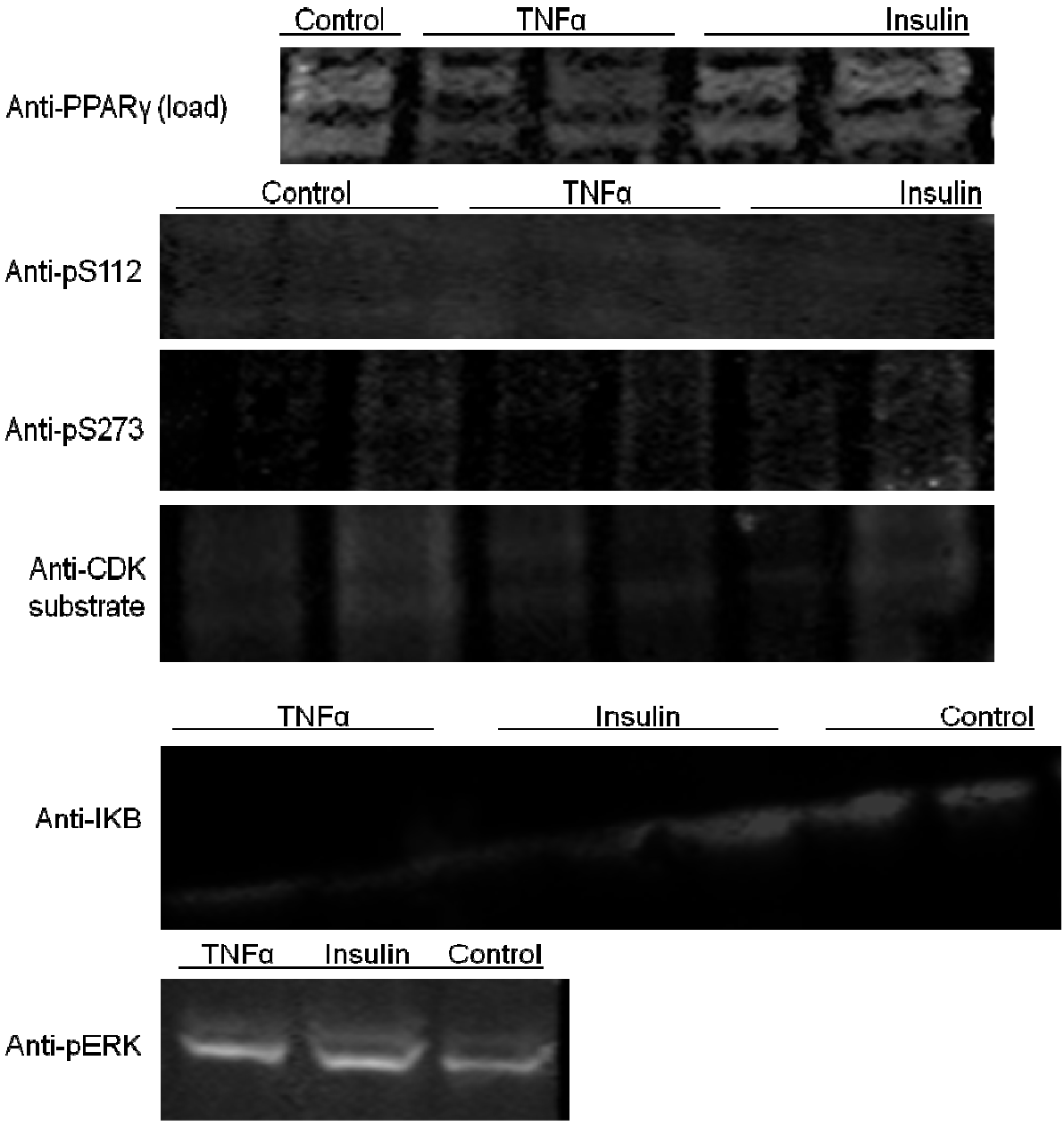

4.2.4 PPARγ phosphorylation in rat adipose tissue.

My studies had been initiated following the report of obesity-induced phosphorylation of PPARγ at Ser-273. All of my *in vitro* and cell based work questioned whether PPARγ was phosphorylated at Ser273. However as these were all relatively artificial systems I decided to investigate whether I could observe any alterations in Ser273 phosphorylation, CDK5 activation or p35 modification following high fat feeding of rats. The rat adipose samples were provided from a study performed in our laboratory looking at high fat diet effects on insulin sensitivity and behaviour. The high fat diet increased BMI and generated insulin resistance within the 10 weeks of the study (see Methods for details). I therefore attempted to extract PPARγ from adipose tissue and compare phosphorylation between the obese and the lean animals. However, PPARγ was almost impossible to extract from adipose (both standard chow and high fat fed rat adipose tissue). I used multiple different protocols including different extraction buffers (RIPA, triton-x-100, hepes buffer and solvent extraction methods) but in no case was I able to robustly isolate PPARγ (Figs 4.12, Fig 4.13 and Fig 4.14).

When RIPA buffer was used,actin could be detectedbut not PPARγ (Fig 4.12).I also tried toimmunoprecipitate the PPARγin order to enrich and concentrate it priorto immunoblot. This was performed after extraction in triton-x-100 lysis buffer as the RIPA buffer contains SDS. Recombinant PPARγ extracted from HEK-293 cells was used to confirm the immunoprecipitation and immunoblot was working but immunopreciptationfrom the tissue lysates did not enhance the PPARγ signal (Fig 4.13).

Data from two further attempts to extract PPARγ are shown in Fig 4.14. Firstly a PPARγ blot following an immunoprecipitation performed on adipose tissue lysates extracted in hepes buffer, and an immunoblot of adipose tissue lysates generated by solvent extraction. FABP was detectable in the solvent extractions demonstrating that protein was being extracted, however PPARγ could not be found. The solvent extractions generate an insoluble protein fraction (disc) and an aqueous soluble fraction but PPARγ was not readily detectable in either.

The lysates were also probed with the PPARγ phospho-specific antibodies despite the lack of detection of PPARγ and perhaps not surprisingly there was no evidence found for Ser273 phosphorylation in either the lean or obese tissue (data not shown).

In summary despite multiple approaches I was not able to generate solid evidence that PPARγ phosphorylation occurs in response to high fat feeding, and indeed I was not able to detect CDK5 or p35 in rat adipose tissue (data not shown).

Figure 4.12 – Adipose tissue (from rats fed either standard chow or high fat diet as indicated) was homogenized in RIPA buffer (as described in Methods) and lysates probed by immunoblot with the indicated antibodies.

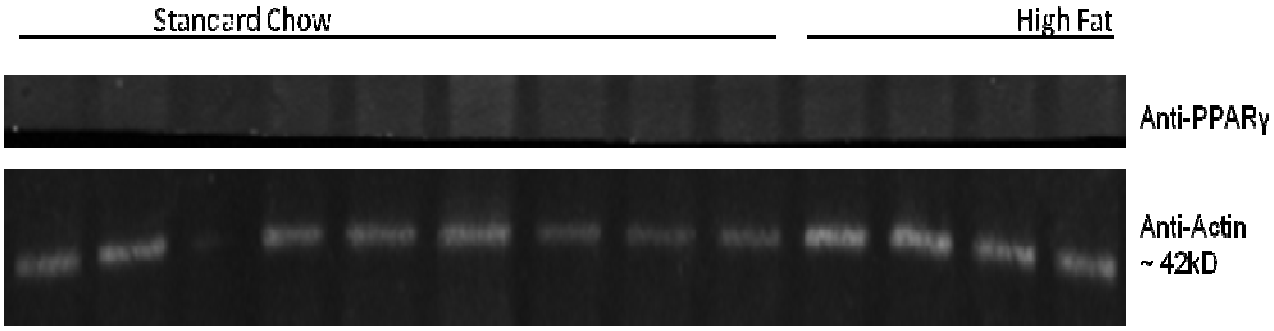


Figure 4.13 – PPARγ was immunoprecipitated using antiPPARγ (from Santa Cruz) either from (A) Hek293 cells expressing WT PPARγ1 or Ser273Ala PPARγ1, or from adipose tissue (B), prior to immunoblot analysis with anti-PPARγ (generated by Prof Colin Palmer, Dundee).

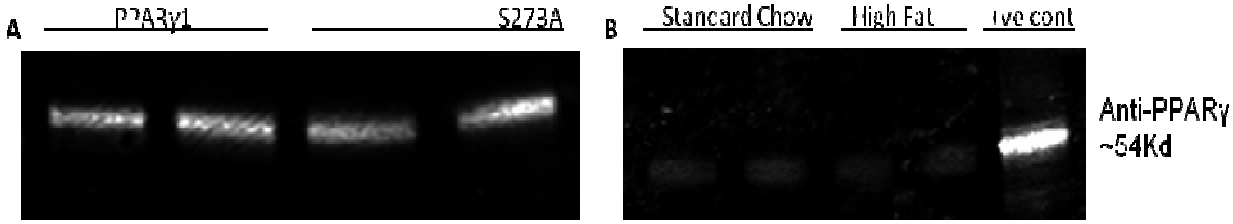


Figure 4.14 – Adipose tissue from chow fed rats was either (A) homogenized in Hepes Buffer or (B) solvent extracted as described in Methods section. Protein fractions were analysed by immunoblot using the antibodies indicated.

## 4.3 Discussion

I have analysedvarious cell lines for phosphorylation of PPARγ at Ser273 site, including 3t3-L1 adipocytes where I was able to detect endogenous PPARγ but not phosphorylation. Over-expression of recombinant human PPARγ transiently in HEK-293 or HeLa cells also failed to provide evidence that phosphorylation of PPARγ at Ser273 occurs. In addition stable expression ofPPARγ in HEK-293 cells generated sufficient quantities of PPARγ to allow visualization of Ser112 phosphorylation butI was unable to detect phosphorylation at Ser273. Attempts to stimulate phosphorylation using palmitate, TNF-αor insulin were also unsuccessful.Of course all of these experiments relied on a phospho-Ser273 antibody which we have not been able to characterize against the intact PPARγ, as we have not identified a protein kinase that will phosphorylate this site. The antibody does recognize a peptide based on the phosphorylated sequence surrounding the Ser273 site of PPARγ but it remains possible that this antibody is not sensitive enough to detect the phosphorylation.

I had one attempt at mapping the phosphorylation of recombinant PPARγfrom HEK-293 cells by mass spectroscopy (in collaboration with Dr Lamont, University of Dundee), however the results of this study were inconclusive and should really be performed on endogenous PPARγ from adipose, which awaits the development of improved extraction protocols. However, should extraction become possible, then the peptide mapping of PPARγ may be the most appropriate approach to definitively assess whether Ser273 is truly phosphorylated *in vivo*.

It is also worth reiterating that although I was able to extract housekeeping proteins such as actin and FABP from adipose tissue I was not able to detect CDK5 nor p35 or p25, even after high fat feeding. Taken together with my in vitro phosphorylation studies and the analysis of PPARγ phosphorylation in cells and tissues these resultsdisagree with the hypothesis that initiated my thesis; namely that obesity induces p35 modification, generation of p25, activation of CDK5 and phosphorylation of PPARγ at Ser273.

Although the results obtained during my research are in conflict with the published data by Professor Bruce Spiegelman,my data is consistent with that of Dhavan (2001), who reported no changes in phosphorylation of PPARγ when any of the proline-directed sites were mutated. My data was also in agreement with previously published data indicating that Ser112 was aregulatablephosphorylation site on PPARγ (Adams *et al* 1997), and I show preliminary evidence that Thr296 is worthy of further investigation as phosphorylation site involved in PPARγ regulation. My data could have conflicted with Professor Bruce Spiegelman's due to the different antibodies used, the confliction with the data already produced by previous groups, or the fact that CDK5 does not contain a known consensus sequence for the phosphorylation of PPARγ.

Finally, much of the work presented here is negative; however it questions the need for development of new drugs that target this modification. The tools generated during my studies (phospho-specific antibody and mutant PPARγ constructs and proteins) provide opportunities to broaden the analysis of PPARγ regulation by phosphorylation at sites other than Ser273 and by kinases other than CDK5.

## Chapter 5 – References


- ABEL, E. D. *et al*. (2001). Adipose-selective Targeting of theGLUT4 Gene Impairs Insulin Action in Muscle and Liver. *Nature*, **409** (8), 729-733.

- ABE, M.K.*et al.* (2002). ERK8, a New Member of the MAP kinase Family.*J. Biol. Chem,* **277** (19), 16733-43.

- ADAMS, M. *et al.* (1997). Transcriptional activation by peroxisome proliferator-activated receptor γis inhibited by phosphorylation at a consensus mitogen-activated protein kinase site. *Journal of Biological Chemistry*, 272 **(8)**, 5128–5132.

- ARANDA, S. *et al*. (2011). DYRK Family of Protein Kinases: Evolutionary Relationships, Biochemical Properties, and Functional Roles. *FACEB Journal,* **25** (2), 449-62.

- BARNARD, R. J. and YOUNGREN, J. F. (1992).Regulation of Glucose Transport in Skeletal Muscle.*FASB Journal*http://www.ncbi.nlm.nih.gov/pubmed/1426762,**6** (14), 3238-3244.

- BARNET, A.H. and SUDHESH, T.K. (2005). *Obesity and Diabetes.* Hoboken, Wiley.

- BARNETT, A. (2008). *Type 2 Diabetes*. Oxford, Oxford University Press

- BERG, J. *et al.* (2007).*Biochemistry*. 6th ed,. New York, W.H. Freeman and Company.

- BERGER, J. P., AKIYAMA, T.E. and MEINKE, P.T. (2005). PPARs: Therapeutic Targets for Metabolic Disease. *Trends in Pharmacological Sciences,* **26**, (5), 244-251.

- BERGER, J. and MOLLER, D.E. (2002). The Mechanisms of Action of PPARs**.** *Annu Rev Med*, **53,** 409–435.

- BOULTON, T.G. *et al.* (1991). ERKs: A Family of Protein-Serine/Threonine Kinases that are Activated and Tyrosine Phosphorylated in Response to Insulin and NGF. *Cell*, **65** (4), 663-675.

- BRADFORD, M.M. (1976). A Rapid and Sensitive Method for the Quantification of Microgram Quantities of Protein Utilizing the Principle of Protein-Dye Binding. *Analytical Biochemistry*. **72,** 248-254.

- BURNS, K. and HEUVEL, J. (2007). Modulation of PPAR Activity via Phosphorylation. *BiochimBiophysActa,***1771** (8), 952-960.

- CAMP, H.S. and TAFURI, S.R. (1997). Regulation of peroxisome proliferator-activated receptor g activity by mitogen-activated protein kinase. *Journal of Biological Chemistry,* 272 **(16)**,10811-10816

- CELL SIGNAL (2013). *CMGC Group* [online]. Last accessed 19 December at:

  http://www.cellsignal.com/reference/kinase/cmgc.html

- CHANG, L., CHIANG, S.H. and SALTIEL, A.R. (2004). Insulin Signaling and the Regulation of Glucose Transport**.** *Molecular Medicine*, **10** (7), 65-71.

- CHEN, L. *et al*. (2006). Peroxisome Proliferator-activated Receptor Gamma Promotes Epithelial to Mesenchymal Transformation by Rho GTPase-dependent Activation of ERK1/2. *Journal of Biological Chemistry,***281** (34), 24575-24587.

- CHOI, J.H. *et al*. (2010). Anti Diabetic Drugs Inhibit Obesity-Linked Phosphorylation of PPARγ by Cdk5.*Nature*, 466 (7305), 451-456.

- CHOI, J.H. *et al*. (2011). Antidiabetic Actions of a Non-Agonist PPARγ Ligand Blocking Cdk5-Mediated Phosphorylation.*Nature,* 477 (7365), 477-481.

- COMPE, E. *et al*. (2005). Dysregulation of the Peroxisome Proliferator-Activated Receptor Target Genes by XPD Mutations. *Molecular and Cell Biology*, **25** (14), 6065-6076.

- DAINTITH, J. and MARTIN, E. (2005). Oxford Dictionary of Science. 5th ed,. Oxford, Oxford University Press.

- DENNER, L.A. *et al*. (2012). Cognitive Enhancement with Rosiglitazone Links the Hippocampal PPARγ and ERK MAPK Signaling Pathways. *Journal of Neuroscience*, **32** (47), 16725-16735.

- DHAVAN, R. and TSAI, L.H (2001). A Decade of CDK5. *Nat Rev Mol Cell Bio*, **2** (10), 749-759.

- DIABETES (2014). [online]. Last accessed on 31 Mar at: http://www.diabetes.co.uk/diabetes-history.html

- DIABETES UK (2012). [online]. Last accessed on 15 January at:

  http://www.diabetes.org.uk/Guide-to-diabetes/What-is-diabetes/

- DIABETES UK (2013). [online]. Last accessed on 19 December at:

  http://www.diabetes.org.uk/Guide-to-diabetes/What-is-diabetes/Diabetes-treatments/

- DISTEL, R. J., RO, H. S., ROSEN, B. S., GROVES D. L. and SPIEGELMAN, B. M. (1987). Nucleoprotein Complexes that Regulate Gene Expression in Adipocyte Differentiation: Direct Participation of C-fos. *Cell,* **49** (6), 835-844.

- EVANS, R.M., BARISH, G.D. and WANG. Y.X. (2004). PPARs and the Complex Journey to Obesity. *Nature Medicine*, **10** (4), 355-361.

- FEINGLOS, M. N. and BETHAL, M. A. (2008). Type 2 Diabetes Mellitus An Evidence-Based Approach To Practical Management. Totowa, Humana Press.

- FIUME, R. *et al*. (2011). Nuclear PLCs Affect Insulin Secretion by Targeting PPARγ in Pancreatic β cells. *FASEB Journal*, **26** (1), 203-210.

- GELMAN, L. *et al.* (2005). Kinase Signaling Cascades that Modulate Peroxisome Proliferator-Activated Receptors. *Current Opinion in Cell Biology*, **17** (2), 216-222.

- GIRALT, M. and VILLARROYA, F. (2013). White, Brown, Beige/Brite: Different Adipose Cells for Different Functions? *Endocrinology*, **154** (9), 2992–3000.

- GREGOIRE, F.M., SMAS, C.M. andSUL, H.S. (1998). Understanding Adipocyte Differentiation. *Physiological Reviews*, **78** (3), 783-801.

- GROSS, B. and STAELS, B. (2007).PPAR Agonists: Multimodal Drugs for the Treatment of Type-2 Diabetes. *Best Practice & Research Clinical Endocrinology & Metabolism*, **21** (4), 687–710.

- HOLMAN, G.D. and KASUGA, M. (1997). From Receptor to Transporter: Insulin Signalling to Glucose Transport. *Diabetologia*, **40** (9), 991-1003.

- HOUTKOOPER, R. and AUWERX, J. (2010). Obesity: New Life for Antidiabetic Drugs. *Nature,* **466** (7305), 451-456.http://www.diabetes.co.uk/

- JONES, J. (2005). Deletion of PPARγ in Adipose Tissues of Mice Protects Against High Fat Diet-Induced Obesity and Insulin Resistance. *PNAS*, **102** (17), 6207-6212.

- JURESA, D. and METALKO, Z. (2009). PPARγ - A New Concept of Treatment?*DiabetologiaCroatica,* **38** (2), 23-29.

- KAHN, S.E., HULL, R.L. and UTZSCHNEIDER, K.M. (2006). Mechanisms Linking Obesity to Insulin Resistance and Type 2 Diabetes. *Nature*, **444** (7121), 840-846.

- KAJITA, K. *et al*. (2008). Effect of Fasting on PPARγ and AMPK Activity in Adipocytes. *Diabetes Research and Clinical Practice,* **81** (2), 144-149.
- KARKI, S. *et al*. (2011). The Multi-Level Action of Fatty Acids on Adiponectin Production by Fat Cells. *PLoS One*, **6** (11).
- KIM, J.K. *et al*. (2001). Glucose Toxicity and the Development of Diabetes in Mice with Muscle-specific Inactivation of GLUT4. *The Journal of Clinical Investigation,***108** (1), 153-160.
- KÖNIG, M., BULIK, S. and HOLTZHÜTTER, H.G. (2012). Quantifying the Contribution of the Liver to Glucose Homeostasis: A Detailed Kinetic Model of Human Hepatic Glucose Metabolism. *PLoS One,* **8** (6).
- KOTA, B.P., HUANG, T.H.W. and ROUFOGALIS, B.D. (2005). An overview on biological mechanisms of PPARs. *Pharmacological Research*, **51** (2), 85-94.

- LAMELLI, U.K. (1970). Cleavage of S*tructural* **P**roteins during the Assembly of the Head of Bacteriophage T4. *Nature*, **227** (5259), 680-685

- LAZAR, M. A. (1999). *PPARγ in Adipocyte Diffe***ren**tiation. *Journal of Animal Science*, **77** (3), 16-22.

- LEE, H.W and KIM, S.G. (2010). AMPK-Dependent Metabolic Regulation by PPAR Agonists.*PPAR Research,* **2010**, 1-10.

- LEE, Y.S. *et al.* (2012). Nobiletin Improves Obesity and Insulin Resistance in High-Fat Diet-Induced Obese Mice.*Journal of Nutritional Biochemistry*, **24** (1), 156-162.

- LEHMANN, J. M. *et al*. (1995). An Antidiabetic Thiazolidinedione is a High Affinity Ligand for Peroxisome Proliferator-Activated Receptor γ (PPARγ). *Journal of Biological Chemistry,***2** (270), 12953–12956

- LENSTRA, J.A. and BLOEMENDAL, H. (1983). The Major Proteins from HeLa Cells Identification and Intracellular Localization. *European Journal of Biochemistry,***130** (2), 419-426.

- LILJENQUIST, J.E. *et al*. (1974). Effects of Glucagon on Lipolysis and Ketogenesis in Normal and Diabetic Men. *Journal of Clinical Investigation,* **53** (1), 190-197.

- LIZCANO, J.M. and ALESSI, D. R. (2002). The Insulin Signalling Pathway. *Current Biology*, **7** (2), 236-238.

- MALUMBRES, M. *et al*. (2009). Cyclin Dependent Kinases: A Family Portrait. *Nat Cell Biol*, **11** (11), 1275-1276.

- MANNING, G. *et al*. (2002). The Protein Kinase Complement of the Human Genome. *Science,* **298**, 1912-1934.

- MICHALIK, L. *et al.* (2006). International Union of Pharmacology. LXI. Peroxisome Proliferator-Activated Receptors.*Pharmacological Reviews*, **58** (4), 726-741.

- MIYAMOTO, S. *et al.* (1994). Tumor Necrosis Factor α-Induced Phosphorylation of IKBa is a Signal for its Degradation but not Dissociation from NF-KB. *PNAS*, **91**(26), 12740-12744.

- Qu, J. (2011). S-Nitrosylation Activates Cdk5 and Contributes to Synaptic Spine Loss Induced by β-Amyloid Peptide. *PNAS*, **108** (34), 14330–14335

- SABOSCIENCES (2012). *CDK5 Pathway* [online]. Last accessed on 16 January at:

  http://www.sabiosciences.com/pathway.php?sn=CDK5_Pathway

- SABOSCIENCES (2012). *PPAR Pathway* [online]. Last accessed on 15 January at:

  http://www.sabiosciences.com/pathway.php?sn=PPAR_Pathway

- SALTIEL, A.R. and PESSIN, J.E. (2007).*Mechanisms of Insulin Action.* New York, Springer Science.

- SCHMOLL, D. *et al*. (2000). Regulation of Glucose-6-phosphatase Gene Expression by Protein Kinase B a and the Forkhead Transcription Factor FKHR: Evidence for Insulin Response Unit-Dependent and Independent Effects of Insulin on Promoter Activity. *THE JOURNAL OF BIOLOGICAL CHEMISTRY*, 275 (46), 36324-36333.

- SHARMA, P. *et al. (1999).* Regulation of Cyclin-Dependent Kinase 5 Catalytic Activity by Phosphorylation.*PNAS*, **96** (20), 11156–11160.
- SINACORE, D.R. and GULVE, E.A. (1993).The Role of Skeletal Muscle in Glucose Transport Glucose Homeostasis, and Insulin Resistance: Implications for Physical Therapy. *Physical Therapy*,**73** (12), 878-891.
- SONGYANG, Z. *et al. (1996).* A structural basis for substratespecificities of protein Ser/Thr kinases: primary sequencepreference of casein kinases I and II, NIMA, phosphorylasekinase, calmodulin–dependent kinase II, CDK5, and ERK1.*Mol. Cell. Biol.* **16**(11), 6486–6493.

- STEPPEN C. M. *et al*. (2001). The HormoneResistinLinksObesity to Diabetes. *Nature*,409 **(6818)**,307-312.
- STRAMBI, A. *et al.* (2013). Structure Prediction and Validation of the ERK8 Kinase Domain [online].*PLoS One*, **8** (1).
- TAYLOR, S. I. (1999).Deconstructing Type 2 Diabetes. *Cell*, **97** (1), 9-12
- TUCH, B., DUNLOP, M. and PROIETTO, J. (2000).*Diabetes Research: A Guide for Postgraduates*. London, CRC Press.
- UNIVERSITY OF DUNDEE (2013). *Protein Kinase Groups* [online]. Last accessed 19 December at:

  http://www.compbio.dundee.ac.uk/kinomer/families.html
- WHITEHEAD, J. (2011). Diabetes: New Conductors for the Peroxisome Proliferator-Activated Receptor γ (PPARγ) Orchestra. *The International Journal of Biochemistry & Cell Biology*, **43**(8), 1071-1074.
- WHO (2012). *Diabetes*[online]. Last accessed on 15 January at: http://www.who.int/topics/diabetes_mellitus/en/

- WOLF, G. *et al*. (1995). PTB Domains of IRS-1 and SHC Have Distinct but Overlapping Binding Specificities. *The Journal of Biological Chemistry*, **270** (46), 27407–27410.

- WU, J., COHEN, P. and SPIEGELMAN, B. M. (2013). Adaptive Thermogenesis in Adipocytes: Is Beige the New Brown?*Genes and Development*, **27** (3), 234-250.

- YANG, S.L. *et al*. (2010). Pigment Epithelium-derived Factor Induces Interleukin-10 Expression in Human Macrophages by Induction of PPAR Gamma.*Life Sciences*, **87** (1-2), 26-35.

- Ye, J. (2011). Challenges in Drug Discovery for Thiazolidinedione Substitute. *ActaPharmaceuticaSinica B,* **1** (3), 137-142.

ZISMAN, A. *et al.* (2000). Targeted Disruption of the Glucose Transporter 4 Selectively in Muscle Causes Insulin Resistance and Glucose Intolerance.*Nature Medicine*, **6** (8), 924-928.